ADDIS ABABA UNIVERSITY
ADDIS ABABA INSTITUTE OF TECHNOLOGY
SCHOOL OF CIVIL AND ENVIRONMENTAL ENGINEERING

THE EFFECT OF VARYING GEOMETRY ON THE AMPLIFIFCATION OF GROUND MOTION IN ZONED EARTHEN DAMS

A Thesis Submitted to Addis Ababa Institute of Technology in partial fulfillment of the requirements for the Degree of Master of Science in Geotechnical Engineering

By:

Yeabsra Tesfaye

Advisor: **Dr.-Ing Asrat Worku**

2020

Addis Ababa

The undersigned have examined the thesis entitled '**The Effect of varying geometry on the amplification of ground motion on zoned earthen dams'** presented by **Yeabsra Tesfaye**, a candidate for the degree of **Master of Science** and hereby certify that it is worthy of acceptance.

Advisor	Signature	Date
Internal Examiner	Signature	Date
External Examiner	Signature	Date
Chair person	Signature	Date

UNDERTAKING

I certify that research work titled "“**The Effect of varying geometry on the amplification of ground motion on zoned earthen dams**”" is my own work. The work has not been presented elsewhere for assessment. Where material has been used from other sources it has been properly acknowledged / referred.

Signature of Student

Yeabsra Tesfaye

ABSTRACT

Stability and safety are very important issues for embankment dams built in seismic regions. Earthquakes impose additional loads on to embankment dams over those experienced under static conditions that could cause settlement and longitudinal and transverse cracking of the embankment, particularly near the crest of the dam. The main objective of this study is to conduct seismic analysis of a zoned earth dam to observe the effect of dam geometry on the amplification of ground motion within the body of the dam. This can be done using GeoStudio which is a finite element based software. A typical dam cross section with fixed slope and different geometric sizes on top of different foundations have been analyzed. Thus real earthquake records are used as input motion with varying peak ground acceleration. The results obtained from the study show that varying the geometry together with the ground motion and peak ground acceleration values have significant effect on the ground motion amplification within the dam body.

Acknowledgment

I would like to express my deepest gratitude to my advisor Dr-Ing -Asrat worku, who has given me the basics during the course works and for his guidance, patience, valuable remarks and wholehearted encouragements from the initiation to the closing of this thesis.

I am also very grateful to Dr. Assie Kemal for providing me with guidance and support especially during the beginning of my thesis and helping me lay the foundation.

I would also like to thank Leamlak Minwuyelet for his guidance and for providing me with his idea.

My heartfelt gratitude goes to Besrat Eshetu for committing to support me from the beginning this thesis work by giving me necessary feedback and his constant encouragement along with impeccable patience.

I also want to give a great thanks to Zetseat Gashaye for going through my work and providing his insights for improvement of this study. This thesis would have been more challenging without all your help.

My appreciation also goes to Rediet Kebede for helping me fix the technical difficulties I faced during this study.

I am beholden to AAiT room 204 staff members for their patience and guidance during the course work. I would like to extend my heartfelt thanks to Ethiopian Roads Authority for granting me the Sponsorship for my study.

Special thanks goes to my dear parents, family and friends who have helped me in one way or another to complete the study.

Table of Contents

List of tables

List of figures

CHAPTER 1 - INTRODUCTION

1 .1. Background

Dams are structures that are widely used for irrigation and power generation purposes. Dams have made an important and significant impact on the development of society and have considerable benefits in different aspects including renewable energy, agriculture and flood control. Among different types of dams, embankments are usually preferred over concrete gravity dams because of different advantages they have over the latter ones: simplicity of the construction, availability of local materials and requirement of fewer number of skilled labors making them the most widely constructed type of dams (Raja and Mashwari, 2016).

As in any structure, stability and safe performance of dams are basic requirements to be attained. Safe performance of dam structures is very crucial since its environmental and economic impairment is severe. Despite the advancement in geotechnical engineering, earthquake still remains one of the main causes of failure for many dams indicating that the area should be given emphasis. Performance evaluation and the stability of earth dams during earthquakes require a thorough dynamic response analysis to determine acceleration, dynamic stresses, and deformations induced in the dam by the seismic forces (Raja and Mashwari, 2016).

Seismic stability of slopes is complicated due to the need to consider the effect of dynamic stresses induced by earthquake shaking and the effect of those stresses on the strength and stress-strain behavior of the slope materials (Kramer, 1996). When earthquake ground motions propagate through embankments, acceleration amplification and permanent deformations can occur potentially resulting in sliding of the soil mass. Dynamic response of the embankments is to be investigated properly for determining these seismic-induced forces and deformations (Kandolkar et al., 2010).

The seismic slope stability can be ascertained by evaluating factor of safety of the dam using pseudo-static approaches which begun in 1920s. The seismic stability of earth structures has been analyzed by a pseudo static approach in which the effect of an earthquake is represented by horizontal and/or vertical acceleration constants (Kramer, 1996).

The pseudo-static method of analysis, like all limit equilibrium methods, provides an index of stability (the factor of safety) without providing any information on deformations associated with slope failure. Since the serviceability of a slope after an earthquake is controlled by deformations, analyses that predict slope displacement provide a more useful indication of seismic slope stability. Since earthquake induced accelerations vary with time, the pseudo static factor of safety will vary throughout an earthquake (Anis and Jawaid, 2016).

If the inertial forces acting on a potential failure mass become large enough that the total (static and dynamic) driving forces exceed the available resisting forces, the factor of safety will drop below 1.0. Newmark (1965) considered the behavior of a slope under such conditions. When the factor of safety is less than 1.0, the potential failure mass is no longer in equilibrium, and consequently, it will be accelerated by the unbalanced force. The situation is analogous to that of a block resting on an inclined plane. Newmark used this analogy to develop a method for prediction of the permanent displacement of a slope subjected to any ground motion. Newmark's sliding block analysis is the simplest method to calculate the permanent sliding displacements of slopes subjected to any ground motion (Anis and Jawaid, 2016).

This study attempts to analyze stress-deformation of seismic slope stability using dynamic finite- element analyses. Seismically induced permanent strains in each element of the finite-element mesh are integrated to obtain the permanent deformation of slope.

1.2. Objectives

1.2.1. General Objective

The main objective of this study is to analyze the effect of height and foundation type of a zoned embankment dam on the amplification of different ground motions.

1.2.2. Specific objectives

Specific objectives that are addressed in this research include:

- To analyze zoned embankment dam profiles using finite element (FE) based software by varying the height, foundation type, ground motion and peak ground acceleration (PGA)
- To determine the extent and location of maximum acceleration (a_{max}) within the dam profiles and
- To determine permanent deformation caused by the maximum acceleration.

1.3. Statement of the Problem

As was discussed in the previous section in relation to pseudo-static analysis approach, there is no exact way of selecting a pseudo-static coefficient and the location of the force for design, yet (Duncan et al., 2014). It seems clear, however, that pseudo-static coefficients should be based on the actual, anticipated level of acceleration in the failure mass; and that should correspond to some fraction of the anticipated peak acceleration. Although engineering judgment is required in all cases, the criteria for the coefficient proposed by Hynes-Griffin and Franklin (1984) and Terzaghi (1950) for the location of the pseudo-static force is commonly taken in the analysis of most slopes. Despite these suggestions, accuracy is an issue with Terzaghi (1950) himself expressing his uncertainties of earthquake effect on slopes, and that a slope could still be unstable even if the computed pseudo-static factor of safety was greater than one having considered the aforementioned criteria for the coefficient and location. Historical and recent earthquake-induced landslides have shown significant shortcomings of the pseudo-static approach (Kramer, 1996).

1.4. Methodology

To meet the objectives of the study, the following steps are followed:

- literature review of seismic response and stability analysis of zoned embankment dams,
- selection of simplified dam model,
- selection of different dam cross-sections,
- selection of ground motion and peak ground acceleration,
- simulation of different dam profiles using GeoStudio software,
- obtain static factor of safety, maximum acceleration within the height of the dam and deformation caused by ground, and
- specify range of maximum acceleration (in terms of pseudo-static coefficient k_h), the point of application of maximum acceleration and deformation.

1.5. Scope

This research investigates the effect of dam height on zoned earth dams in response to earthquake ground motion at a steady-state reservoir condition setting aside rapid drawdown and construction conditions using GeoStudio software package. Since this research is not for a particular dam at a particular site, the range of parameters used for the analysis are genera l(For this reason no attempt is made to analyze every combination of dam dimensions, soil properties, ground motions and peak ground accelerations). The study is restricted to three dam heights, resting on two homogeneous foundations, analyzed using three ground motions scaled to three peak ground acceleration values. Equivalent-linear 2D dynamic analyses with elastic-plastic deformation are conducted for statically stable dam section.

1.6. Organization

This document is organized into five chapters. Chapter 2 deals with definition of embankment dam, failure due to earthquake, and how it is represented in stability analysis. Stress-strain relationship of soils is also presented in this chapter. In Chapter 3, modeling of typical zoned earth dam with appropriate dimension and material assignment is discussed followed by input ground motion and the FE (GeoStudio) software processing. Chapter 4 holds an arranged form of the results from the software output and a discussion that goes with it. Finally, Chapter 5 provides conclusions and recommendations.

CHAPTER 2 - LITRATURE REVIEW

2.1. Embankment dams

Embankment dams are made from mechanically compacted earth fills. There are several types of embankment dams; depending on their designs they have varying degrees of in-built conservatism, usually relating to the degree to which seepage within the dam is controlled by provision of filters and drains, the use of free draining rock fill in the embankment and the control of foundation seepage by grouting, drainage and cutoff construction (Fell et al., 2015). The two most common types of embankment dams are rock-fill and earth-fill dams.

Earth fill dams are composed of suitable soils obtained from borrow areas or required excavation that are spread and compacted in layers by mechanical means. Earth-fill dams may be constructed with homogenous layers (homogeneous dams) or zones of different materials of varying characteristics (zoned-earth dams). Typical zones include a clay core, filter, drain zones and shell materials. Rock-fill dams are constructed from high percentage of rock sand other larger particles. The fill typically drains easily and therefore no drainage layer is required. To prevent seepage, rock-fill dams have an impervious zone on the upstream side of the dam or within the embankment. The impervious zone can be made from a variety of materials including masonry, concrete, plastic, steel pile sheets, timber, or clay (Beadenkopf, 2013).

Earth-fill dams may include a water-tight core and can also be made from asphalt concrete. Dams with this type of core are called concrete-asphalt core embankment dams. Most concrete asphalt dams use rock and/or gravel as the main fill material. These types of dams are considered especially appropriate for areas susceptible to earthquakes due to the flexible nature of the asphalt core (Beadenkopf, 2013).

Earthquakes impose additional loads on to embankment dams over those experienced under static conditions. The earthquake loading is of short duration, cyclic and involves motion in the horizontal and vertical directions. Earthquakes can affect embankment dams by causing settlement and longitudinal and transverse cracking of the embankment, particularly near the crest of the dam. The settlements adversely affect the size of freeboard between the embankment crest and reservoir level which may, in the worst case, result in overtopping of the dam. Internal erosion and piping may develop in cracks. Liquefaction or loss of shear strength due to increase in pore pressures induced by the earthquake may occur in the embankment and its foundations (Fell et al. 2015).

Earthquake loading may result in differential movement between the embankment, abutments and spillway structures leading to transverse cracks that could cause differential settlements that damage outlet works passing through the embankment. Instability of the upstream and downstream slopes of the dam are also one of the main cause of earthquake motion as they bring additional load (Fell et al. 2015).

The potential for such problems depends on the seismicity of the area in which the dam is sited, foundation materials and topographic conditions at the dam site, detailed construction of the dam, and the water level in the reservoir at the time of the earthquake(Fell et al. 2015).

Earthquakes may also result in overtopping of the dam by wave induced in the reservoir in the event of large tectonic movement in the reservoir and by waves due to earthquake induced landslides into the reservoir from the valley sides. The amount of site investigation, design and additional construction measures (over those needed for static conditions) will depend on these factors, the consequences of failure and whether the dam is existing or new (Fell et al., 2015).

2.2. Analysis of inertial instability

2.2.1. Pseudo static coefficient

In the mid-1960s, the state of practice in seismic analysis of earth dams was known as seismic coefficient (pseudo-static) method which is also called pseudo-static analysis. Pseudo-static analysis is the use of a static analysis of the factor of safety against sliding with the addition of a horizontal force to represent the effect of seismic shaking. The selection of a seismic coefficient is based on judgment and experience of slope behavior during past earthquakes, and these coefficients were embodied in seismic design codes. This approach lacked a rational basis for choosing the seismic coefficient, and it did not take into account possible loss of strength and stiffness of the soil as a result of shaking (Marcuson, 1981).

Ambraseys (1960), proposed coefficients based on elastic response analyses of the embankments. Figure 2-1 shows recommended coefficients by Seed and Martin (1966) which are based on maximum elastic response and root mean-square response, and critical damping of 20 percent, together with bands representing typical U.S. practice and the Japanese code (Marcuson, 1981).

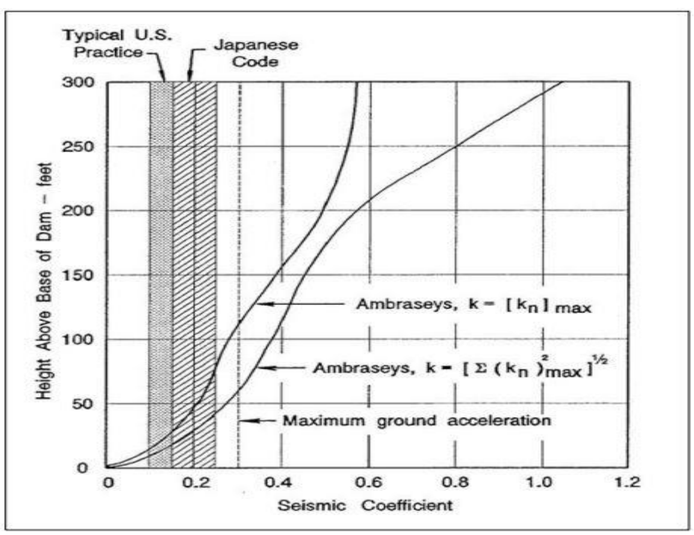

Figure 2-1: Seismic coefficients suggested in 1966 for use in pseudo-static analysis (Seed and Martin, 1966)

The late Nathan Newmark, who served on an advisory board with Taylor for the Corps of Engineers, further developed Whitman's concept and presented a method of analysis in his Rankine Lecture of 1965 (Newmark, 1965). The method, as presented by Newmark assumes rigid-plastic behavior of the embankment during the earthquake, and that the time-history of the earthquake motions is known. The sliding mass is idealized as a rigid block on an inclined plane, which slides on the plane whenever the shearing resistance of the contact is overcome by inertial force due to shaking (Marcuson, 1981).

Various researchers have proposed ways of evaluating static and seismic slope stability and yield acceleration of embankment dams. Usually, a horizontal seismic coefficient (k_h) is either chosen arbitrarily or is selected based on judgment and experience of the behavior of structures during past earthquakes. However, the accuracy and reliability of results mainly depend upon the proper selection of horizontal and/or vertical seismic acceleration coefficients (Kandolka,s.s. et al., 2010). From among the numerous suggestions about the values of seismic coefficients, the most notable ones are the following

- Seed (1979) recommended horizontal seismic coefficient, k_h of 0.10 for sites near faults capable of generating magnitude 6.5 earthquakes and the acceptable pseudo-static factor of safety is of the order of 1.15 or greater. For near-fault sites capable of generating up to 8.5 magnitude earthquakes, a horizontal seismic coefficient, k_h equal to 0.15 was suggested, with the acceptable pseudo-static factor of safety to be 1.15 or greater.
- k_h values suggested by Terzaghi (1950) were 0.10 for "severe" earthquakes, 0.20 for "violent" and "destructive" earthquakes, and 0.50 for "catastrophic" earthquakes.
- Hynes-Griffin and Franklin (1984) estimated that for k_h = 0.5 a_{max}/g and for factor of safety (FS) > 1.0 large deformation will not develop.
- Marcuson (1981) suggested that appropriate pseudo-static coefficients for dams

should correspond to 1/3 to 1/2 of the maximum acceleration, including amplification or de-amplification effect to which the dam is subjected

2.2.2. Pseudo-static Force Location

An issue that arises in pseudo-static analyses is the location of the pseudo static force. Seed (1979) showed that the location assumed for the seismic force can have a small but noticeable effect on the computed factor of safety. Terzaghi (1950) suggested that the pseudo-static force should act through the center of gravity of each slice or through the entire sliding soil mass. This would be true only if the accelerations were constant over the entire soil mass, which they probably are not.

Observed dynamic response of many dams to earthquakes indicate that peak accelerations increase from the bottom to the top of a dam (Makdisi and Seed, 1978). Thus, the location of the resultant seismic force can be expected to be above the center of gravity of the slice

In the case of circular slip surfaces, assuming pseudo-static force will act above the center of gravity will reduce the moment about the center of the circle due to the seismic forces, in comparison to applying the force at the center of gravity of the slice, and the factor of safety would be expected to increase. The assumption that the pseudo-static force acts through the center of gravity of the slice is probably slightly conservative for most dams (Duncun et al., 2014).

2.3. Newmark Sliding Block Analyses

Newmark (1965) suggested a relatively simple deformation analysis based on a rigid sliding block. In this approach, the displacement of a soil mass above a slip surface is modeled as a rigid block of soil sliding on a planar surface. When the acceleration of the block exceeds a yield acceleration, a_y, the block begins to slip along the plane. Any acceleration that exceeds the yield acceleration causes the block to slip and imparts a relative velocity to the underlying mass. The block continues to move after the acceleration falls below the yield acceleration and until the velocity of the block relative to the underlying mass goes to zero. The block will slip again if the acceleration again exceeds the yield acceleration. This stick-slip pattern of motion continues until the accelerations fall below the yield acceleration and the relative velocity drops to zero for the last time. Movements in the upslope direction are neglected since all displacements are assumed to be one way. Limit equilibrium slope stability analyses are used to compute the values of yield acceleration, a_y, used in sliding block analyses. The yield acceleration is usually expressed as a seismic yield coefficient, $k_y = a_y/g$. The seismic yield coefficient is the seismic coefficient that produces a factor of safety of unity in a pseudo-static slope stability analysis.

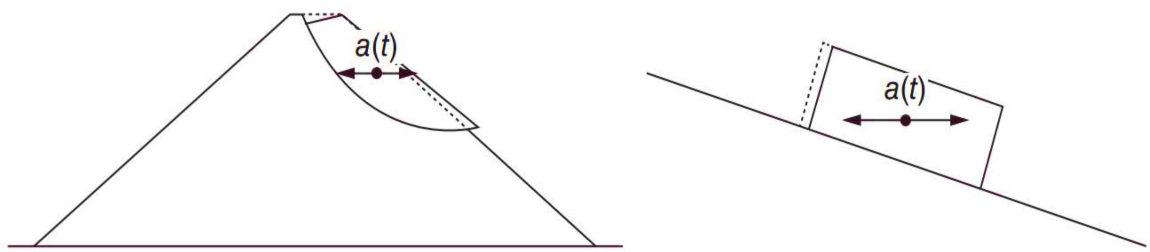

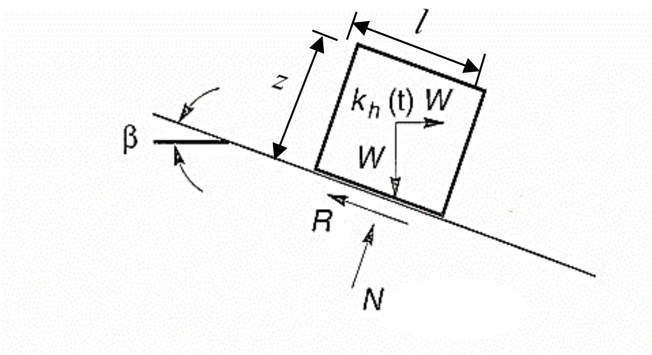

Figure 2-2: Newton's sliding block

Resolving forces perpendicular to slip plane

$$N = W\cos\beta - kW\sin\beta \tag{2-1}$$

Resolving force parallel to slip plane

$$R = W\sin\beta + kW\cos\beta \tag{2-2}$$

Weight of sliding block

$$W = \gamma lz\cos\beta \tag{2-3}$$

Substituting (2-3) in to (2-1) and (2-2)

$$N = \gamma l\cos^2\beta - k\gamma l\cos\beta\sin\beta \tag{2-4}$$

$$T = \gamma lz\cos\beta\sin\beta + k\gamma lz\cos^2\beta \tag{2-5}$$

For the normal and shearing stresses on the slip plane

$$\sigma = \frac{N}{l} = \gamma z\cos\beta\sin\beta - k\gamma z\cos^2\beta \tag{2-6}$$

$$\tau = \gamma z\cos\beta\sin\beta + k\gamma z\cos^2\beta \tag{2-7}$$

Finally, for the factor of safety (total stress)

$$F = \frac{resisting\ force}{driving\ force} = \frac{c+\sigma\tan\phi}{\tau} = \frac{c+(\gamma z\cos\beta\sin\beta - k\gamma z\cos^2\beta)\tan\phi}{\gamma z\cos\beta\sin\beta + k\gamma z\cos^2\beta} \tag{2-8}$$

2.4. Stress-strain relationship of the soil

The stress-strain relationship of soils, particularly granular soil, can be approximated by a hyperbolic curve as illustrated in Figure 2-3. The curve can be defined by two parameters which are the slope at zero strain and the, asymptotes at large strains. In terms of soil properties, the initial slope is the small strain shear modulus G_{max} and the asymptote being the shear strength (GEO-SLOPE International Ltd., 2007).

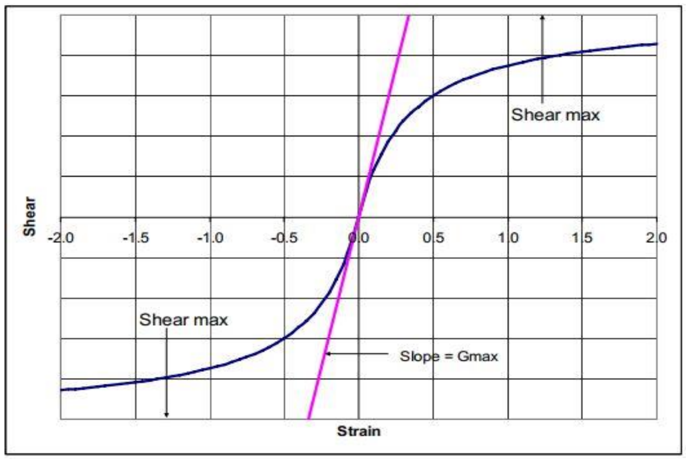

Figure 2-3: Hyperbolic curve relative to τ_{max} and Gmax

When the hyperbolic curve is drawn for both negative and positive shear stresses and strains as in Figure 2-4, the hyperbolic curve is referred to as the backbone.

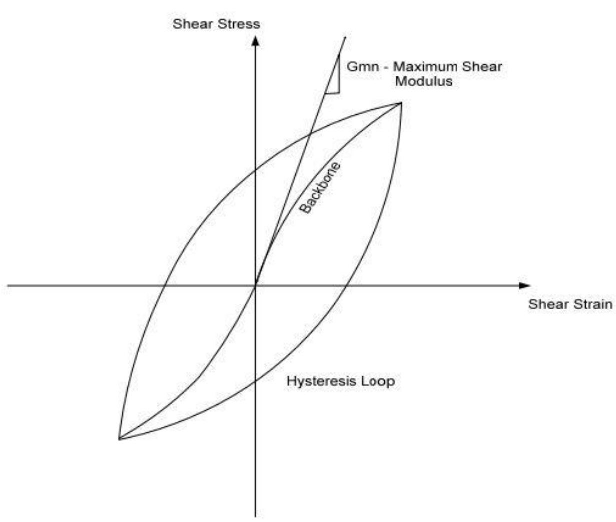

Figure 2-4: Hyperbolic backbone curve

Another key component is that when there is a stress reversal, the shape of the unloading curve is the same as the backbone curve with the exception that the origin moves to the point of the stress reversal. Stated in another way, the shape of the loading, unloading and re-loading curves are all the same. In addition, the curves follow what are known as Masing rules (Kramer, 1996). Only G_{max} and the Mohr-Coulomb shear-strength parameters c' and ϕ' are required soil properties for the hyperbolic model (GEO-SLOPE International Ltd., 2007).

2.4.1. Shear modulus and damping ratio

Seed and Idriss (1970) prepared a proposition of curves of shear modulus and damping ratio for clay, sand and gravely soils and this was later re-analyzed by Seed et al. (1986) as shown in Figure 2-5 and Figure 2-6. A wide variety of procedures, including laboratory and field tests have been used to determine both shear moduli and damping characteristics. Direct determination of stress- strain relationship, forced vibration test, free vibration test, field measurement of wave velocity and analysis of ground response during earth quake are mentioned by Seed and Idriss (1970) as the main procedures.

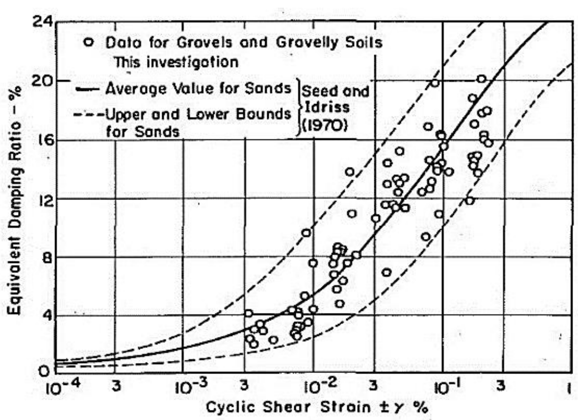

(a)

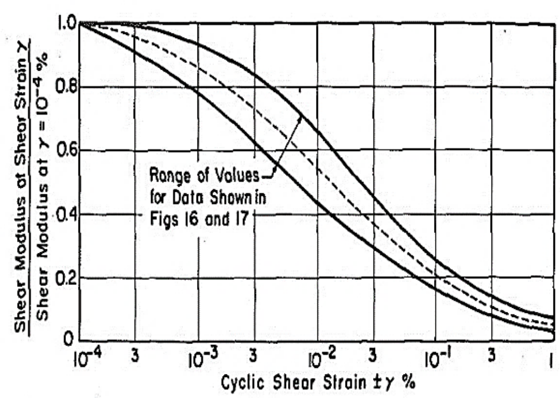

(b)

Figure 2-5: (a) damping ratio curve for gravely soil (b) shear modulus curve for gravely soil

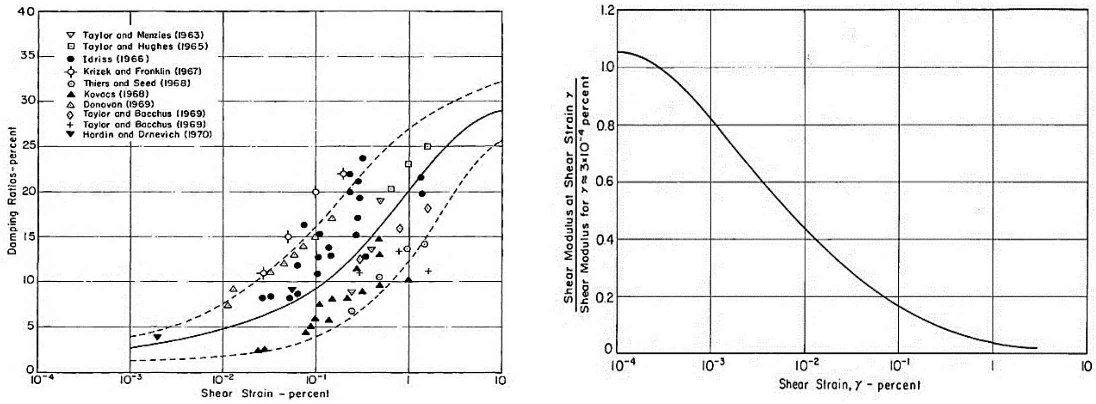

(a) (b)

Figure 2-6: (a) damping ratio curve for clay (b) shear modulus curves for clay

2.5. Related researches

Many Researches on the amplification of ground motion have been done on both particular and more generalized (taking typical cross section and material property) dams.

Shuishen and Liyutan zoned earth dams located in Taiwan were analyzed by Chern (2001), Mamloo dam was also analyzed by Moayed (2008) and zoned rock fill dam located in the seismic zone of northern Greece was analyzed by Anastasiadis (2004). These researches are done to observe the ground motion amplification of a particular dam and no other additional experiments or parametric studies were conducted. Zou (2011) concluded that acceleration amplified factor at the crest (the amplified acceleration divided by the peak ground acceleration) decreases with an increase in height.

Yu (2012) reviewed case histories of earth and rock fill dam behaviors during earth quake and concluded that acceleration amplified factor increases more at the top 1/3 to 1/5 area of the dam. Yu also varying the dam slope gradient has minor effect on the seismic response of the dam. Özener (2014) considered typical cross section and material property of both homogeneous and zoned rock fill dam and implicated that the as dam height increases the amplification decreases and an increase in peak ground acceleration leads to a decrease in amplification. And concerning deformation, Kramer (1996) suggested that a ground motion of short duration may not produce enough load reversals for damaging response to build up in structure , even if the amplitude of the motion is high. Kramer also added that there is reduction of amplitude (acceleration) due to spreading of the energy over a greater volume of material and is reffered to as radiation damping (also as geometric damping and geometric attenuation).

The researchs mentioned above does not include the effect of the foundation on the dam and vise versa.

CHAPTER 3 - MATERIAL MODEL, MATERIAL PROPERTY AND METHODOLOGY

3.1. General Work flow of the study

The study conducted in this research can be summarized by the flowchart shown in Figure 3-1.

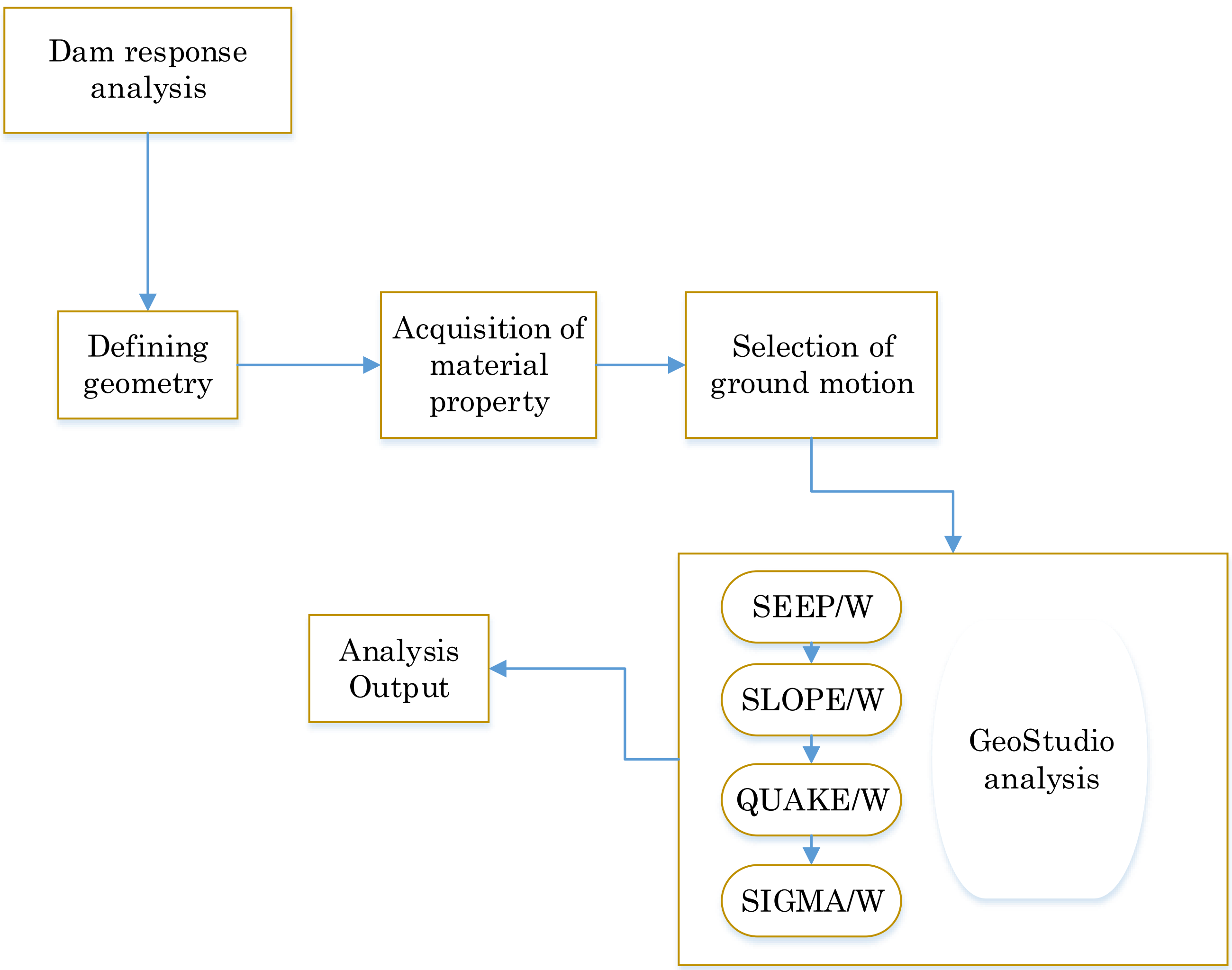

Figure 3-1: General work flow

The flow chart in Figure 3-1 shows the procedure required to accomplish the objective of this study. The chart shows four major parts that are discussed below.

1) Defining geometry – this section involves selecting an acceptable dimension for static stability and to meet seepage criteria of the zoned earth dam and to fulfill the required factor of safety.
2) Assigning of material property – assigning static and dynamic soil properties that represent the type of material used in zoned earth dam.
3) Ground motion selection – this refers to the selection of ground motions that are used as input for the FEM software. Known earthquakes with certain unique behaviors are selected.
4) Software analysis – this part involves analyses of the embankment dam through four integrated sub divisions that perform FEM analysis using different software under the GeoStudio package. Dam cross-section, material property and ground motion are used as input for this section.

3.2. Model and Parts

A finite element model needs a simplified geometry that represents actual field conditions. Including all surface irregularities is unnecessary in most situations, as doing so can cause numerical irregularities in the result which distract from the main overall solution (GEO-SLOPE International Ltd., 2007). Figure 3-2 shows a simplified geometry for a typical zoned earth dam selected for the purpose of this study.

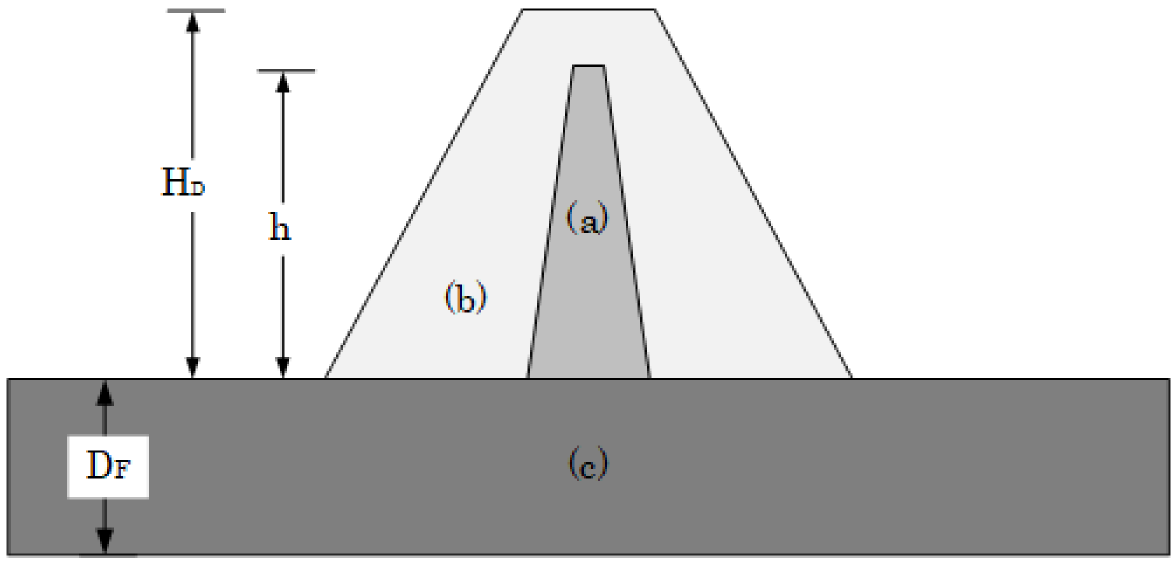

Figure 3-2: Simplified dam Model considered

Zoned embankments take advantage of the availability of various materials. A zoned earth fill dam commonly comprises of a central impervious core flanked by upstream transition zones, downstream filters and drains, and then outer zones or shells composed of gravel-fill, rock-fill, or random-fill, which are considerably stronger than the core. Depending on the gradation of available materials, transition zones may not be necessary (Engomoen et al., 2014). But for the sake of simplicity, this study uses only three zones as shown in Figure 3-2 and described below:-

(a) Earth-fill core - controls seepage through the dam. Mostly constructed out of fine materials like clay, silty clay, and sandy clay (Fell et al., 2015 ; Engomoen et al., 2014). Clay core is used for this study.

(b) Shell - provides stability, commonly free draining to allow discharge of seepage through the dam and prevents erosion. The shell is mostly constructed out of coarse materials such as rock fills (for rock fill dams), sandy gravels and gravely sand (for earth-fill dams) (Fell et al., 2015 ; Engomoen et al., 2014). Sandy-gravel shale is hence used for this study.

(c) Foundation - a material having adequate strength to support the embankment. For this study, two types of foundations are used, a rock foundation and a sandy gravel foundation, to observe the effect of foundation stiffness on dam response.

3.3. Geometry

There is no fixed geometry for a dam. Height depends on the amount of water one wants to retain. While side-slopes depend on the type of soil used, and freeboard depends on the fetch length, climate condition of the area. So it is mostly dependent on location and for what the dam is intended to be used for. Since this study is not about a specific dam, recommended dimensions are taken from literature and common dam designs. Later on it will be checked for seepage and static stability so the dimensions can be acceptable. Each main dimension of the dam is described in this sub-section.

1. **Dam height (H)**

This study is not about a particular dam and there is a need to see the effect of different dam heights on the amplification of ground motion. Basing this study on ICOLD's (1974) definition of large dams (>15 m) as sited by (Fell et al., 2015), three different dam heights of 50m, 150m and 250m are selected with the aim of representing different heights within the "large-dams" category.

2. **Core height (h)**

In zoned dams the core height is usually limited to few meter below the crest. The top of the impervious core should be at or above the maximum reservoir water surface. This is because impervious zones extending to the top of the dam are subjected to damage by desiccation and frost action, which causes loosening and cracking of the soil (Engomoen et al.,2014). For this analysis a core height is taken to be equal to the maximum water surface level. The maximum water level is the total height of the dam minus the freeboard, where the freeboard is the vertical distance between a specified reservoir water surface level and the crest of the dam. Most of the hydraulic failures of earth dams have occurred due to overtopping of dams. Because of this, the freeboard must be sufficient enough so as to avoid any possibility of overtopping (Fell et al., 2015). U.S.B.R (2012) recommends a freeboard greater than 3 percent of the embankment height to avoid potential seismic failure. A freeboard board of 4m, 6m and 8m and a corresponding core heights of 46m, 144m and 242m for 50m, 150m, and 250m respectively have been used for the models.

3. **Foundation depth (D_F)**

Soils to be homogeneous for a longer depth is uncommon. There will be different layers of different soils as a dam foundation and the depth of investigation for the different dam height will defer. However, to iterate mesh size and to observe the effect of the foundation on different dam heights, the foundation depth must be fixed for every dam height. After observing a foundation depth from other studies on constructed dams an average depth of 50m has been used for this study.

4. **Side boundary**

In order to minimize the disturbance due to the boundary-related wave reflection, an appropriate distance of the side boundary from the dam toe must be fixed; from different literature and research report, it is usually taken to be 2-3 times the dam height (Seged and Haile, 2010; Gikas and Sakellariou, 2008; Gopal and Kumar, 2014). The side boundaries are taken to be 3 times the dam height for this study.

5. **Crest width**

The crest width has no appreciable influence on the overall stability of a dam and is determined by the minimum practicable width for construction purposes, and possible other requirements (Fell et al., 2015). Any earth fill zone should be at least 3 m wide at the crest to allow compaction with normal rollers. No dam should have a crest width less than 3 m so as to allow vehicular access for maintenance purposes (Fell et al. 2015).

In this analysis core top widths of 3m, 4m and 5m are taken for the 50m, 150m and 250m dam heights, respectively. Filters are mostly used in zoned dams, the width of the filter should be considered and added to the core top width to give the overall crest width, taking 2.5m, 3m and 3m for the 50m, 150m, and 250m dam heights respectively in both sides of the core (Fell et al. 2015; United States Department Of Interior, 1987). By this the overall crest width would be 8m, 10m and 11m for 50m, 150m and 250m dam heights respectively.

6. **Slope**

The upstream and downstream side-slopes should be designed as to be stable under worst condition of loading. These critical conditions occur for the upstream slope during sudden draw-down of reservoir, and for the downstream slope during steady seepage under full reservoir. The upstream and downstream slopes should be flat enough, so as to provide sufficient base width at the foundation level, such that the maximum shear stress developed remains well below the corresponding maximum shear strength of the soil (Garg, 1980) . Fell (2015) recommended base line minimum acceptable factors of safety of 1.5 for downstream slope when reservoir is at full supply level.

In earth and rock fill dams, inclination of upstream slope can range from very flat (1V:3H) to very steep (1V: 1.4H) and those of a downstream slopes from 1V:2.5 H to 1V:1.2H (Khanna et al., 2017). The side-slopes depend upon various factors such as the type and nature of the dam, foundation material, height of dam, and dam material property. The recommended values of side slopes of 3H: 1V for upstream and 2.5H: 1V for downstream are given by Terzaghi (Garg,1980). Slopes of 2.5H: 1V for the downstream and 3H: 1V for the upstream side of the dam are used in this analysis.

If the thickness of the core inside an earth dam is increased beyond a critical value, it can cause a decrease in stability of downstream slope. A critical core thickness at the bottom of the dam ranges from 50% to 150% of dam height for different values of relative strength, pore water ratio and height of dams (Khanna et al., 2017). A recommended Slope of 0.3H: 1V has been used for the core which makes the core thickness 60% of the dam height.

3.4. Finite Element Formulation in GeoStudio

Integrated GeoStudio software allows us to combine multiple analyses using different products into a single modeling project. New analyses can be easily created by cloning an existing analysis and adjusting its properties. When the model is ready to be analyzed, GeoStudio solves the analyses in the appropriate order. The result from one analysis can be used as an input for another one. This kind of approach can be used to model construction sequences, establish initial conditions, and perform sensitivity analyses, model complex time sequences and more manageable analysis (GEO-SLOPE International Ltd., 2007). GeoStudio contains eight analysis types that can be integrated with one another, out of these, four have been used for this study:

- SEEP/W- for the analysis of seepage and identification of phreatic line,
- SLOPE/W- for analyzing the static slope stability of the dam,
- QUAKE /W- to analyze the static load effect and dynamic response of the dam,
- SIGMA /W- to analyze the deformation caused by the ground motion.

Each analysis has been used according to the GeoStudio manual is briefly discussed in the following subsection (GEO-SLOPE International Ltd., 2007).

3.4.1. Seepage analysis using SEEP/W

Flow quantity is often considered to be the key parameter in quantifying seepage losses from a reservoir or determining the amount of water available for domestic or industrial use. The pore-water pressure, whether positive or negative, has a direct bearing on the shear strength and volume change characteristics of the soil. SEEP / W is based on the following formulation:

$$\frac{\partial}{\partial x}\left(k_x \frac{\partial H}{\partial x}\right) + \frac{\partial}{\partial_y}\left(k_y \frac{\partial H}{\partial y}\right) + Q = \frac{\partial \theta}{\partial t} \tag{3-1}$$

Where:

H = total head

k_x = hydraulic conductivity in the x-direction

k_y = hydraulic conductivity in the y-direction

Q = applied boundary flux

θ = volumetric water content

t = time

The hydraulic conductivity is a function of volumetric water content, which in turn is some function of pore-water pressure. The ability of a soil to transport or conduct water under both saturated and unsaturated conditions is reflected by the hydraulic conductivity function (GEO-SLOPE International Ltd., 2007).

3.4.1.1. Analysis Types

There are two fundamental types of finite element seepage analyses: steady-state analysis and transient analysis. In steady-state analysis the pore pressure condition is estimated for long term steady-state situation. Transient seepage analysis, on the other hand, is carried out in a changing condition of pore-water pressure. It is changing because it considers how long the soil takes to respond to the user specified boundary conditions.

Dams experience steady-state seepage for long portion of their life time, hence the probability of experiencing an earthquake will be higher within this period. This study assumes the dam to be in steady-state condition.

3.4.1.2. Material models and properties

There are four different material models to choose from when using SEEP/W. A summary of two of the models and the required soil properties are given below.

Material models in SEEP/W

"Saturated-only" and "Saturated/Unsaturated" model are the two main material models in SEEP/W. The "Saturated-only" soil model is very useful for quickly defining a soil region that will always remain below the phreatic surface, but it should not be used for soils that will at some point during the analysis become partially saturated. If this model is considered, it would mean that the unsaturated zone can transmit the water at a similar rate as that of a saturated soil. This will result in an overestimation of flow quantity and an unrealistic water table. If there is any doubt about which model to choose for a soil region, one should select the "Saturated/Unsaturated" model (GEO-SLOPE International Ltd., 2007) soil properties required for saturated/unsaturated are listed as follows:-

- Hydraulic saturated conductivity (k_{sat})
- Saturated water content
- Coefficient of compressibility(m_v)

This study uses Saturated/Unsaturated material model since it has unsaturated zone above the phreatic line.

3.4.2. Slope stability analysis using SLOPE/W

SLOPE/W is a limit equilibrium method software package and has different methods available for slope stability analysis. The differences between the methods are the equations of statics that are included and satisfied, whether the interslice forces are included and the assumed relationship between the interslice shear and normal forces.

3.4.2.1. Analysis type

Limit equilibrium analyses applied in practice should at the very least use a method that satisfies both force and moment equilibrium such as the Morgenstern-Price or Spencer method. With software such as SLOPE/W, it is just as easy to use one of the mathematically more rigorous methods as to use the simpler methods that only satisfy some of the statics equations. Simpler methods that do not include all interslice forces and do not satisfy all equations of equilibrium sometimes can err on the unsafe side. This methods are included in SLOPE/W for "historic reasons and teaching purposes" (GEO-SLOPE International Ltd., 2007).

There are around 14 methods to calculate factor of safeties in SLOPE/W; among these methods Morgenstern-Price and Spencer methods include all interslice forces and satisfy all equations of statics. The Morgenstern-Price method considers both shear and normal interslice forces, satisfying both moment and force equilibrium and allows for a variety of user-selected interslice force function, whereas Spencer method assumes a constant interslice force function. Hence, Morgenstern-Price method has been used in the present study.

How the interslice shear forces are handled and computed is a fundamental point. The Morgenstern-Price and General Limit equilibrium (GLE) methods allow for user-specified interslice functions. Some of the functions available are the constant, half-sine, clipped-sine, trapezoidal and data-point specified. The most commonly used functions are the constant and half-sine functions (GEO-SLOPE International Ltd., 2007).

SLOPE/W (2007) by default uses the half-sine function for the Morgenstern-Price and GLE methods. The half-sine function tends to concentrate the interslice shear forces towards the middle of the sliding mass and diminishes the interslice shear in the crest and toe areas. Hence, the half-sine function method has been used in the present study.

3.4.2.2. Material models and properties

Out of 14 material models presented in SLOPE/W, two are used for stability analysis. Mohr-Coulomb for the soil and Bed Rock-Impenetrable for the rock.

1. **Mohr-Coulomb model**

The most classic way of describing the shear strength of geotechnical materials is by Coulomb's equation which is:

$$\tau = c + \sigma_n \tan\phi \qquad (3\text{-}2)$$

Where:

τ = shear strength

c = cohesion

σ_n = normal stress on shear plane

ϕ = angle of internal friction

This equation represents a straight line on a shear strength versus normal stress Plot as shown in Figure 3-3 .The intercept on the shear strength axis is the cohesion (c) and the slope of the line represents the angle of internal friction(ϕ).

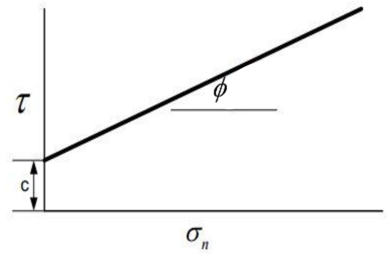

Figure 3-3: Graphic representation of coulomb shear strength equation

The strength parameters c and ϕ can refer to total strength parameters or effective strength parameters. SLOPE/W makes no distinction between these two sets of parameters. The user must decide which set is appropriate for a particular analysis. From a slope stability analysis point of view, effective strength parameters give the most realistic solution, particularly with respect to the position of the critical-slip surface. When using only undrained strengths in a slope stability analysis, the position of the slip surface with the lowest factor of safety might not necessarily be close to the position of the actual slip-surface if the slope should fail (GEO-SLOPE International Ltd., 2007).

Soil properties required for the model

- Unit weight
- Cohesion
- Angle of internal friction
- Volumetric water content

2. Bed Rock-Impenetrable model

The Impenetrable strength option is really not a strength model, but a flag for the software to indicate that the slip-surface cannot enter this material. It is an indirect mechanism for controlling the shape of trial slip-surfaces. This rock model type is also sometimes referred to as bedrock (GEO-SLOPE International Ltd., 2007).

3.4.3. Dynamic analysis using QUAKE/W

This topic discusses the properties that can be used in QUAKE/W to describe the soil. Generally, there are two groups of properties in this context; one is related to the soil stiffness and the other group is related to the generation of excess pore-pressures. The most common soil property in a dynamic analysis is the shear modulus, G. There are several ways in QUAKE/W to specify G and how G is affected by cyclic stresses. Closely related to the soil stiffness is damping which is the soil's ability to dissipate energy associated with seismic waves. Many of the properties related to the generation of excess pore-pressures are not constants, but they are functions of various variables (GEO-SLOPE International Ltd., 2007).

3.4.3.1. Analysis Type

There are basically four types of analyses available in QUAKE/W

- Initial Static
- Equivalent Linear Dynamic
- Equivalent Linear PWP Only
- Nonlinear Dynamic

Static loading of the dam is considered in "Initial static" analysis. On the other hand, "Equivalent Linear Dynamic" analysis is used for dynamic analyses. If the user wants to re-compute the magnitude of excess pore-pressure without repeating the "Equivalent Linear dynamic" analysis, "Equivalent linear PWP Only" analysis can be selected. "Nonlinear dynamic" analysis requires additional material properties and/or parameters which makes it difficult to define in this study, since it is not for a particular site provided with soil investigation and laboratory results.

Out of the four analysis, this study uses initial static and equivalent linear dynamic analysis type of analysis and discussed as follows.

1. **Initial static**

In a QUAKE/W analysis it is always necessary to establish the initial insitu stress conditions before conducting dynamic analysis. Material properties like the shear modulus (G) are usually functions of the effective stress in the ground. Other variables like the Cyclic Stress Ratio are based on the initial effective stresses. Consequently, it is essential to know the initial state of stress in the ground before starting the dynamic analysis. Establishing the static insitu stresses is a separate step in QUAKE/W. In an initial static analysis, QUAKE/W uses the specified Poisson's ratio (υ) and a specified total unit weight. All other specified soil properties, including the soil stiffness (G) are considered not in the Initial Static analysis as this context is limited with static condition (GEO-SLOPE International Ltd., 2007).

2. **Equivalent Linear Dynamic**

Performing a dynamic analysis is the main essence of using QUAKE/W. It is that part of the analysis that models the response of an earthen structure to some kind of oscillating or sudden impulse force – forces such as those that arise from earthquake shaking or blasting. In relation to earthquakes, the dynamic driving forces are the seismic forces associated with earthquake shaking. A time-history can be specified for the horizontal and vertical directions (GEO-SLOPE International Ltd., 2007).

QUAKE/W 2007 is formulated in such a way that the motion of the structure or domain is relative to some kind of specified displacement. Often a good portion of the boundary is specified as being fixed. For all QUAKE/W analyses, there must be specified displacements in order to compute a solution. It is numerically not possible to obtain a finite element solution if there are no specified displacements (GEO-SLOPE International Ltd., 2007). The left and right boundaries of the foundation are constrained in the vertical direction, to allow a horizontal free movement of the soil along with the ground motion, and the bottom is fixed while performing this analysis.

3.4.3.2. Material model and properties

There are three main different material models to choose from when using QUAKE/W.

- Linear model
- Equivalent-Linear model
- Non-linear model

Linear-elastic material properties generally do not produce realistic dynamic responses for actual field problems for the Treating the soils as linear-elastic usually results in amplifications that are too high. Non-linear analyses, using either the Equivalent-linear or truly Non-Linear formulation, are required to obtain meaningful responses from a dynamic analysis of actual field problems (GEO-SLOPE International Ltd., 2007).

Out of the three material models equivalent linear model is used for this study. Equivalent Linear model starts a dynamic analysis with the specified soil stiffness. QUAKE/W (2007) steps through the entire earthquake record and identifies the peak shear strains at each Gauss numerical integration point in each element. The shear modulus is then modified according a specified G reduction function and the process is repeated. This iterative procedure continues until the required G modifications are within a specified tolerance.

Soil properties required

- Unit weight, Poisson's ratio, c' and ϕ'
- Damping ratio constant or function
- k_a and k_s functions
- Pore-water pressure function
- G reduction function
- G_{max} constant or function

3.4.3.3. Mesh generation

Discretization or meshing is one of the three fundamental aspects of finite element modeling, where the other two are defining material properties and boundary conditions. Discretization involves defining geometry, distance, area, and volume. It is the component that deals with the physical dimensions of the domain (Rao, 2004).

In GeoStudio (2007), all meshing is fully automatic. When a geometric region or line is initially drawn it is by default un-meshed. A default mesh is generated for the soil regions when one first uses the Draw-Mesh Properties command, with a modification option. Mesh density can be specified as a real length unit, as a ratio of the global mesh size, or as the number of divisions along a line edge. Generally, however, it is recommended to limit altering the mesh to changing the global density and then, if necessary, at a few limited locations where finer or coarser density is needed (GEO-SLOPE International Ltd., 2007).

Out of 5 mesh types and patterns available in the Geo-Studio package, the following two are widely used and fits the model for this study.

1. Structured mesh

It is called structured mesh because the elements are ordered in a consistent pattern and are of only two shapes and size. A structured mesh for a non-symmetrical geometry shape requires that several soil regions are created and the meshing is controlled within each region. This is likely to accomplish more work and will not yield a significant improvement in results. A structured mesh is created using either a rectangular grid of quads or a triangular grid of quads/triangles (GEO-SLOPE International Ltd., 2007).

2. Unstructured quad and triangle mesh

A fully structured mesh may require several regions to be defined so that one can control the meshing at a detailed level in order to maintain structure. GeoStudio has meshing pattern available that will automatically generate a well-behaved unstructured pattern of quadrilateral and triangular elements. GeoStudio manual recommends this mesh option should be the first one to choose as it will meet the needs in most cases (GEO-SLOPE International Ltd., 2007).

By the recommendation of the software manual and by observing what is fit for the shape of the dam, the unstructured quad and triangle mesh has been used for this study as shown in the Figure 3-4 .

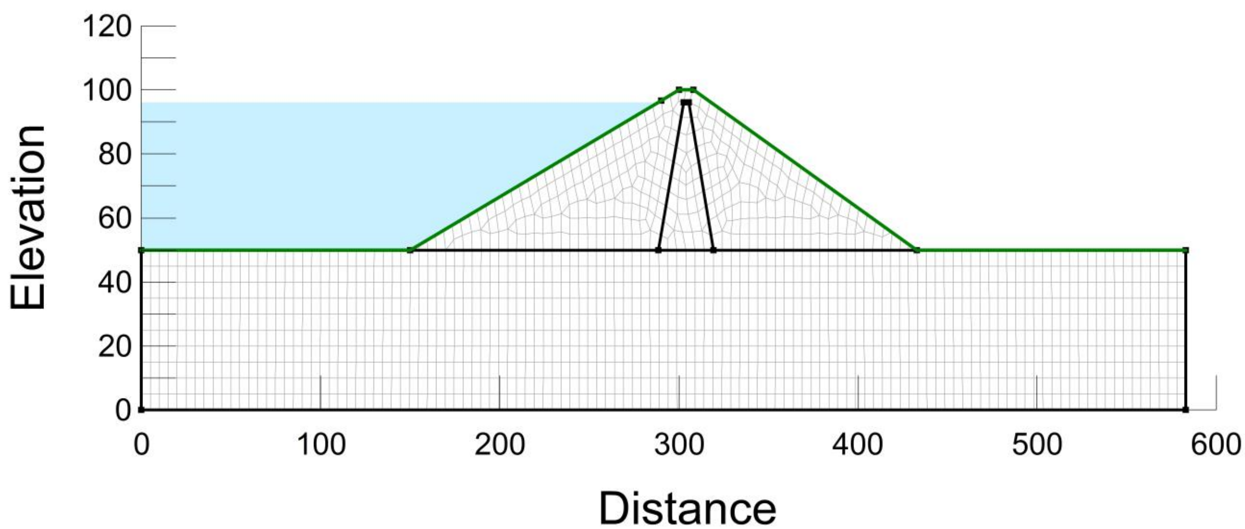

Figure 3-4: Unstructured quad and triangle mesh

An appropriate finite element mesh is problem-dependent and consequently, there are no hard and fast rules for how to create a mesh. In addition, the type of mesh created for a particular problem will depend on the experience and creativity of the user. However, according to GeoStudio 2007 manual there are some broad guidelines that are useful to follow (GEO-SLOPE International Ltd., 2007).

The size of an element directly influences the convergence of the solution directly and hence has to be chosen with care. Although an increase in the number of elements generally means more accurate results for any given problem, there will be a certain number of elements beyond which the accuracy cannot be improved by any significant amount. Furthermore, the use of elements of smaller size will also mean more computational time as more elements implies more degrees of freedom to the process, which will demand more computer memory (Rao, 2004).

It is recommended to use as few elements as possible at the start of an analysis. It is seldom necessary to use more than 1000 elements to verify concepts and get a first approximate solution. QUAKE/W modeling and analysis can be unmanageable if the mesh gets too large. There is not a specific limit in QUAKE/W on mesh size, but for practical reasons meshes generally should not be much greater than about a 1000 elements (GEO-SLOPE International Ltd., 2007). The mesh number should be selected to answer a specific question, and it should not include features that do not significantly influence the system behavior. This is particularly true for a multi-time step dynamic analysis (GEO-SLOPE International Ltd., 2007) .

Having the recommendations in mind, it was appropriate to find the balance between the number of elements and the computational time for the model used in this study. Six samples were selected, a typical ground motion of higher and lower PGA values, were analyzed in QUAKE/W after going through both SEEP/W and SLOPE/W analyses with the same property and size but different number of elements. Table 3-1 shows the trial mesh setting used to compare number of elements and computational time.

Table 3-1 - Mesh setting for each height of the dam.

Dam Height	Global Element size	Number of Nodes	Number of Elements	Time taken for QUAKE/W analysis
50m	5m	1603	1529	20min-40min
	3m	4326	4145	4hr-5hr
150m	10m	1683	1493	20min-40min
	6m	4369	4138	4hr-5hr
250m	15m	1556	1387	20min-40min
	9m	4149	4149	5hr-6hr

The results for maximum acceleration and their respective locations in the analysis with higher number of elements were identical to that of the lower number of elements. However, higher number of elements took longer computational time, therefore mesh that is generated by setting the smaller number of elements is used for this study.

3.4.3.4. Time step

Stepping through the acceleration time history is inherent to the direct integration method used in the QUAKE/W formulation. Due to the dramatic, very sudden changes in motion it is necessary to step though the time history in small steps.
Earthquake shaking often lasts a few seconds and to capture all the characteristics of the motion, the time steps must be fractions of a second. A typical value is two hundredths (0.02) of a second. This consequently results in a large number of time steps (GEO-SLOPE International Ltd., 2007).

Smaller time steps are more accurate, but require considerably more computing time and can also produce substantially more data. As with all numerical analyses, it necessary to try to maintain a balance between numerical objectives and practical consequences such as computing time and the volume of data created (GEO-SLOPE International Ltd., 2007).

There are no firm rules on selecting time step sizes. Conceptually, the time steps should be such that most of the peaks and sudden changes are approximately captured. To assists with setting up an appropriate time integration sequence, QUAKE/W has a feature that makes it possible to develop the time integration scheme from the earthquake record. This is a very useful feature and the recommended procedure unless there is some other compelling reason to develop an alternate time stepping sequence. The specified change in time (time step) integration should not be longer than the time interval in the available earthquake record (GEO-SLOPE International Ltd., 2007). For instance, the acceleration data of Hachinohe record is available at an interval of 0.01 second, hence the time step used is 0.01 sec.

3.4.4. Deformation analysis using SIGMA/W

SIGMA/W is a finite element software product that can be used to perform stress and deformation analyses of earth structures. SIGMA/W includes six different soil constitutive models:-

- Linear-Elastic
- Anisotropic Linear-Elastic
- Nonlinear Elastic (Hyperbolic)
- Elastic-Plastic (Mohr-Coulomb)
- Soft Clay - Modified Cam-Clay (Critical State)

For each of these models, the behavior will be different depending on whether one is assigning the model to a total stress, effective stress with no pressure change, or effective stress with pore-water pressure change categories. SIGMA/W can be used to compute stress-deformation with or without the changes in pore-water pressures that arise from stress state changes. The most common application of SIGMA/W is to compute deformations in earthworks such as foundations, embankments, excavations and tunnels (GEO-SLOPE International Ltd., 2007)

3.4.4.1. Analysis Type

Dynamic deformation analysis

GeoStudio has the ability to link SIGMA/W with the output from a QUAKE/W dynamic analysis. An already solved analysis must be selected for an output stress when choosing this analysis type. The SIGMA/W model will then determine the necessary time stepping scheme such that an incremental load is applied for every change in saved output of the source file. SIGMA/W computes an incremental load vector based on the stress difference between two time steps. Each load step may produce some elastic strains and some plastic strains. It is the accumulation of the plastic strains and deformations that are measure of the permanent deformation (GEO-SLOPE International Ltd., 2007) .

3.4.4.2. Material model and properties

Elastic –Plastic model

The Elastic-Plastic model in SIGMA/W describes an elastic, perfectly-plastic relationship. A typical stress-strain curve for this model is shown in Figure 3-5. Stresses are directly proportional to strains until a yield point is reached. Beyond the yield point, the stress-strain curve is perfectly horizontal.

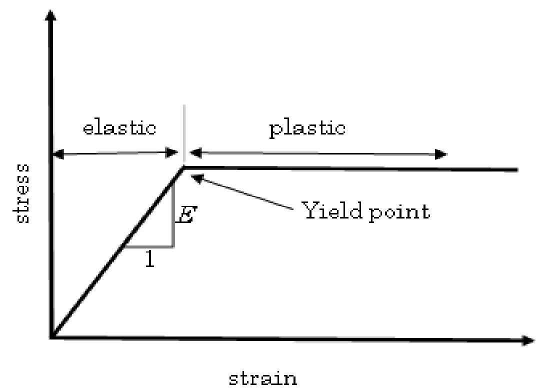

Figure 3-5: Stress-Strain graph for young modulus

Soil parameters required

- Cohesion
- E-modulus
- Unit weight
- Angle of internal friction
- Poisson's ratio
- Dilation angle

3.5. Soil Properties

Every analysis discussed previously mention soil parameter requirements. Since this study is not about a specific site, the soil properties that one chooses should be reasonable and representative of the soil type used. This properties are gathered from different engineering references and presented in this subsection.

3.5.1. Definitions of soil properties

1. **Coefficient of compressibility**

The coefficient of volume compressibility is the slope of the volumetric water content function in the positive pore-pressure range .In physical terms it describes how much a saturated soil volume will swell or shrink for a given change in pore pressure (GEO-SLOPE International Ltd., 2007).

2. **Hydraulic conductivity**

The ability of a soil to conduct water under both saturated and unsaturated conditions is reflected by the hydraulic conductivity function (GEO-SLOPE International Ltd., 2007).

3. **Volumetric water content function**

The volumetric water content function describes the capability of the soil to store water under changes in matric pressures. It describes what portion or volume of the voids remain water filled as the soil drains. Saturated water content is used as an input to generate the function in SEEP/W (GEO-SLOPE International Ltd., 2007).Figure 3-6 shows the volumetric water content verses the matric suction graph of each materials used.

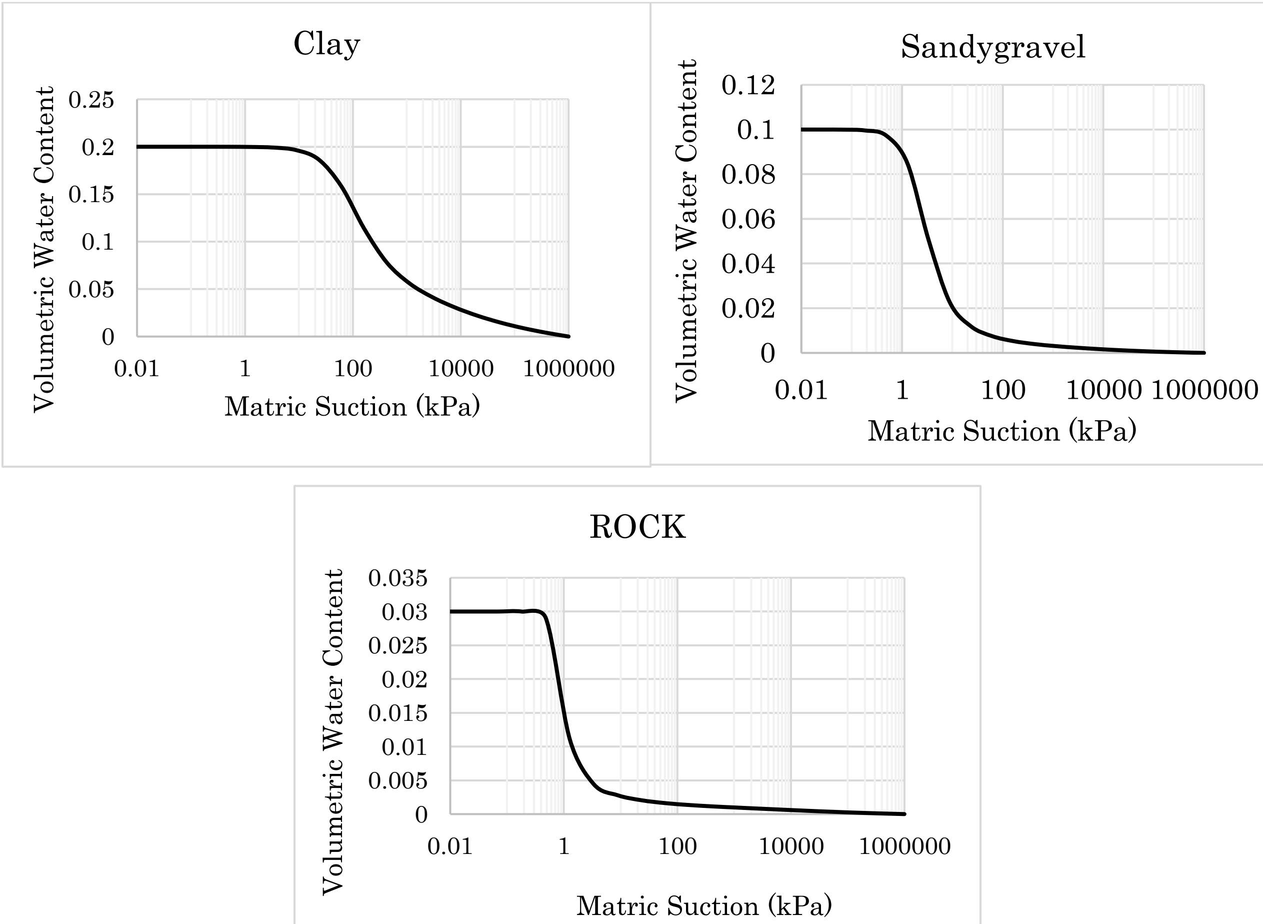

Figure 3-6: Volumetric water content verses Matric suction graph

4. Shear strength

Shear strength of a soil is defined as the maximum resistance to shearing stresses which can be mobilized. Shear strength is usually quantified through two shear strength parameters:

- apparent cohesion, c, essentially arising from the complex electrical forces binding clay-size particles together;
- Angle of shearing resistance, ϕ, developed by interparticle frictional resistance and particle interlocking.

Steady-state, reservoir full analysis is expressed in terms of effective stress shear strength parameters c' and ϕ'. Total stress parameters, c and ϕ, are suitable only for a short-term and approximate analysis (Novak et al., 2007). The majority of dam embankment design is based on peak drained effective strength parameters (Fell et al., 2015).

Due to high compaction effort made during construction of zoned dams, higher values of c' and ϕ' are considered that corresponds to stiffness of the material. Cohesion assigned for sandy gravel material is considered to prevent tumbling of sandy gravel material at the upstream and downstream face of the dam.

5. **Soil unit weight**

The sliding mass weight or gravitational force is applied by assigning the soil a unit weight. The slice cross-sectional area multiplied by the specified unit weight determines the weight of the slice. SLOPE/W is formulated on the basis of total forces; and the unit weight consequently needs to be specified as the total unit weight. Unit weight of the soil is the total weight of the soil divided by total volume. SLOPE/W allows for a separate unit weight for the soil above the water table, but the use of this parameter is seldom necessary (GEO-SLOPE International Ltd., 2007).

Factor of safety calculations are not very sensitive to the unit weight. If the slice weight increases, the gravitational driving force increases, but the shear resistance also increases because of a higher normal at the slice base, and vice versa. Therefore, defining different unit weights above and below the water table usually has little effect on the resulting factor of safety (GEO-SLOPE International Ltd., 2007).

3.5.2. Values of soil properties taken for the analysis

The soil properties are determined by taking average values from the ranges of values found from reference literature that are provided in Table 3-2.

Table 3-2: Input material property

	Dam			
	Core	Shell	Foundation	
PROPERTY	Clay	Sandy Gravel	Rock	
k-Permeability [m/s]	1.00E-10	1.00E-04	1.00E-13	Briaud, (2013); Novak et al. (2007) ; Budhu, (2010); Bowles (1997) ; United states Department of
Saturated Water content (m^3/m^3)	0.2	0.1	0.03	Novak et al. (2007); United states Department of interior (1987)
m_v**-coefficient of compressibility[1/kPa]**	0.00015	0.000075	0	Novak et al. (2007)
γ **-Unit weight[kN/m³]**	18	20	25	Budhu, (2010); Bowles (1997) ; Novak et al. (2007)
c **-Cohesion[kPa]**	15	5	33	Briaud, (2013);Novak et al. (2007);Bowles (1997); Pariseau, (2006)
ϕ **-Angle of internal friction[°]**	20	35	30	
υ **-Poisson's ratio**	0.4	0.3	0.2	Briaud, (2013);Budhu, (2010);Bowles (1997) ;Pariseau, (2006)

3.5.3 Dynamic soil properties

1. **Shear modulus [G_{max}]**

The maximum/initial shear modulus is referred to as G_{max}. It is considered to be a small-strain shear modulus and therefore the maximum value for a particular soil and consequently the designation G_{max}.

It is much more common and realistic to define G_{max} as a function of the stress state in the soil. Generally, the soil stiffness increases with increasing in confining or overburden stress. To capture this behavior, G_{max} values in QUAKE/W can be specified as functions (GEO-SLOPE International Ltd., 2007).

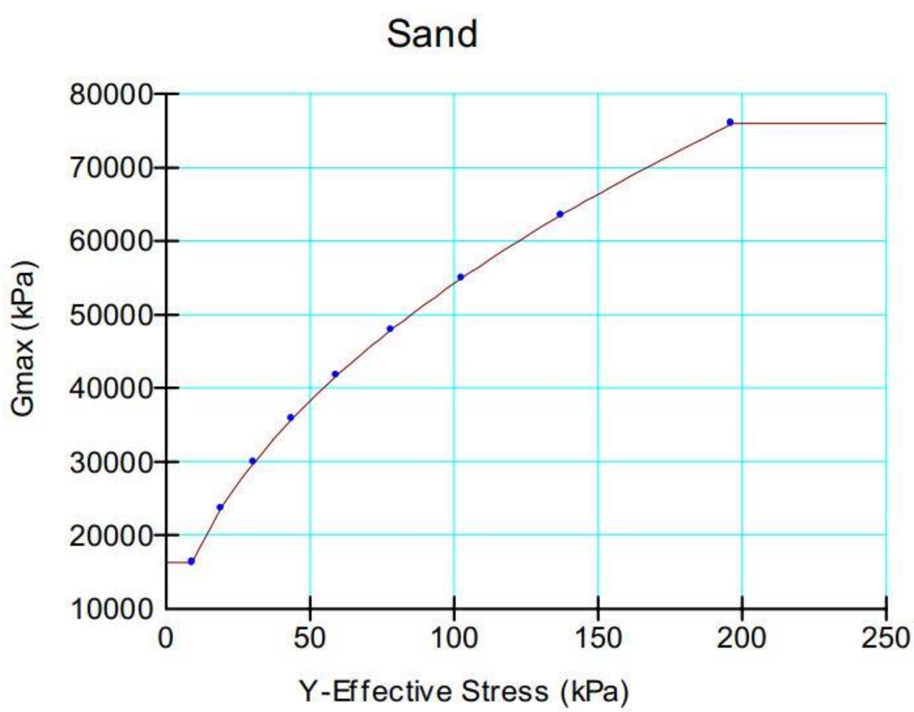

Figure 3-7: Typical G_{max} function of granular soil

Figure 3-7 shows a typical G_{max} function and while defining G_{max} as a function, it is possible to insert the minimum G_{max} value. Which in the case of a dam cross section means the G_{max} value at the crest, that hasn't been stressed with any over burden pressure. As it can be seen in Figure 3-7 the short straight line as the vertical effective stress approaches to zero. This is a useful feature for limiting or cropping the function which makes it possible for user to control the minimum G_{max} value that will be used in the analysis. The increase in G_{max} due to over burden pressure starts from the minimum G_{max} given (GEO-SLOPE International Ltd., 2007).

i. Granular soils

For granular soils the sample functions for the maximum shear modulus are based on the following equation

$$G_{\max} = k\sqrt{\sigma'_m} \tag{3-3}$$

Typical soil modulus (K) numbers have been published for mean stresses. So to use the published values, QUAKE/W estimates the G_{max} function using an approximate mean stress computed as follows:

$$\sigma'_m = \frac{\sigma_v + k_o\sigma_v + k_o\sigma_v}{3} \tag{3-4}$$

Where σ_v is the depth is times the unit weight of the soil (overburden). k_o is the at-rest earth pressure coefficient or the insitu ratio of $\frac{\sigma_h}{\sigma_v}$.

ii. Cohesive soils

Based on the works by Hardin & Drnevich (1972), Hardin (1978) and Mayne & Rix (1993), the G_{max} of cohesive soils can be estimated from,

$$G_{\max} = 625\left(\frac{1}{0.3+0.7e^2}\right)(OCR)^k\sqrt{P_a\sigma'_m} \tag{3-5}$$

Where e is the void ratio, OCR the over-consolidation ratio and k an exponent related to the soil plasticity index PI and σ'_m is as defined in Equation (3-3).

The k exponent is computed from,

$$k = \frac{PI^{0.72}}{50} \tag{3-6}$$

QUAKE/W can estimate the G_{max} function by specifying a depth value for a function stress range together with values for OCR, e, PI, and k_o.

Table 3-3: Initial G_{max} value

	Dam			
	Core	**Shell**	**Foundation**	
PROPERTY	**Clay**	**sandy gravel**	**Rock**	
Initial $\mathbf{G_{max}}$	25Mpa	250Mpa	(Constant) 30000MPa	Briaud(2013);Pariseau (2006);Budhu (2010)

G_{max} functions

The graphs presented in Figure 3-8,Figure 3-9 ,Figure 3-10 and Figure 3-11 are G_{max} functions generated by the software according to their height, soil type and initial G_{max} value that are used for this analysis.

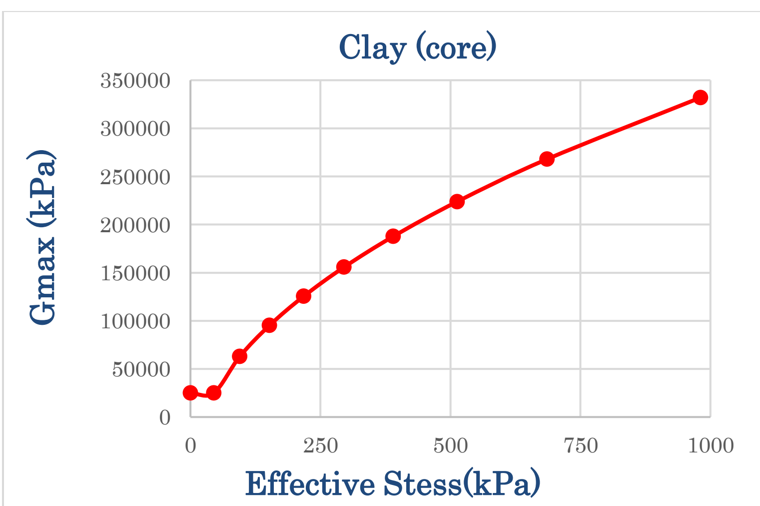

(a)

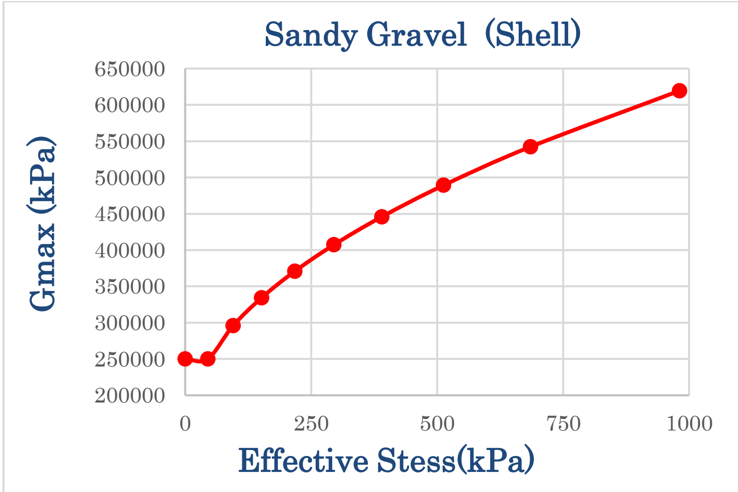

(b)

Figure 3-8: G_{max} function for 50m high dam – (a) clay (core) and (b) sandy gravel (shell)

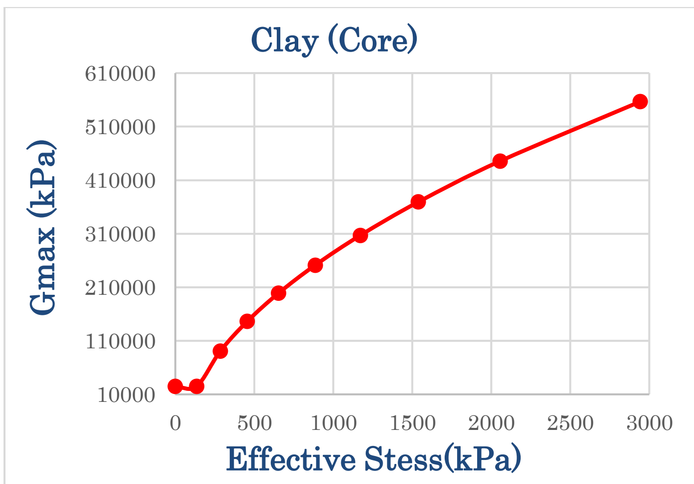

(a)

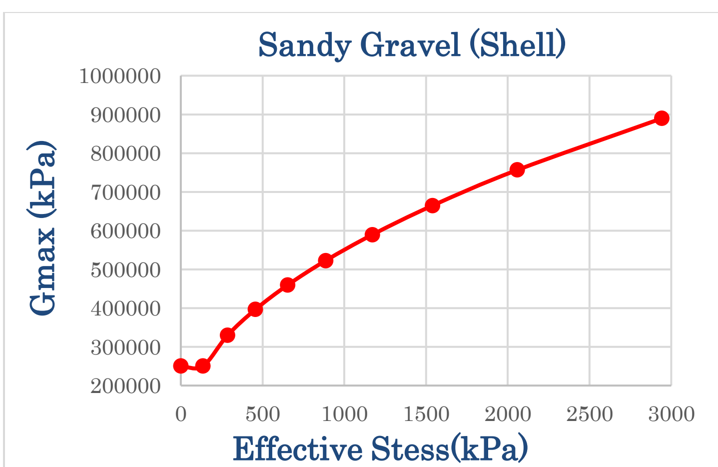

(b)

Figure 3-9: G_{max} function for 150m high dam – (a) clay (core) (b) sandy gravel (shell)

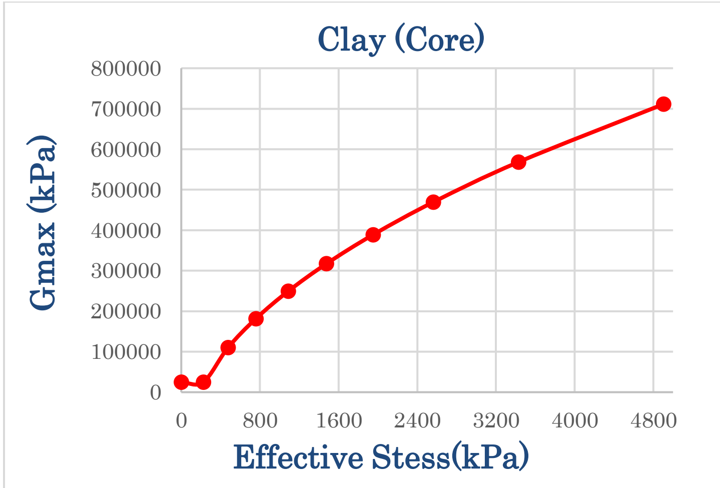

(a)

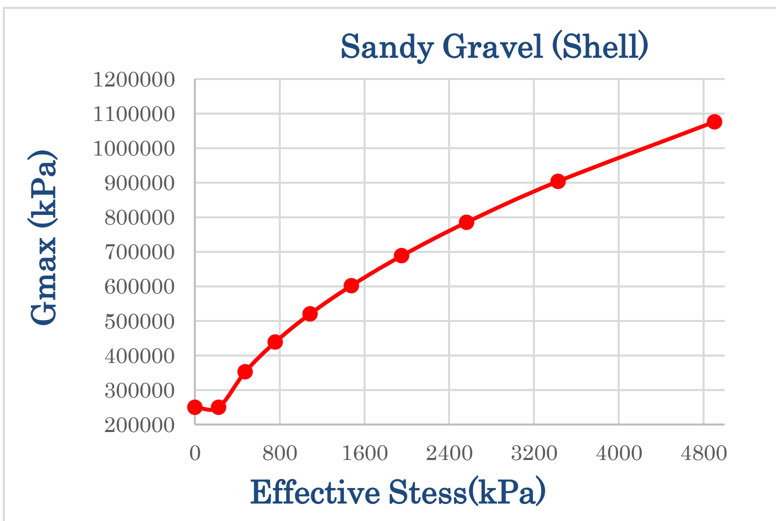

(b)

Figure 3-10: G_{max} function for 250m high dam – (a) clay (core) (b) sandy gravel (shell)

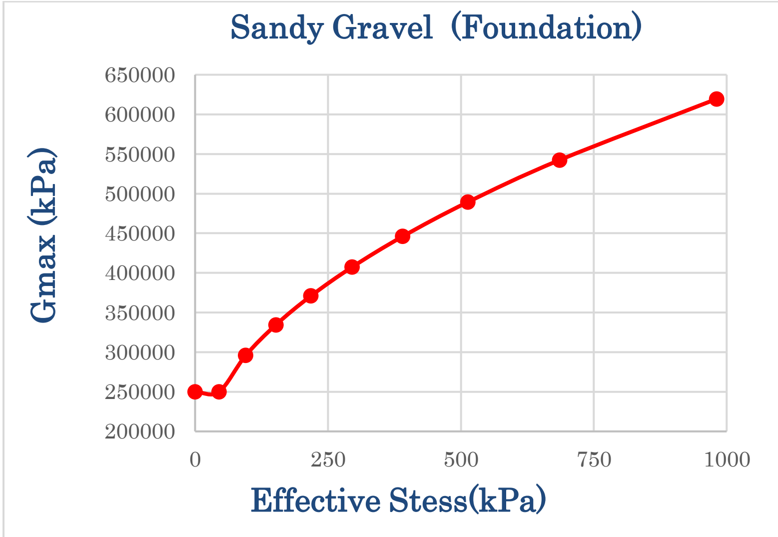

Figure 3-11: G_{max} function for 50m deep sandy gravel foundation

2. **G-reduction function**

A soil subjected to dynamic stresses tends to 'soften' in response to a cyclic shear strain. In the Equivalent Linear soil model, this softening is described as a ratio relative to G_{max}. This is called a G-reduction function. The cyclic shear strain comes from the finite element analysis. The computed shear strain together with the function and the specified G_{max} are used to compute new G values for each of the iterations (GEO-SLOPE International Ltd., 2007).

As with all the material property functions in QUAKE/W, it is not a must to use the samples or estimating features. It is possible to define a function by entering data points that are obtained from some other sources.

For this study the soil G-reduction function curve is obtained from Seed and Idriss (1970). Getdata graph digitizer is used to retrive the G-reduction curve from Seed and Idriss (1970) and are presented in Figure 3-12. For the rock foundation, inbuilt G-reduction curves in SHAKE 2000 is directly used and presented in Figure 3-13.

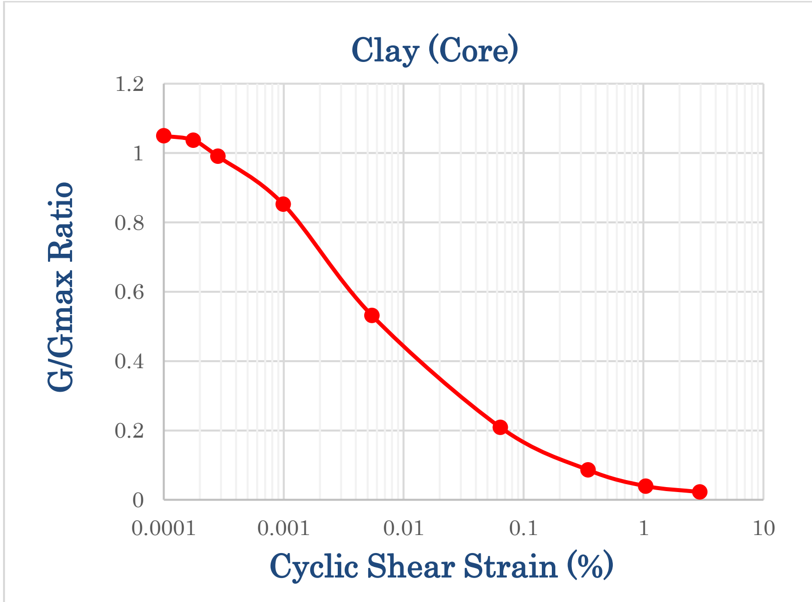

(a)

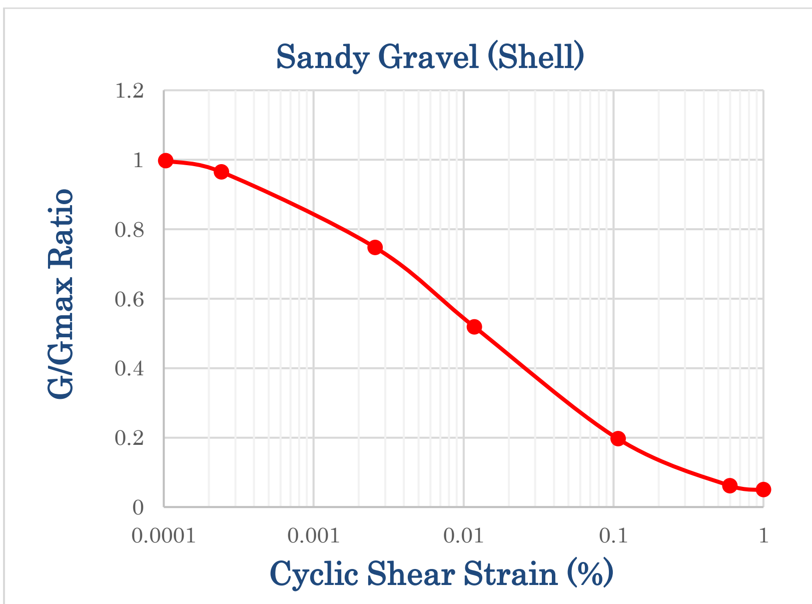

(b)

Figure 3-12: G-reduction function traced from Seed H.B. and Idriss, soil moduli and damping factor for dynamic response (1970). (a) Clay, (b) sandy gravel

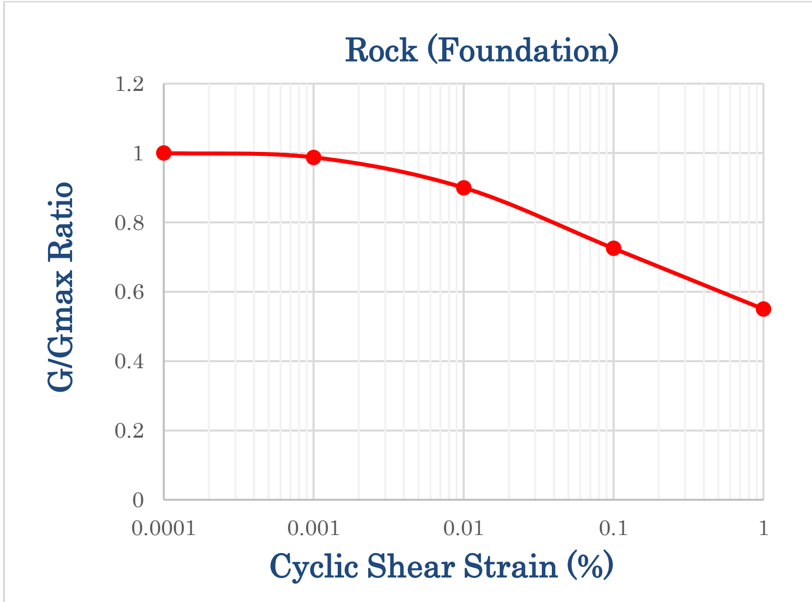

Figure 3-13: G-reduction function for rock taken from SHAKE 2000

3. Damping Ratio

As with G_{max}, the damping ratio in QUAKE/W can be specified as a constant or as a function. The damping ratio is a function of the cyclic shear strain, the same as the G-reduction function.

Like in the case with G-reduction curve, it is not a must to use the samples or estimating features. It is possible to define a function by entering data points that are obtained from some other source.

For this study the soil damping ratio curve is obtained from Seed and Idriss, (1970). As in the G-reduction curve, Getdata graph digitizer is used to retrive the damping curve from Seed and Idriss (1970) and are presented in Figure 3-14. For the rock foundation, inbuilt damping ratio curve in SHAKE 2000 is directly used and presented in Figure 3-15.

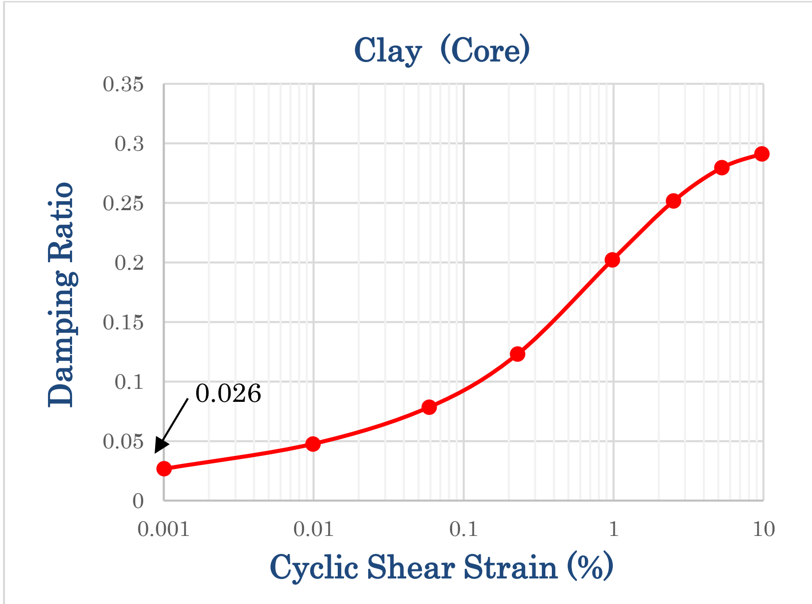

(a)

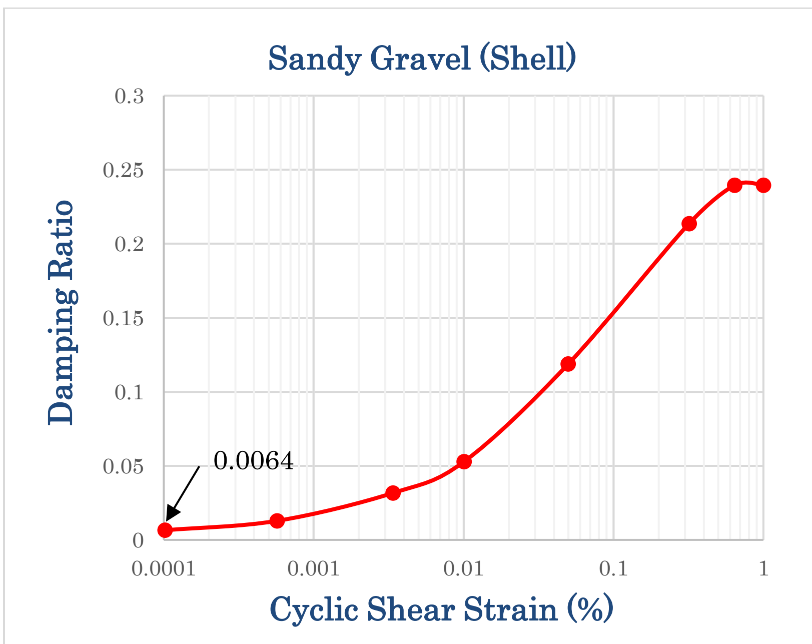

(b)

Figure 3-14: Damping ratio function traced from Seed H.B. and Idriss, soil moduli and damping factor for dynamic response, 1970. (a) Clay, (b) sandy gravel

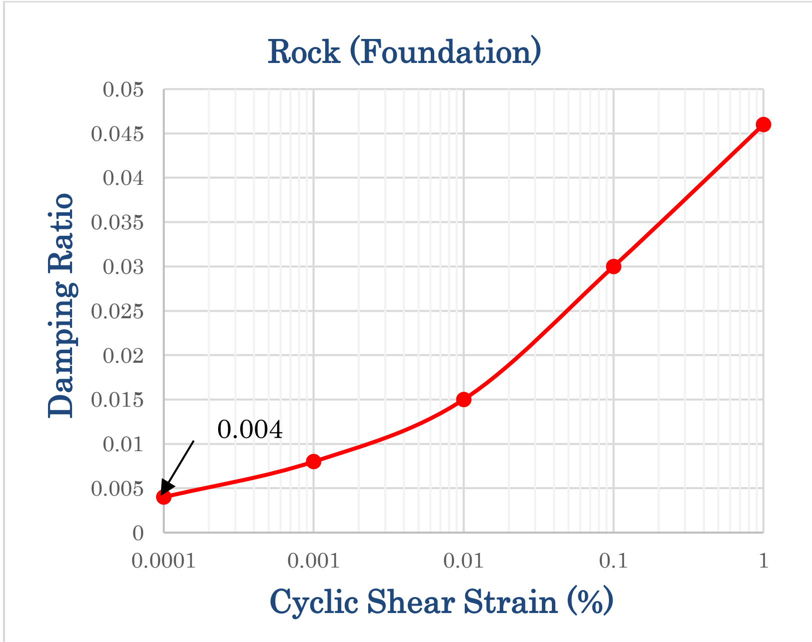

Figure 3-15: G-reduction function for rock taken from SHAKE 2000

4. Elastic-modulus (E)

The soil stiffness modulus, E, can be specified as a constant or as a function of the effective overburden stress.

$$E = k\left(\sigma'_m\right)^n \tag{3-7}$$

Where k soil property and n is an exponent

$$\sigma'_m = \frac{\sigma_v + k_o\sigma_v + k_o\sigma_v}{3} \tag{3-9}$$

Table 3-4 shows values of k and n that are presented in Duncan et al. (1980) after extensive laboratory testing programs carried out on a wide range of soils in University of California (GEO-SLOPE International Ltd., 2007).

Table 3-4: soil stiffness properties presented by Duncan et al. (1980) taken from Idriss and Duncan (1988).

Unified classification	γ **(kN/m³)**	*k*	*n*
GW,GP,SW,SP	16.48 - 23.5	600	0.4
	15.7 - 22.7	450	0.4
	14.91 - 21.9	300	0.4
	14.13 - 21.2	200	0.4
SM	17.27 - 21.2	600	0.25
	16.48 - 20.4	450	0.25
	15.7 - 19.6	300	0.25
	14.91 - 18.8	150	0.25
SM-SC	18.05 - 21.2	400	0.6
	17.27 - 20.4	200	0.6
	16.48 - 19.6	150	0.6
	15.7 - 18.8	100	0.6
CL	18.05 - 21.2	150	0.45
	17.27 - 20.4	120	0.45
	16.48 - 19.6	90	0.45
	15.7 - 18.8	60	0.45

To estimate an E-modulus function in SIGMA/W, one needs to specify a maximum depth (high of the dam), a $K_{modulus}$ number, a k_o value and exponent n. The important issue is to establish the correct match between E and the overburden (vertical) stress.

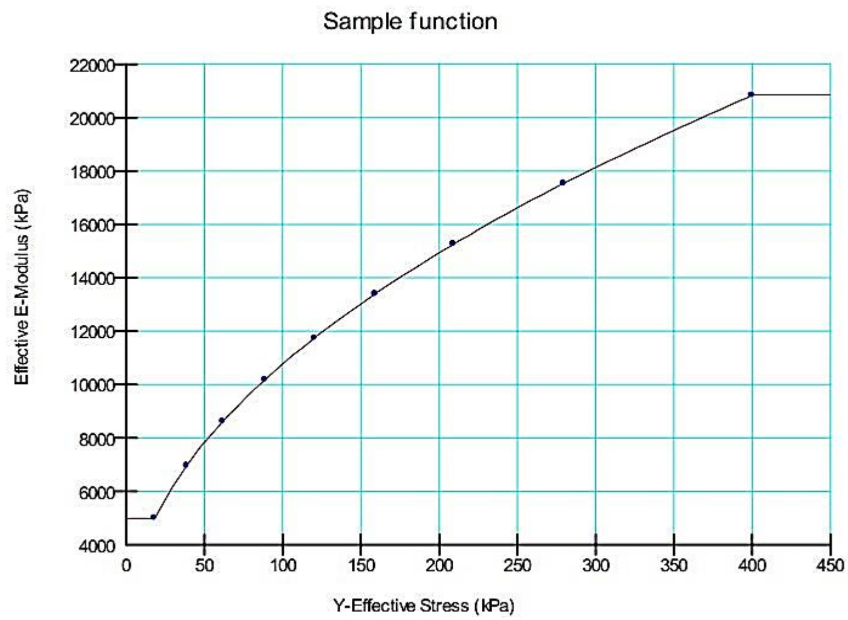

Figure 3-16: sample E-modules function

While defining E-modulus as a function, it is possible to insert the Initial or minimum E-modulus .Which in the case of a dam cross section means the E-modulus value at the crest, which is not under any over burden pressure. This means the minimum (and initial) value will be the first data point on the left. This is a useful feature for limiting or cropping the function which makes it possible for user to control the minimum E-modulus value that will be used in the analysis. The increase in E-modulus due to over burden pressure starts from the minimum E-modulus given.

Compatibility with G_{max} must be considered while estimating the Initial E-modulus. Initial E-modulus values estimated using Hooke's Stress-Strain Relation (Equation 3-10) are presented in Table 3-5.

$$E = G_{\max}\left(2\left(1+\upsilon\right)\right) \tag{3-10}$$

Table 3-5: Initial E-modulus

Soil Type	Initial G_{max} (MPa)	υ	Initial E-modulus(MPa)	k	n
Clay	25	0.4	70	60	0.45
Sandy gravel	250	0.3	650	200	0.4
Rock	(constant) 30000	0.2	(constant) 72000		

E-modulus function

The graphs Figure 3-17 to 3-20 are E-modulus functions formulated by the software according to their height, soil type and initial E-modulus that are used for this analysis.

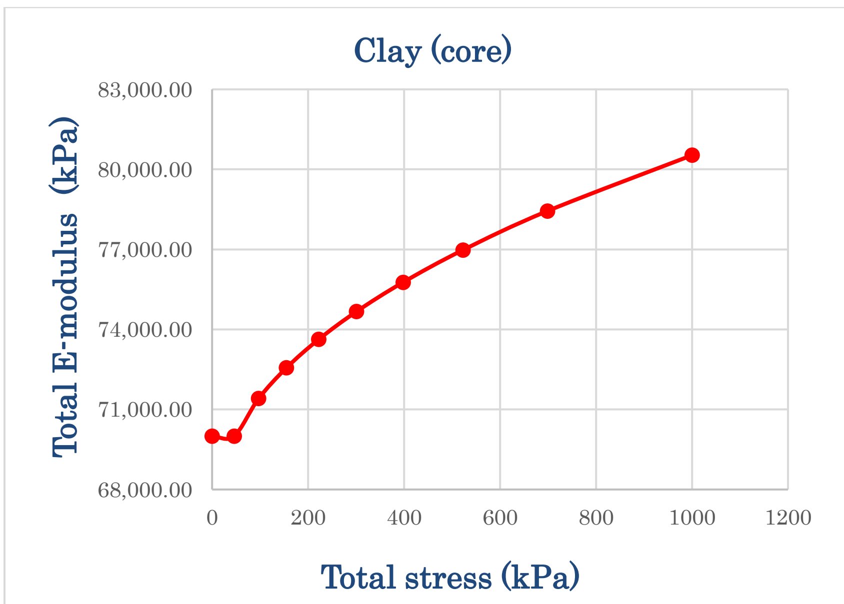

(a)

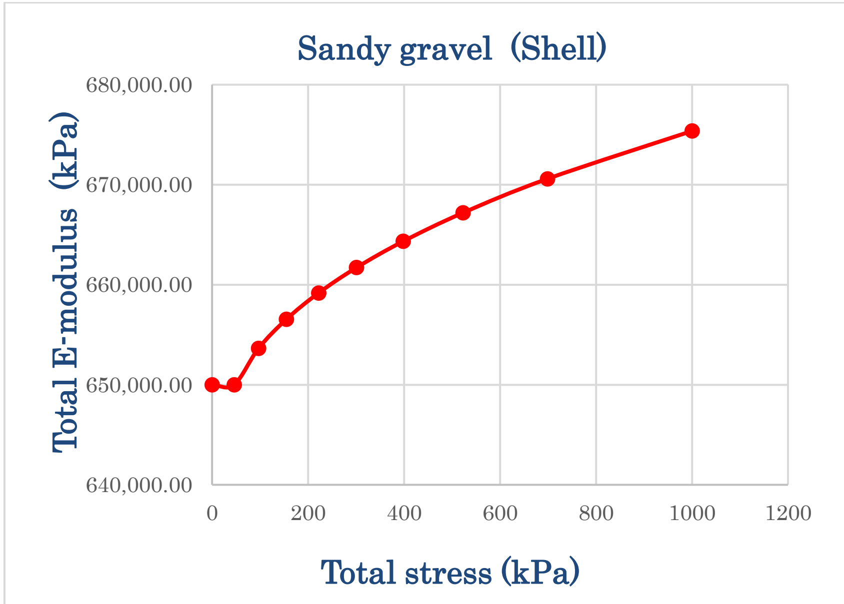

(b)

Figure 3-17: E-modulus function for 50m high dam – (a) clay (core) (b) sand gravel (Shell)

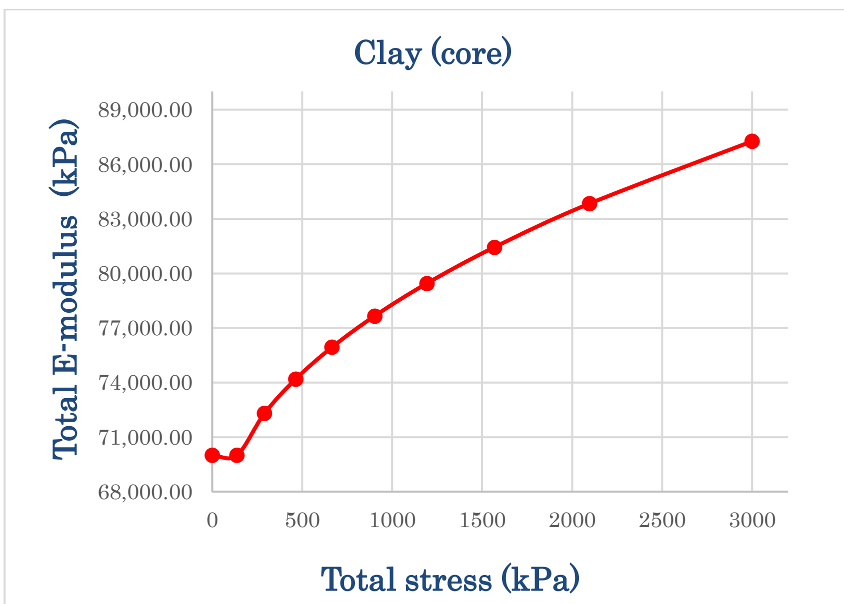

(a)

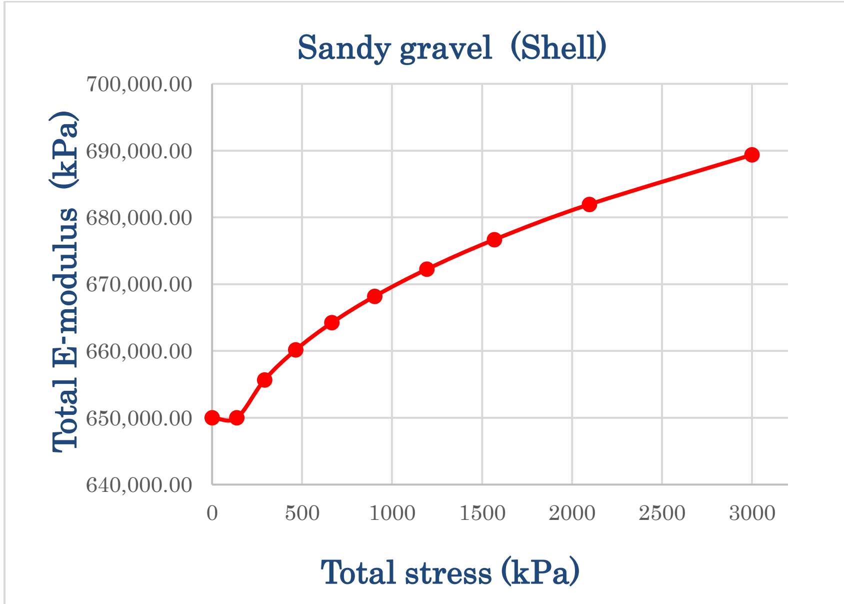

(b)

Figure 3-18: E-modulus function for 150m high dam – (a) clay (core) (b) sand gravel (shell)

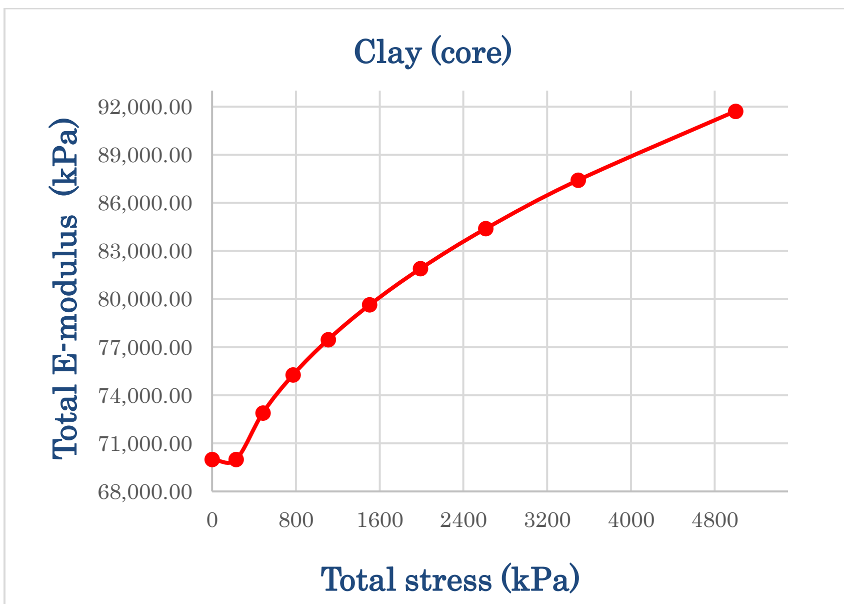

(a)

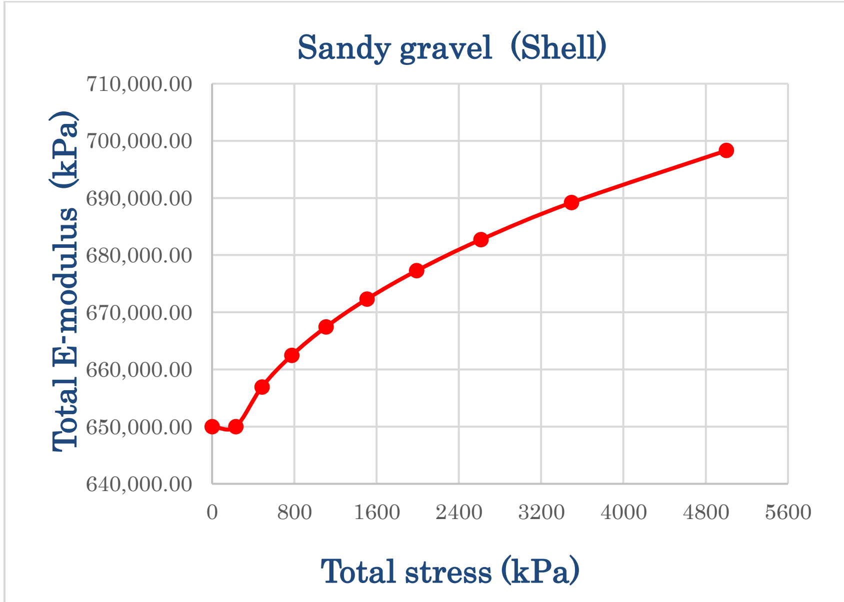

(b)

Figure 3-19: E-modulus function for 250m high dam – (a) clay (core) (b) sand gravel (shell)

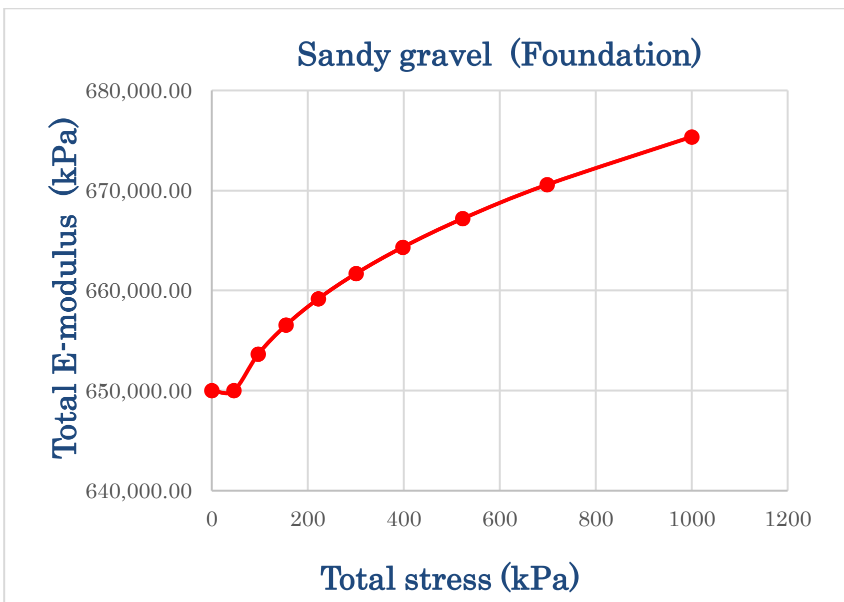

Figure 3-20: E-modulus function for 50m deep sandy gravel foundation

3.6. Input motion

3.6.1. Acceleration Time-History

Horizontal acceleration time-histories are key input parameters for the dynamic QUAKE/W analysis. For an analysis of a dam, site specific acceleration time-history is use; this study is generalized and not specific for one particular place so the following three recorded acceleration time-histories that are recorded elsewhere having their own different unique features are used.

- Imperial Valley Earthquake (1940) Elcentro record, USA (M=6.7, H=11km, R=11.5km)

  -Multiple peaks in short period, high frequency rich motion

- Tokachi-oki Earthquake (1968) Hachinohe record, Japan (M=7.9, H=0, R=200km)

  -Longer duration

- Hyogoken-nanbu Earthquake (1995) Kobe JMA Record, Japan (M=7.2, H=14.3km, R=19km)

  -Short duration, big pulse

Where M is ground motion magnitude, H is focal depth (distance from the epicenter to the focus) and R is the epicentral distance (distance from point of interest to the epicenter) from a near source (Haile, 1996).

3.6.2. Peak Ground Acceleration (PGA)

As recommended by the International Commission on Large Dams (ICOLD), these following three types of earthquakes must be considered while designing a dam and are described as follows:-

1. **Maximum Credible Earthquake (MCE)**

A Maximum Credible Earthquake (MCE) is the largest reasonably conceivable earthquake magnitude that is considered possible along a recognized fault or within a geographically defined tectonic province, under the presently known or presumed tectonic framework. The most severe ground motion affecting a dam site due to an MCE scenario is referred to as the MCE ground motion (ICOLD, 2010).

2. **Safety Evaluation Earthquake (SEE)**

The Safety Evaluation Earthquake (SEE) also referred as maximum design earthquake (MDE) and design base earthquake (DBE) is the maximum level of ground motion for which the dam should be designed or analyzed (ICOLD, 2010).

3. **Operating Basis Earthquake (OBE)**

The Operating Basis Earthquake (OBE) represents the level of ground motion at the dam site for which only minor damage is acceptable. The dam, appurtenant structures and equipment should remain functional and damage should be easily repairable, from the occurrence of earthquake shaking not exceeding the OBE (ICOLD, 2010).

While considering a PGA for a particular dam, we consider the seismic hazard of the area the dam is located. Since this study is not about a particular area, it's based on the earthquake levels described above and other previous studies on ground motions. A PGA values of 0.05g, 0.15g and 0.3g are taken for this study as an amplitude of the ground motions considered with the aim of representing lower, medium and higher PGA values.

Acceleration time history of the three motions scaled to a PGA of 0.05g, 0.15 g and 0.3g are plotted in Figure 3-21, Figure 3-22 and Figure 3-23. And to view their frequency content, their spectral acceleration is shown in Figure 3-24. Smoothed Fourier amplitude is also presented in Figure 3-25, narrow spectrum implies that the motion has "dominant frequency" and a broad spectrum relates to motion that contains "variety of frequencies that produce a jagged, irregular time history" (Kramer, 1996).

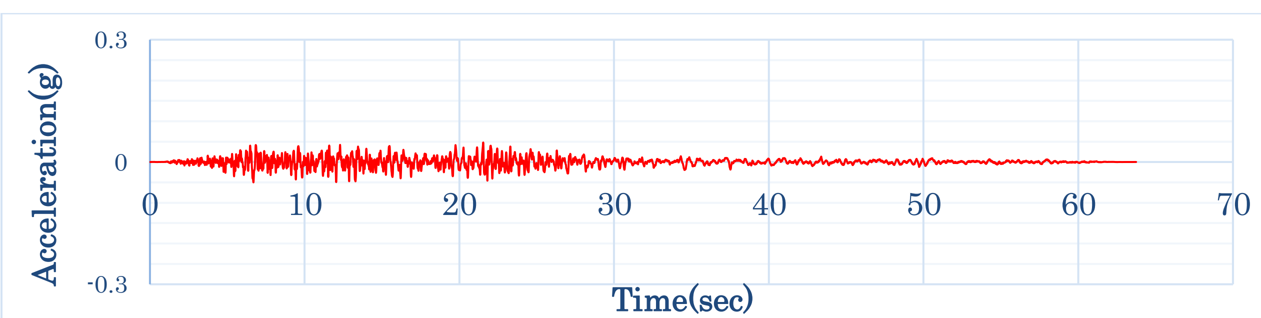

(a)

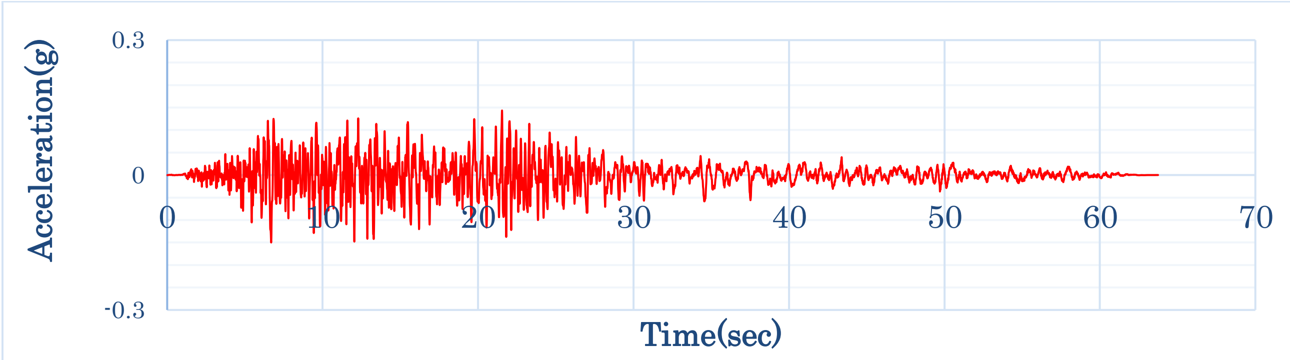

(b)

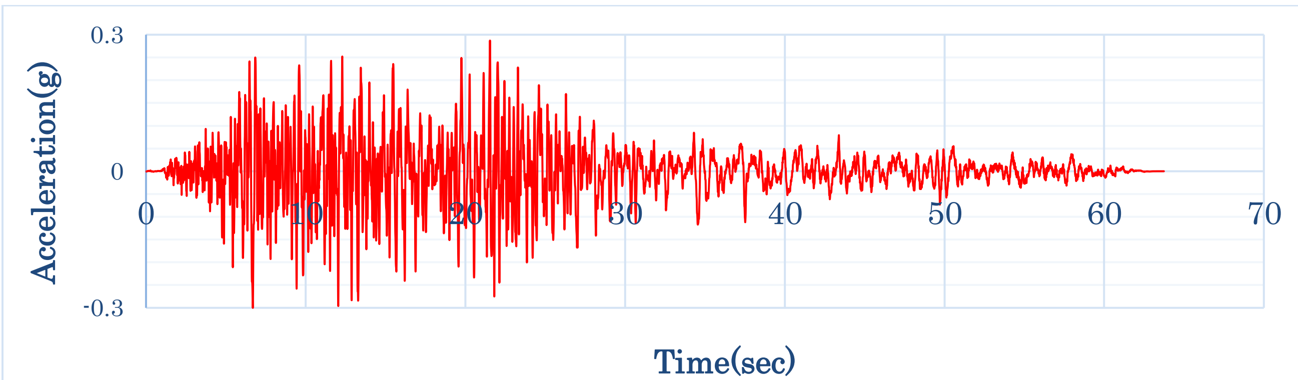

(c)

Figure 3-21: Imperial Valley Earthquake (1940) Elcentro Record (Haile, 1996), (a) scaled to PGA of 0.05g ,(b) scaled to PGA of 0.15g, (c) scaled to PGA of 0.3g

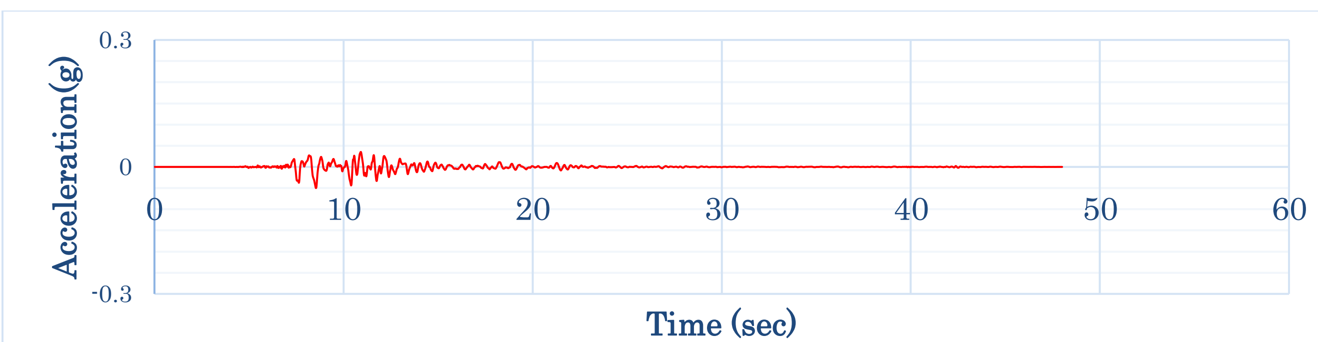

(a)

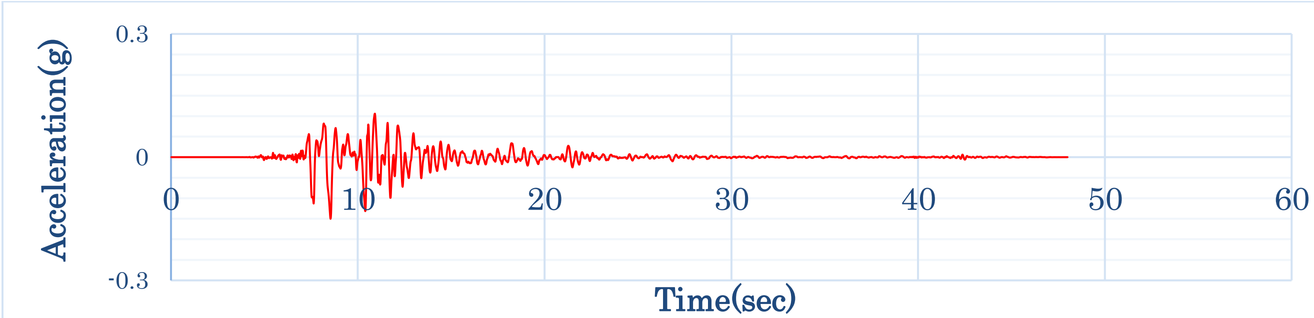

(b)

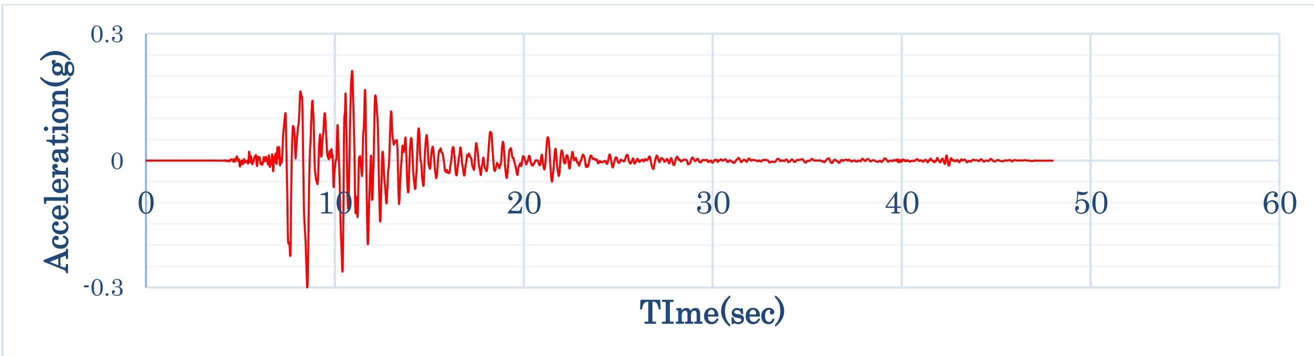

(c)

Figure 3-22: Hyogoken-nanbu Earthquake (1995) Kobe JMA Record (Haile, 1996), (a) scaled to PGA of 0.05g ,(b) scaled to PGA of 0.15g ,(c) scaled to PGA of 0.3g

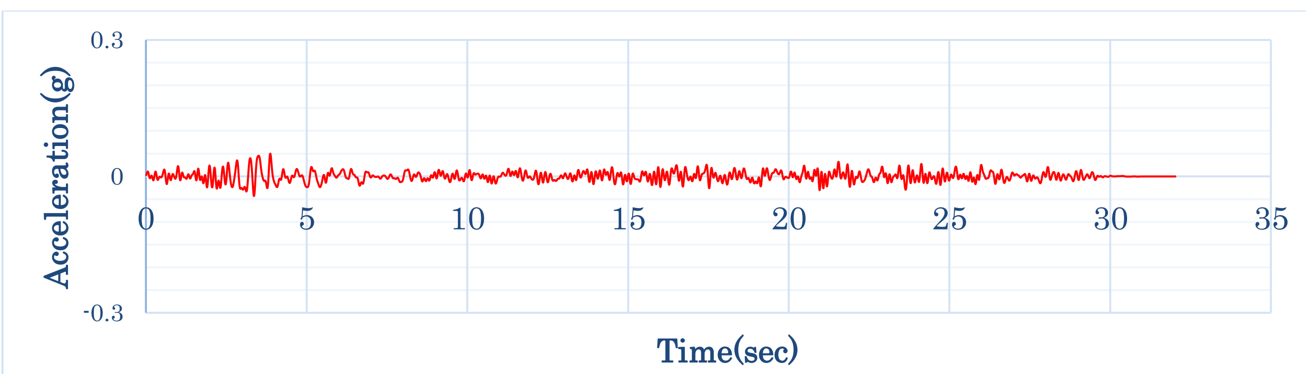

(a)

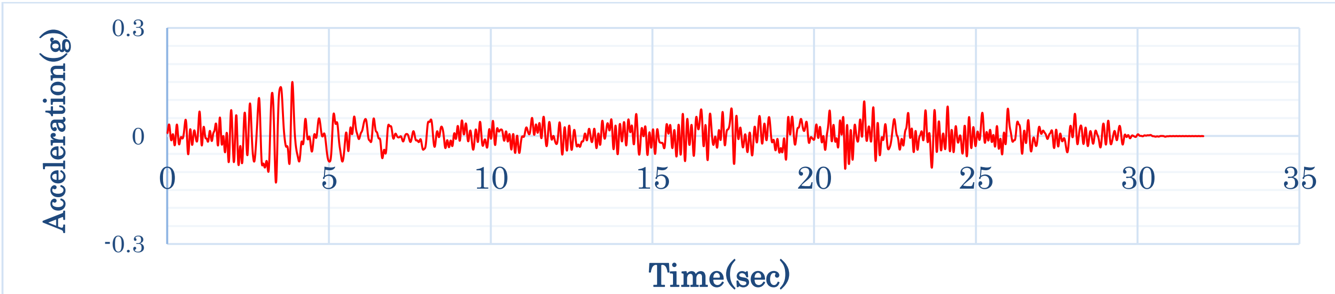

(b)

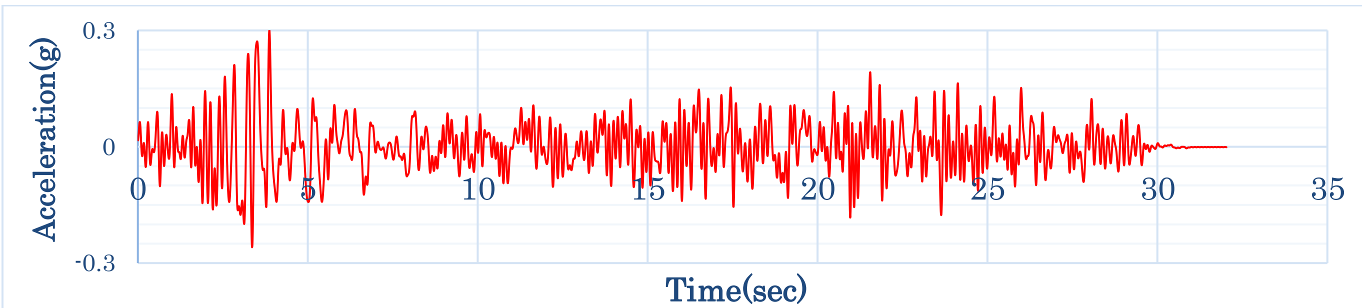

(c)

Figure 3-23: Tokachi-oki Earthquake (1968) Hachinohe Record (Haile, 1996), (a) scaled to PGA of 0.05g ,(b) scaled to PGA of 0.15g ,(c) scaled to PGA of 0.3g

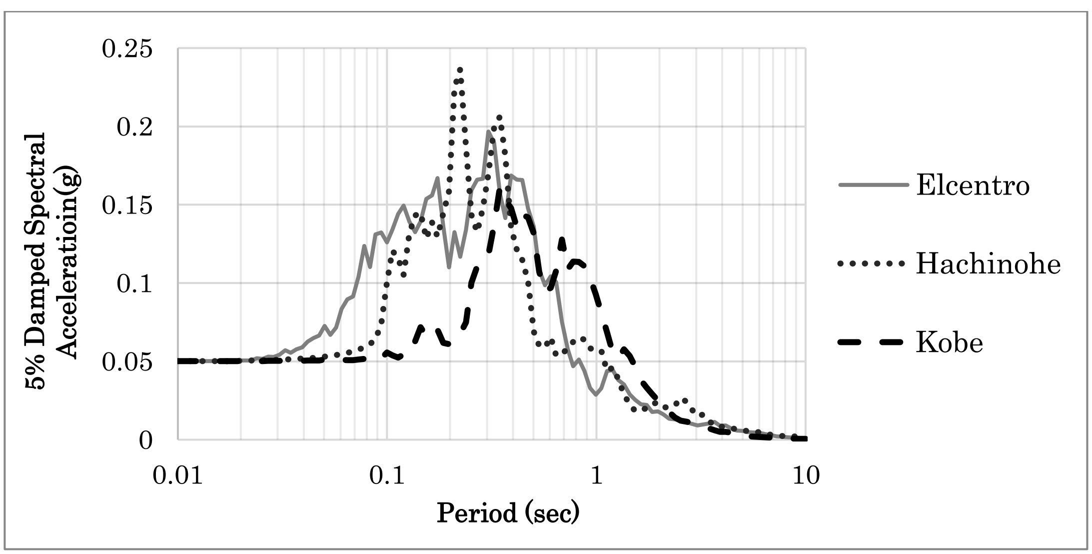

Figure 3-24: Spectra acceleration of Kobe, Hachinohe and Elcentro ground motion

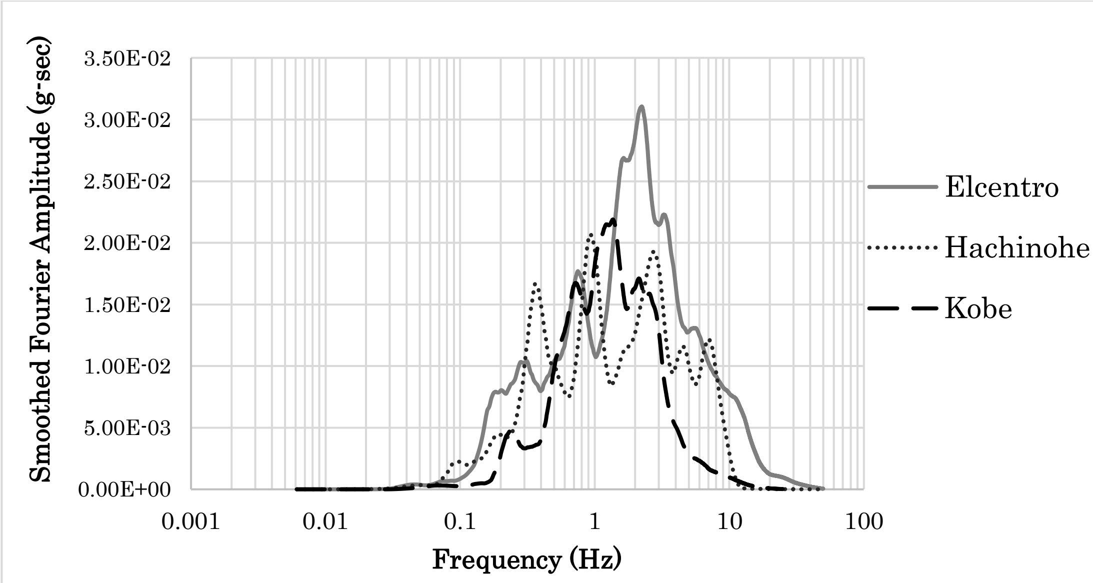

Figure 3-25: Smoothed Fourier amplitude Kobe, Hachinohe and Elcentro ground motion.

3.7. Staged/multiple analysis in GeoStudio

As mentioned in section 3.4, components of GeoStudio package can be integrated and for this study, the four type of analysis described before are integrated.

The first is SEEP/W for the seepage analysis in which the result will be the parent analysis for the SLOPE/W, which will analyze the slope stability. The result of the SEEP/W and SLOPE/W is to check the stability of the dam under static condition. The results for both are presented in the chapter four. The result from SLOPE/W is used as a parent analysis for the initial static analysis which will, in turn, be the parent analysis of the QUAKE/W dynamic analysis. To see the permanent deformation on the dam caused by the effect of the motions, SIGMA/W analysis is performed using the result of QUAKE/W as a parental analysis. A clear and step by step process is shown in Figure 3-26.

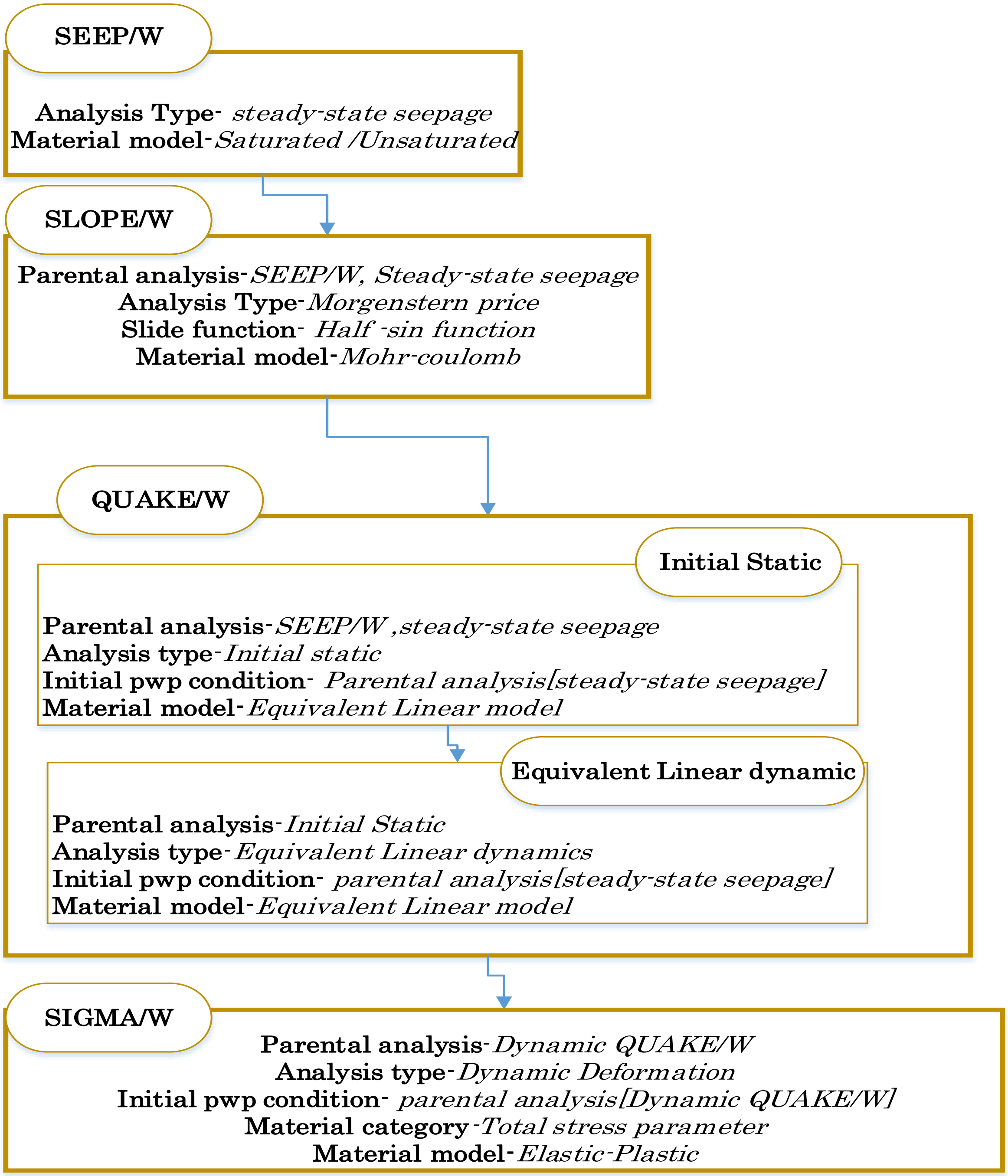

Figure 3-26: Staged multiple analysis in geo studio

CHAPTER 4 - ANALYSIS RESULT AND DISCUSSION

4.1. Analyzed dam Model and combination of analysis

The dam cross-section has been modeled on GeoStudio 2007 in such a way that it is founded on two different foundations as shown in Figure 4-1.

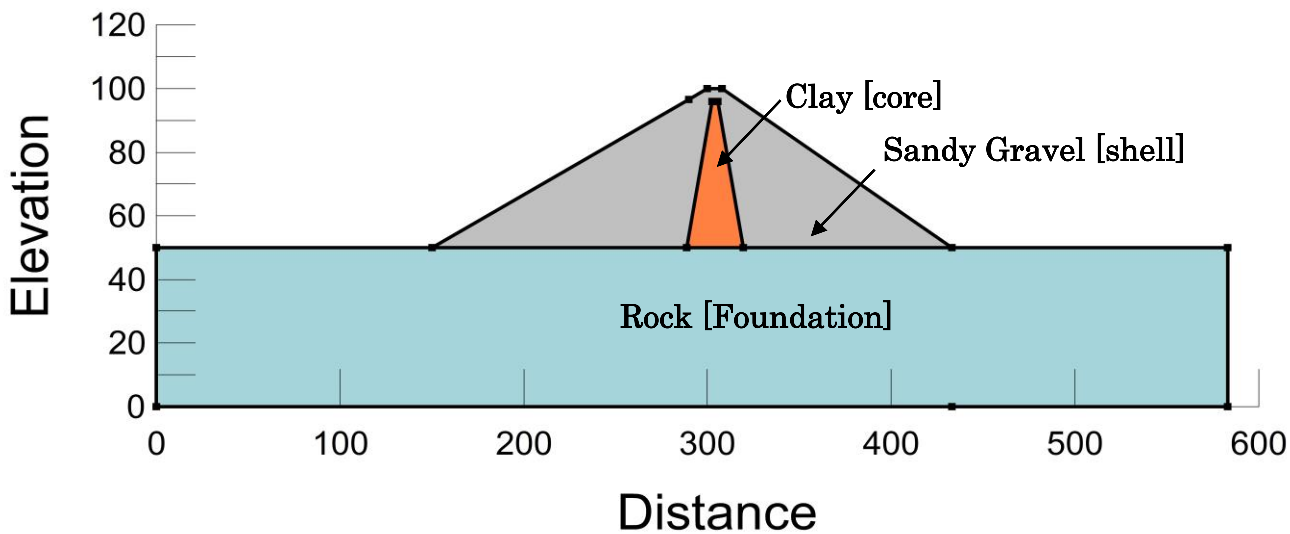

(a)

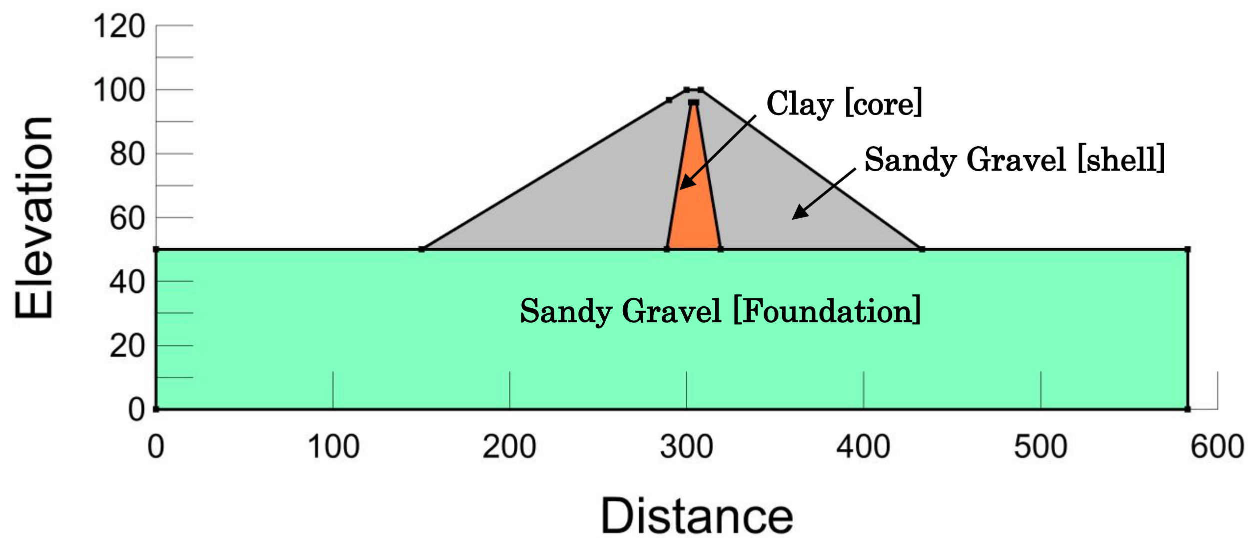

(b)

Figure 4-1: Model of dam cross-section on, (a) Rock foundation, (b) Sandy gravel foundation

The dynamic analyses are conducted as per the flow chart in Figure 4-2. Here, four parameters – dam height, foundation type, ground motion and PGA – have been selected from among other parameters that one can employ for comparison purposes. The results are presented in the following manner:-

-The three PGA [0.05g, 0.15g and 0.3g] are used as control variable and shown on every result.

-The model has two major parts, the foundation and the dam. The results for the effect of ground motion on both have been presented separately in the following order:-

1. Comparison of a_{max} value for the foundation
    - Variation of a_{max} values with respect to different ground motions.
    - Variation of a_{max} values with respect to different foundation types.
    - Variation of a_{max} values with respect to different dam heights.
2. Comparison of a_{max} value for the dam
    - Variation of a_{max} values with respect to different ground motions.
    - Variation of a_{max} values with respect to different foundation types.
    - Variation of a_{max} values with respect to different dam heights.
3. Summary of a_{max} values

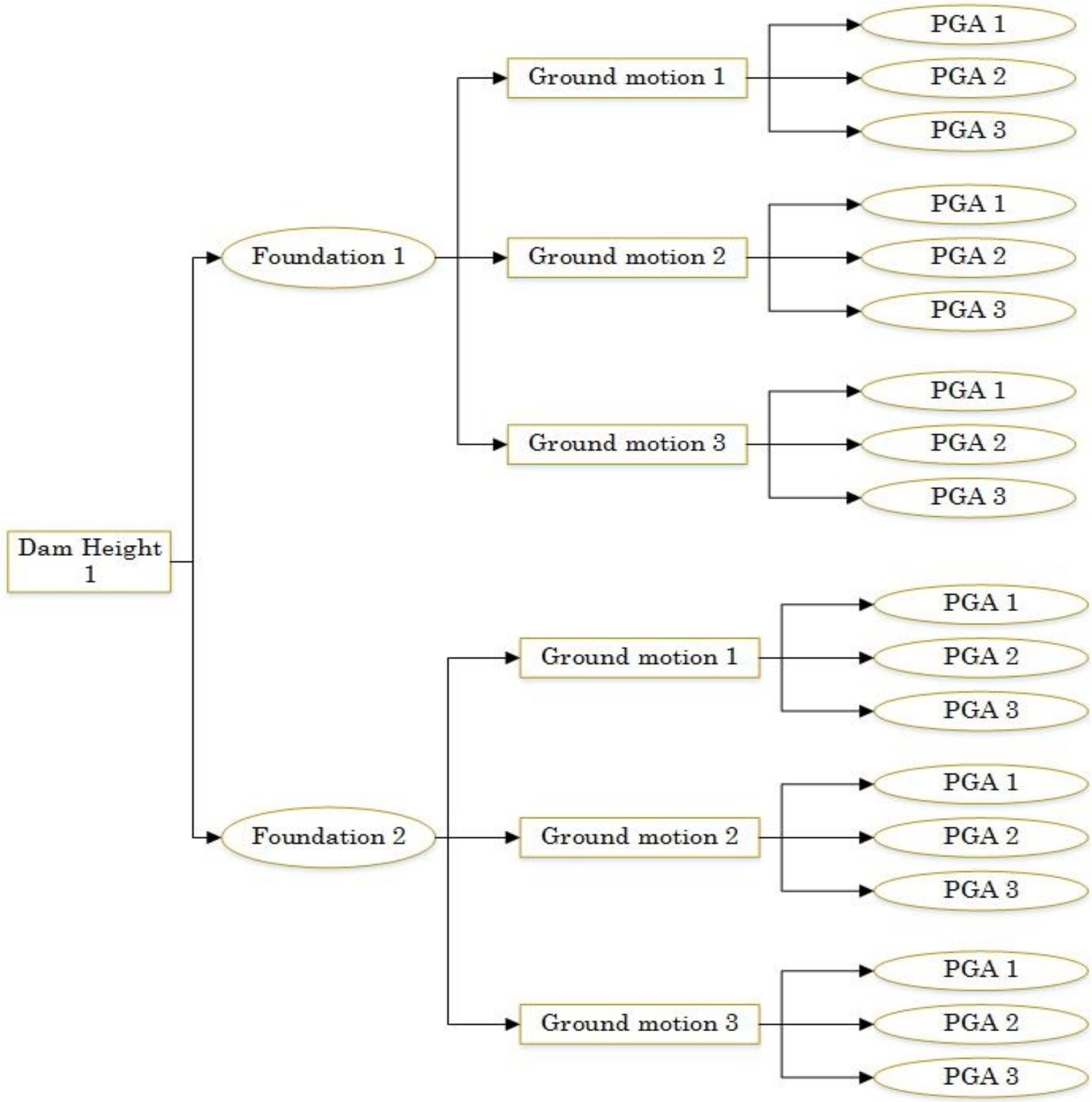

Figure 4-2: Analysis combinations

For one dam height there are two types of foundations, three types of ground motions and three peak ground accelerations, which gives 18 analyses. Since three dam heights are used in this study, altogether it becomes 54 analyses.

4.2. Seepage (SEEP/W) analysis results

Having modeled the dam using SEEP/W and inserting the necessary hydraulic parameters, the results of the analysis are shown in Figures 4-3, Figure 4-4 and Figure 4-5 for different height and foundation type. It can be seen that the phreatic line does not cross the downstream slope; and it is worth mentioning that below the phreatic line prevails positive pore water pressure while above it is the negative pore water pressure. The generated pore pressure from SEEP/W is taken to SLOPE/W for stability analyses. The models are analyzed with a slope of 3H: 1V for upstream, 2.5H: 1V for downstream and a core slope of 0.3H: 1V with 50m deep foundation.

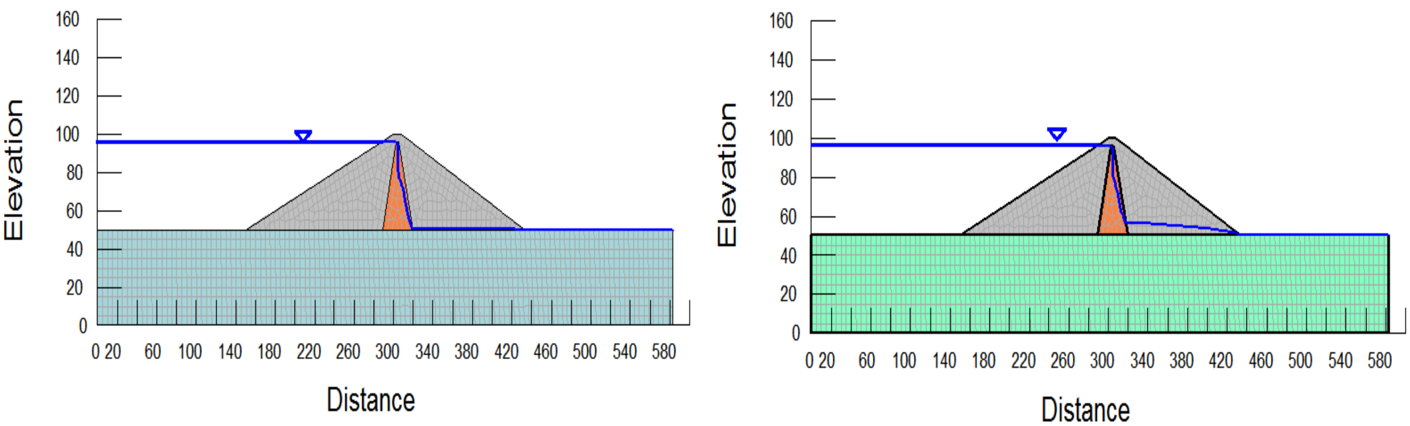

(a) (b)

Figure 4-3: Seepage analysis results for 50m high dam on top of - (a) Rock foundation (b) Sandy gravel foundation

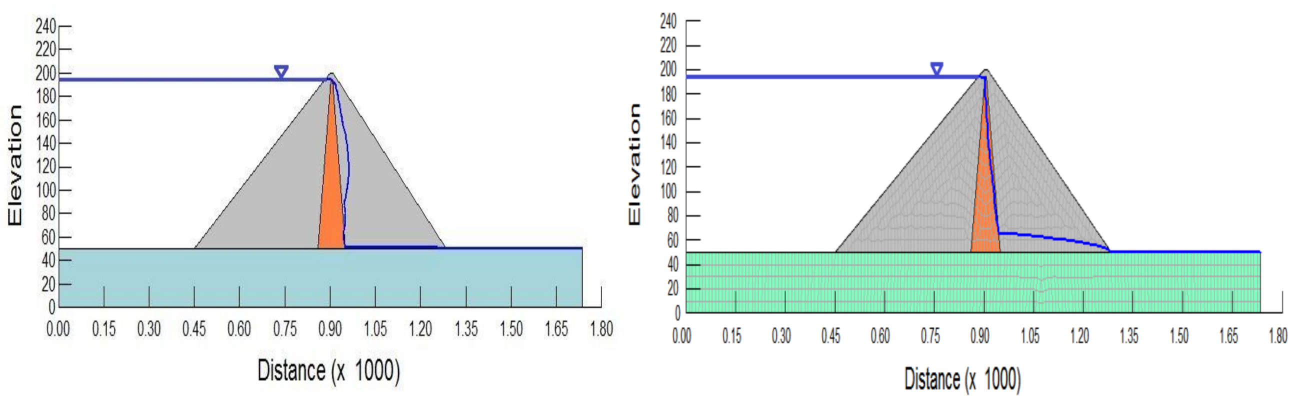

(a) (b)

Figure 4-4: Seepage analysis results for 150m high dam on top of - (a) Rock foundation (b) Sandy gravel foundation

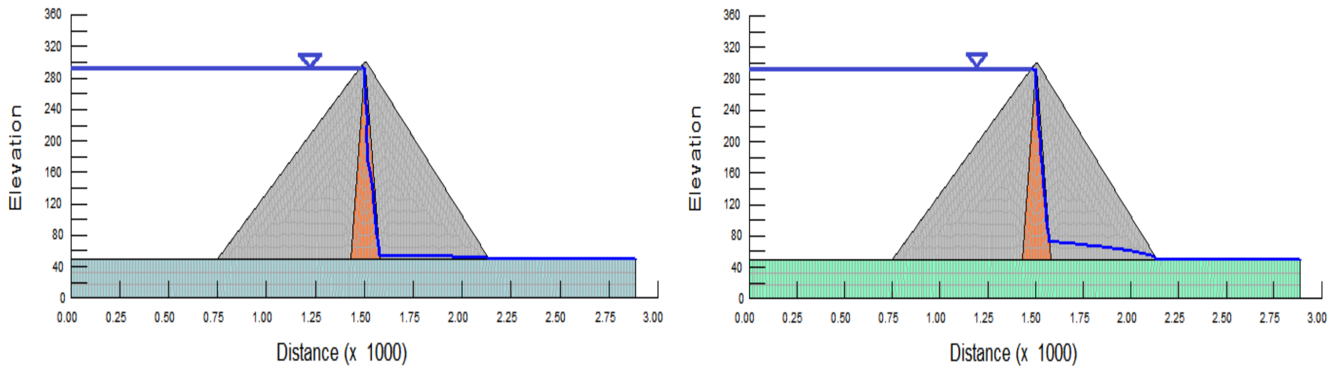

(a) (b)

Figure 4-5: Seepage analysis results for 250m high dam on top of - (a) Rock foundation (b) Sandy gravel foundation

4.3 Slope stability (SLOPE/W) results

The stability of the dam has been analyzed using SLOPE/W which is based on limit equilibrium. The stability analyses was conducted in order to determine the factor of safety for three different heights of the dam on two different foundations. Figure 4-6, to Figure 4-11 show factor of safeties for both downstream and upstream slopes under static condition.

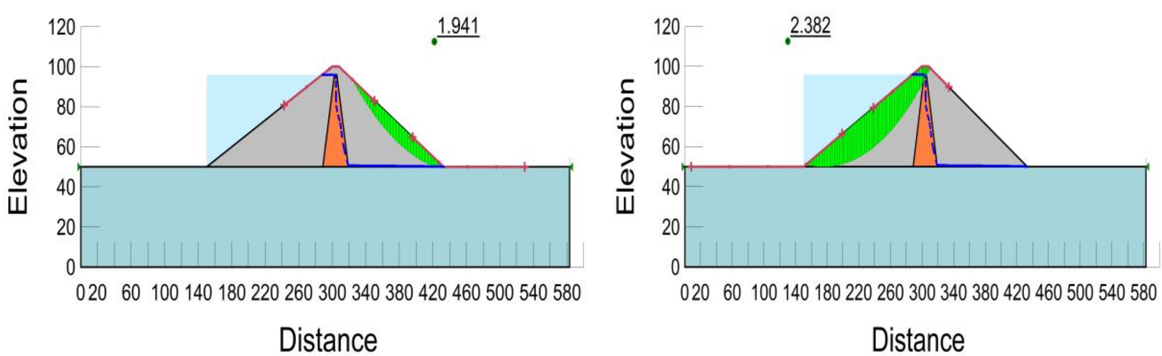

(a) (b)

Figure 4-6: Slope stability results of 50m high dam on a rock foundation – (a) downstream slope (b) upstream slope

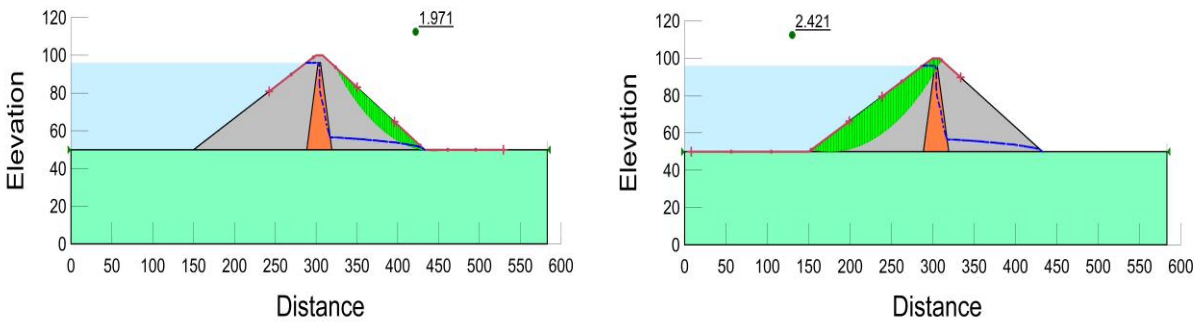

(a) (b)

Figure 4-7: Slope stability results of 50m high dam on a sandy gravel foundation – (a) downstream slope (b) upstream slope

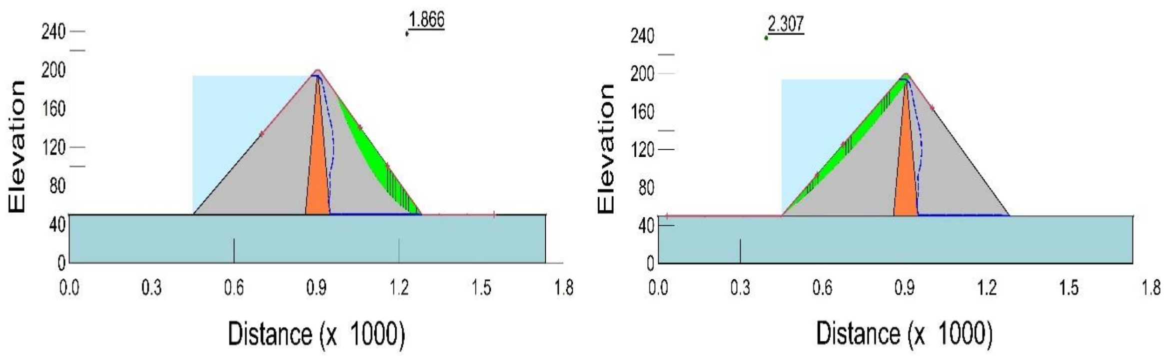

(a) (b)

Figure 4-8: Slope stability results of 150m high dam on a rock foundation – (a) downstream slope (b) upstream slope

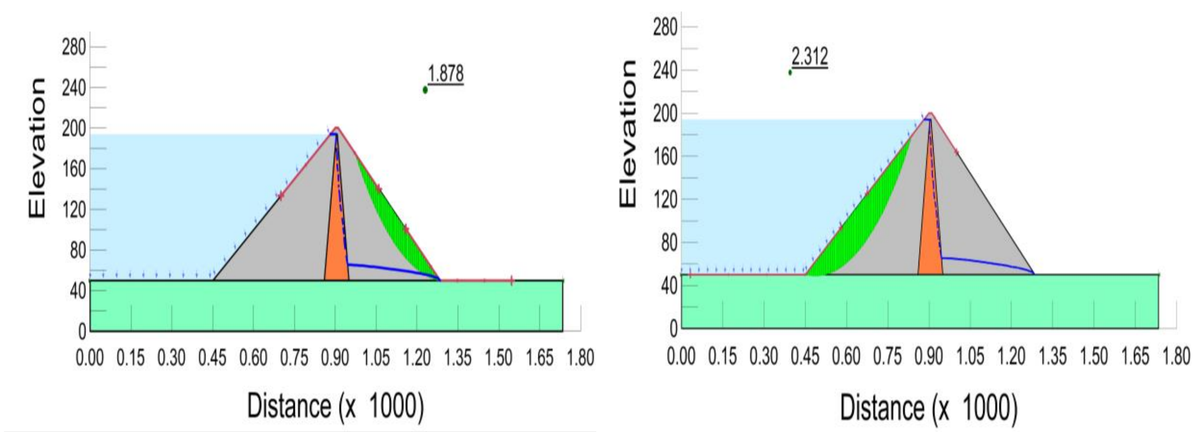

(a) (b)

Figure 4-9: Slope stability results of 150m high dam on a sandy gravel foundation – (a) downstream slope (b) upstream slope

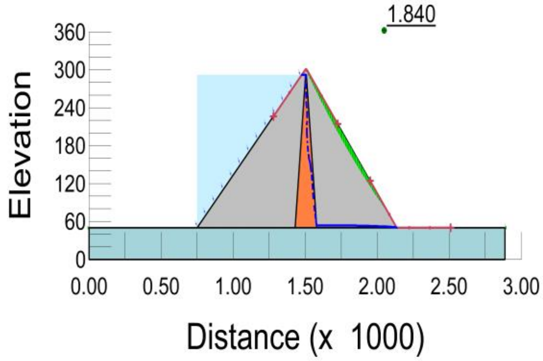

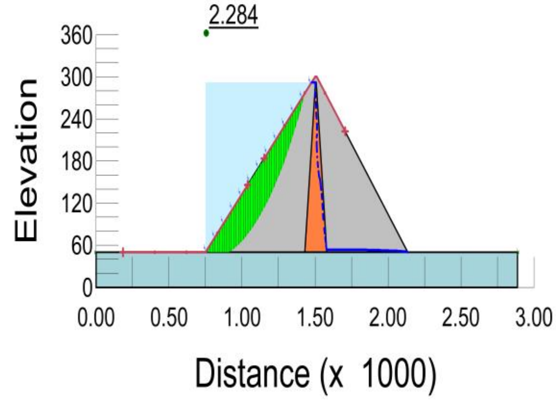

(a) (b)

Figure 4-10: Slope stability results of 250m high dam on a rock foundation – (a) downstream slope (b) upstream slope

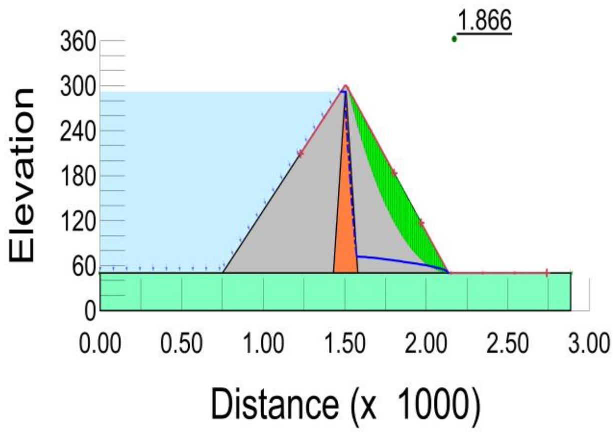

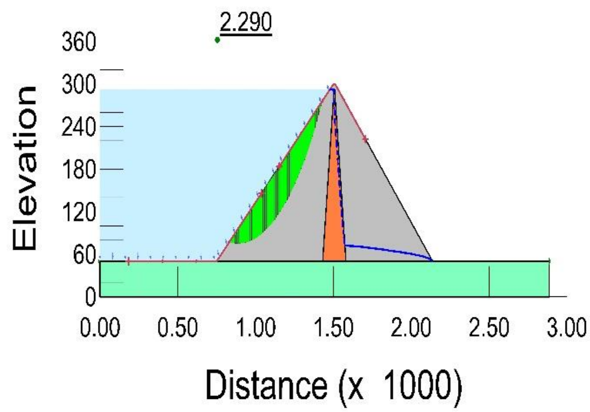

(a) (b)

Figure 4-11: Slope stability results of 250m high dam on a sandy gravel foundation – (a) downstream slope (b) upstream slope

Table 4.1 gives a summary of safety factors. The static stability is checked and the factor of safety of both upstream and downstream slope was found to be greater than 1.5 as it is the minimum factor of safety for a reservoir-full long term operational dam (Fell et al., 2015). Hence, we can proceed to QUAKE/W with this cross section and material properties.

Table 4-1: A summary of factor of safety

Foundation	Dam Height	Upstream slope	Downstream slope
Rock	50	2.382	1.914
Sandy Gravel	50	2.421	1.971
Rock	150	2.307	1.866
Sandy Gravel	150	2.312	1.878
Rock	250	2.285	1.84
Sandy Gravel	250	2.29	1.866

4.3. Dam dynamic response (QUAKE/W) result

A sample output for the horizontal maximum acceleration is shown in Figure 4-12. The dam is 50m high resting on 50m deep sandy gravel foundation subjected to Kobe ground motion at an amplitude of 0.3g. The side slope is 3H: 1V and 2.5H: 1V for upstream and downstream, respectively, with 0.3H: 1V core side slope. The maximum acceleration at the top of the foundation and in the dam are presented in this section.

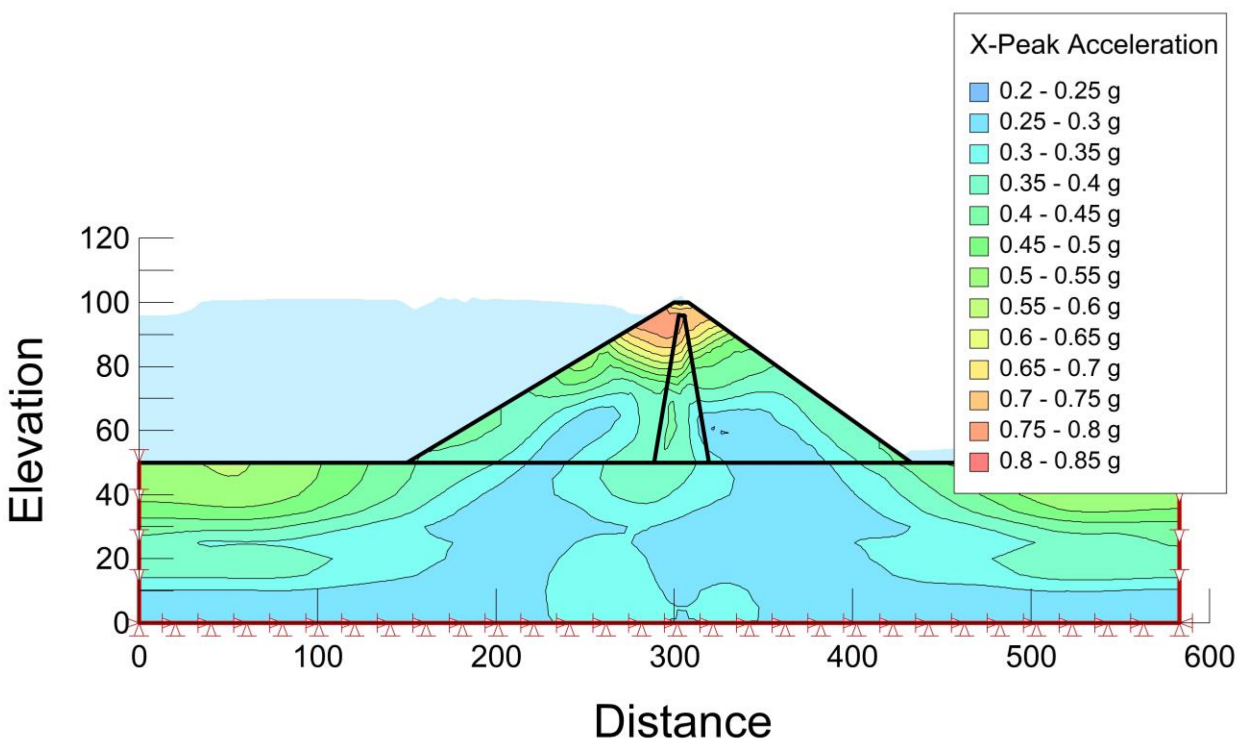

Figure 4-12: Sample software output for horizontal maximum acceleration

4.3.1. Summary of maximum-acceleration results

4.3.1.1. Maximum-accelerations at the top of foundation

a) Comparison of a_{max} for the same foundation under different ground motions

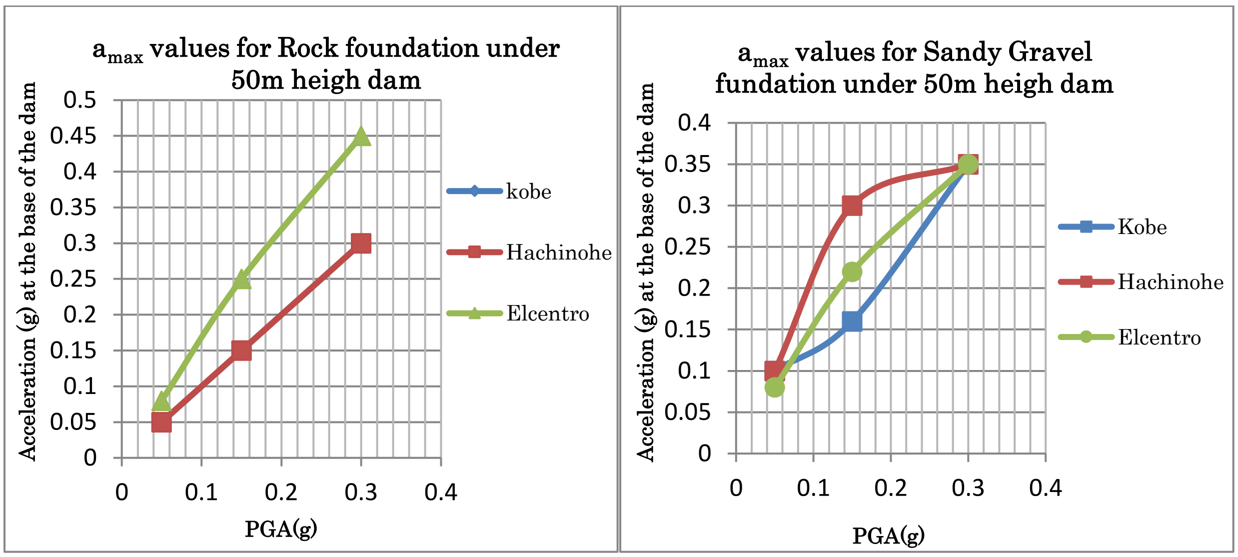

(a) (b)

Figure 4-13: a_{max} value for foundations found under 50m high dam subjected to different ground motions - (a) Rock foundation, (b) Sandy Gravel foundation

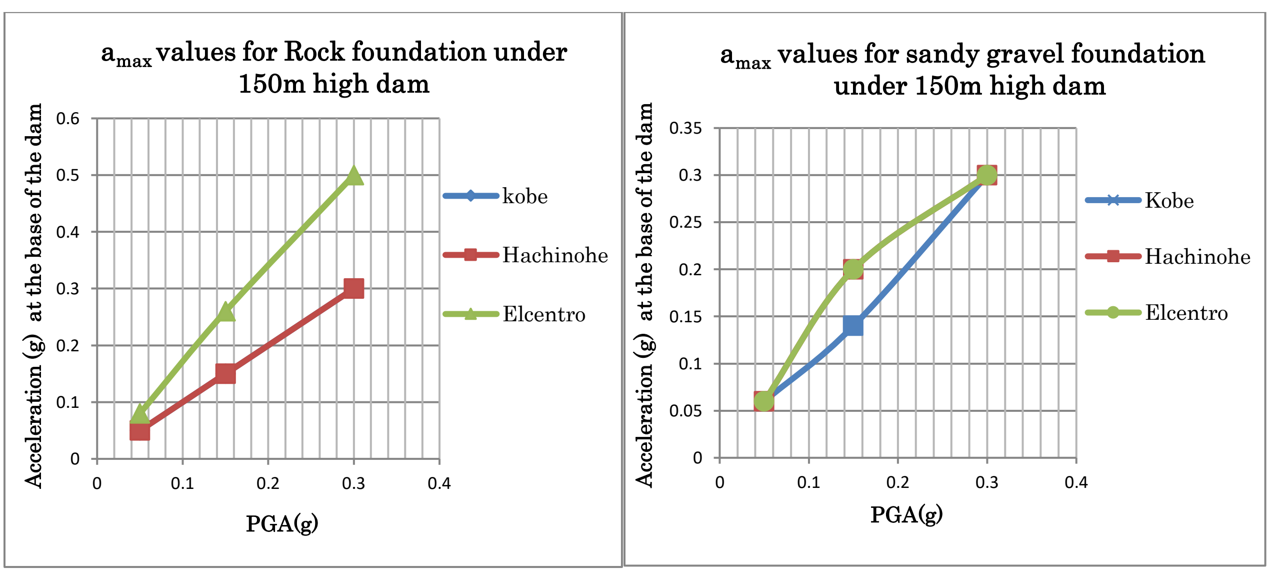

(a) (b)

Figure 4-14: a_{max} value for foundation found under 150m high dam subjected to different motion - (a) Rock foundation, (b) sandy gravel foundation.

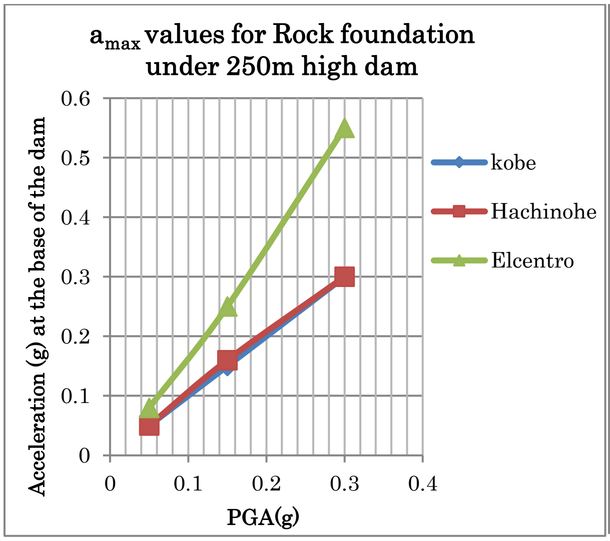

(a)

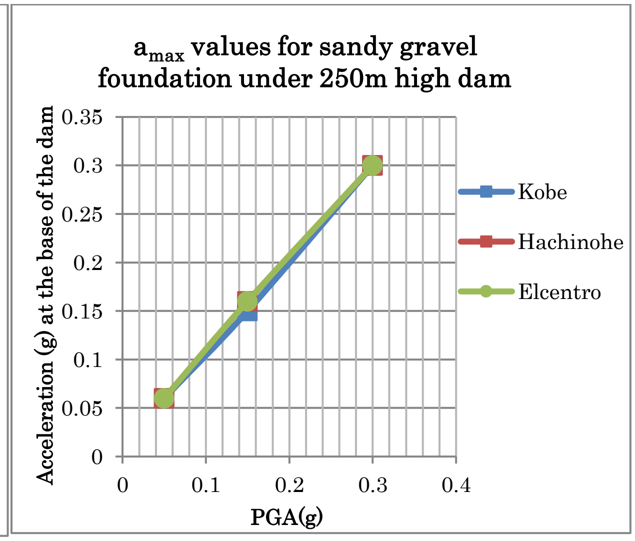

(b)

Figure 4-15: a_{max} value for foundation found under 250m high dam subjected to different motion - (a) Rock foundation, (b) sandy gravel foundation.

Amplification behavior for Hachinohe and Kobe ground motions have been found to overlap as can be seen in Figure 4-13(a), Figure 4-14(a) and Figure 4-15(a). Elcentro ground motion contains more high frequency content as could be seen in Figure 3-23 and Figure 3-24 compared with the other two ground motions. Hence, rock foundation (which is a stiff and low period material) results in higher amplification of the ground motion. This effect can also be clearly observed in Figure 4-16(c), Figure 4-17(c) and Figure 4-18(c).On the other hand, lower frequency ground motions show relatively higher amplification on sandy gravel foundation as can be observed in Figure 4-16((a),(b)), Figure 4-17((a),(b)) and Figure 4-18((a),(b)).

As the dam height increases, so does the weight of the dam, stressing the under laying foundation. This stress creates confinements making the foundation stiffer as the height increases. This effect is clearly observed in Figure 4-13 (b), Figure 4-14 (b) and Figure 4-15 (b), as the dam height increases it shows lowering of amplification and similarity of a_{max}.

b) Comparison of a_{max} for the same ground motion under different foundation

i. Amplification of foundation under 50m

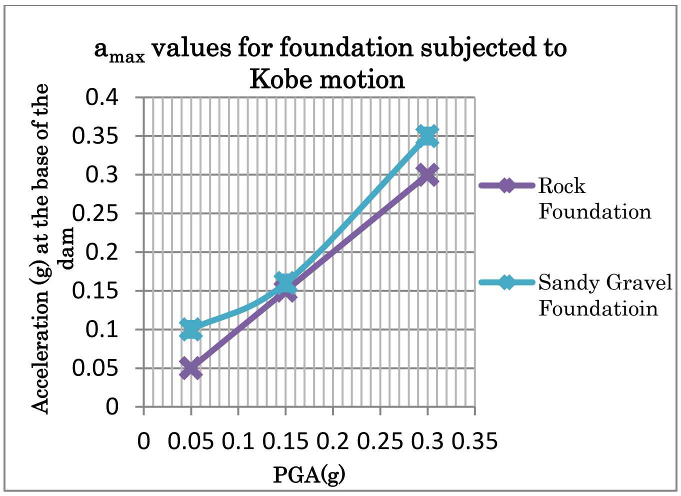

(a)

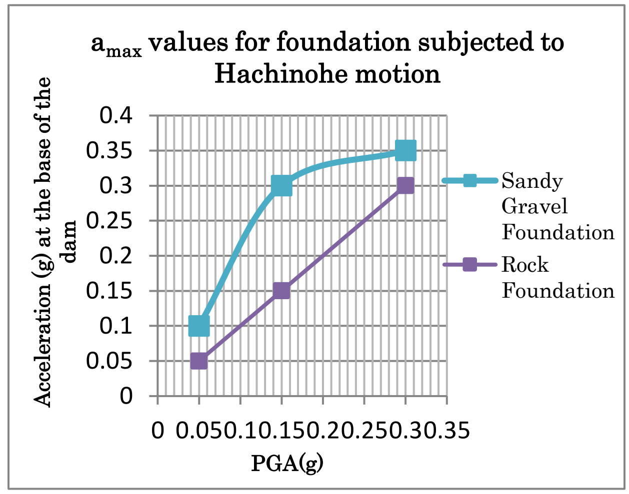

(b)

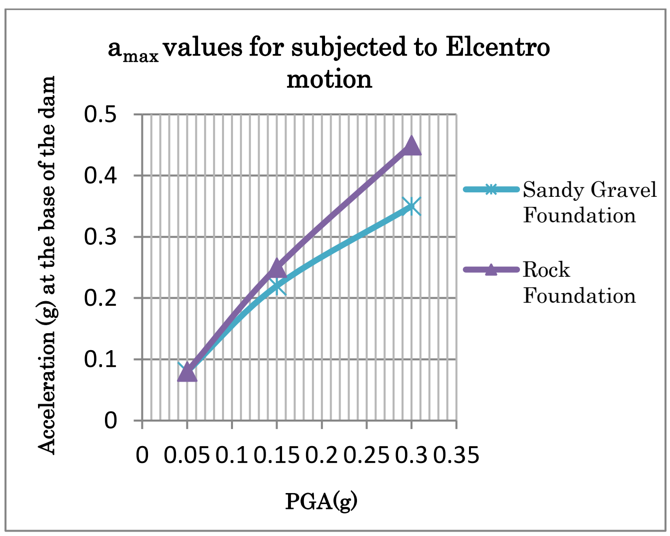

(c)

Figure 4-16: a_{max} values for different foundations found under 50m high dam subjected to same motion - (a) Kobe ground motion, (b) Hachinohe ground motion, (c) Elcentro ground motion

ii. Amplification of foundation under 150m

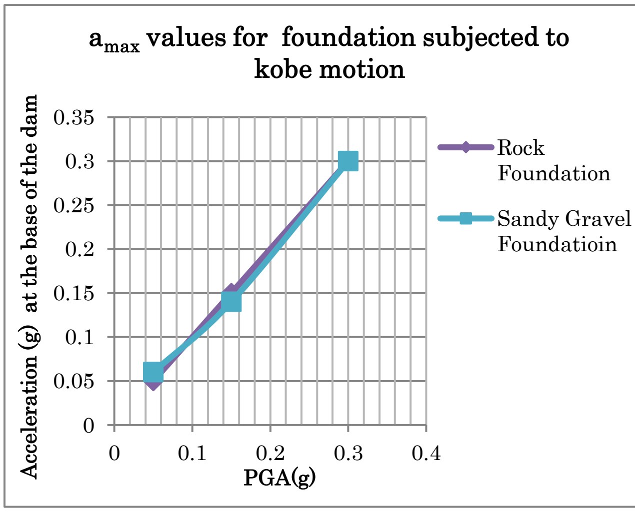

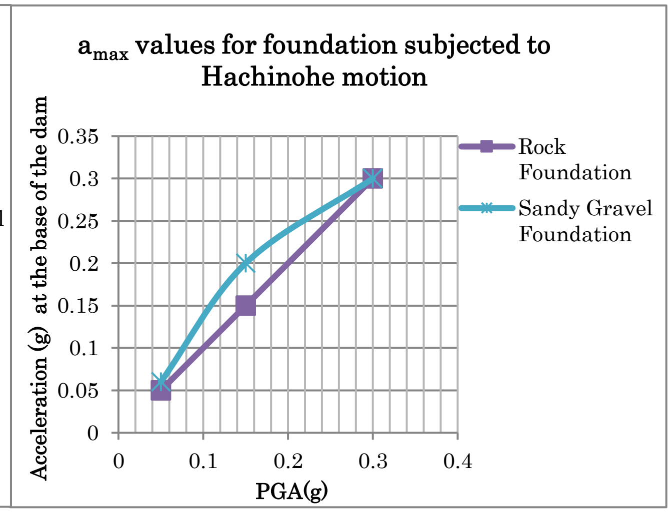

(a)

(b)

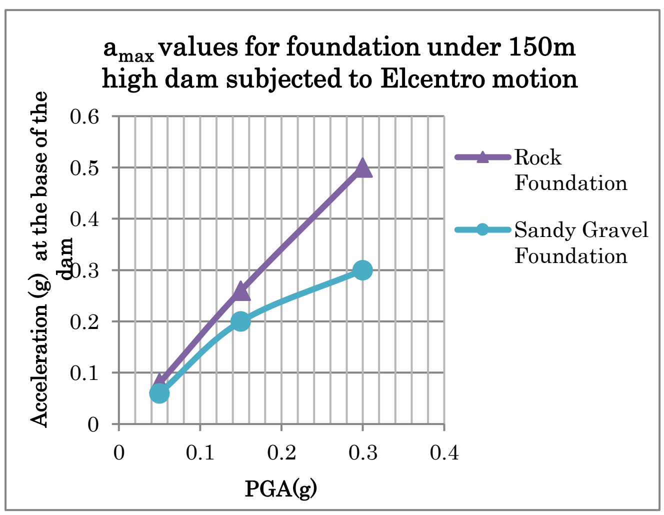

(c)

Figure 4-17: a_{max} values for different foundations found under 150m high dam subjected to same ground motion - (a) Kobe ground motion, (b) Hachinohe ground motion, (c) Elcentro ground motion

iii. Amplification of foundation under 250m

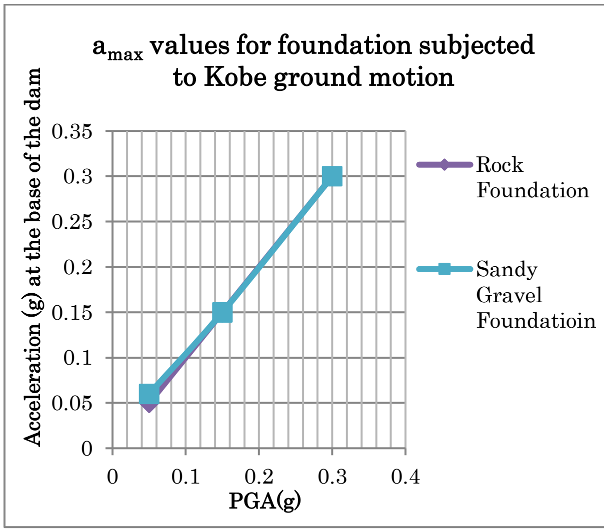

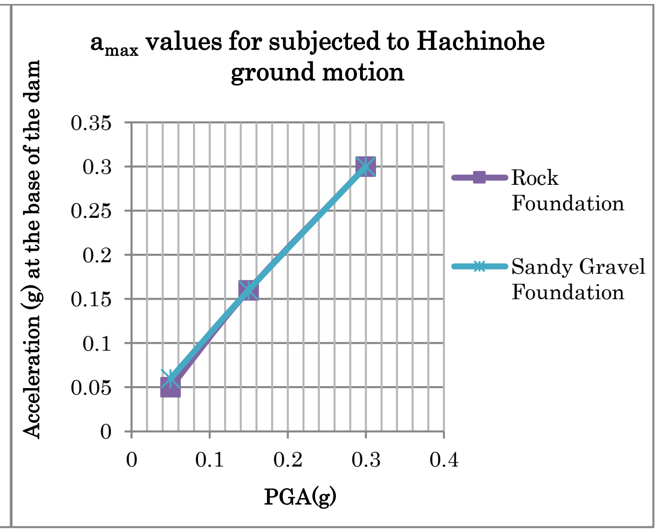

(a) (b)

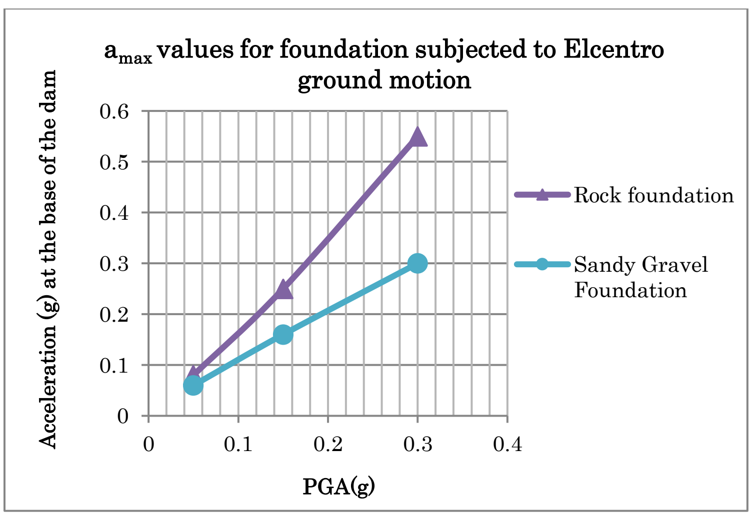

(c)

Figure 4-18: a_{max} value for different foundation found under 250m high dam subjected to same motion - (a) Kobe ground motion, (b) Hachinohe ground motion, (c) Elcentro ground motion

c) Comparison of a_{max} for the same ground motion and foundation but under different dam height

i. Rock foundation

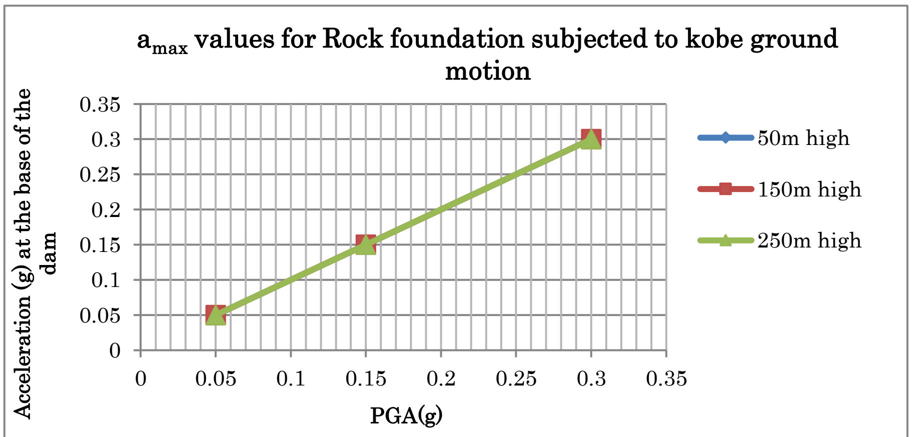

(a)

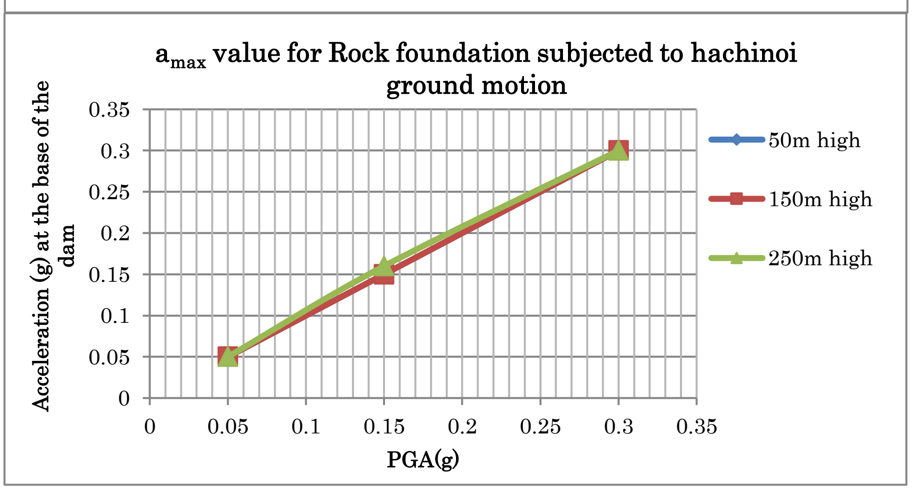

(b)

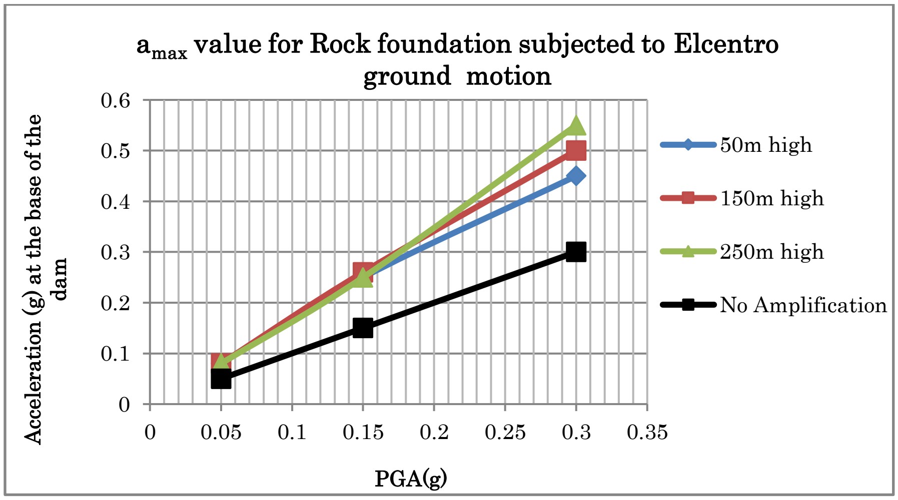

(c)

Figure 4-19: Comparison of a_{max} for Rock foundation under different height dam subjected to motion (a) Kobe ground motion (b) Hachinohie ground motion (c) Elcentro ground motion

ii. Sandy Gravel foundation

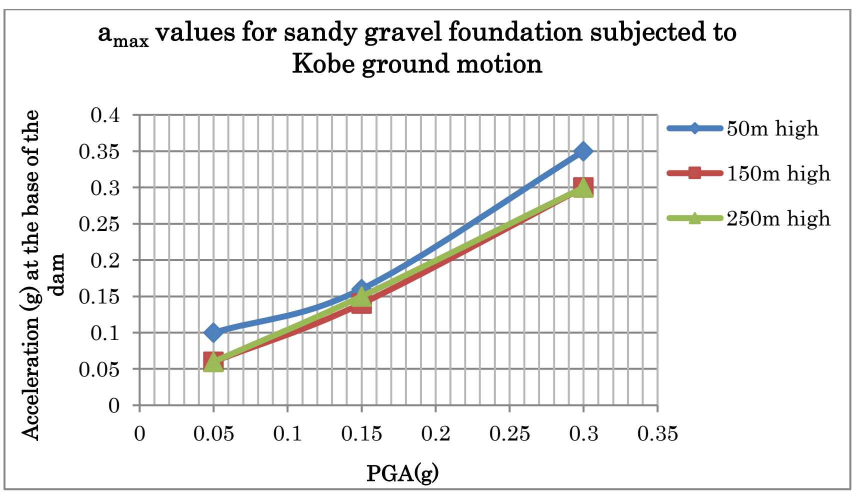

(a)

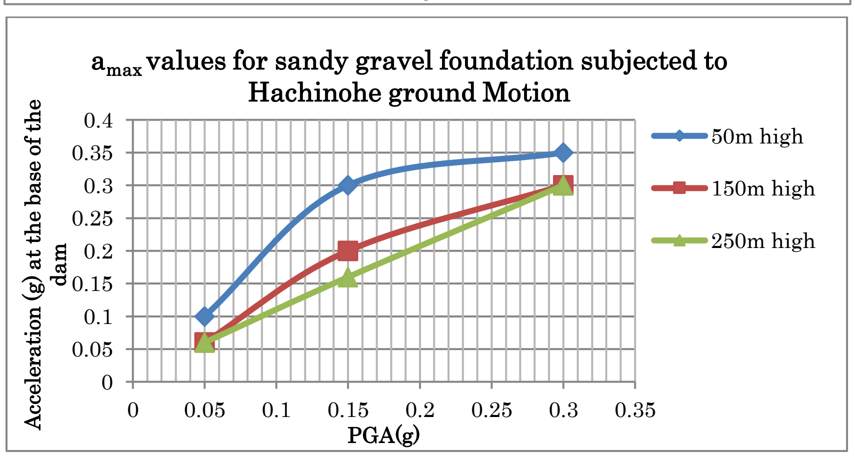

(b)

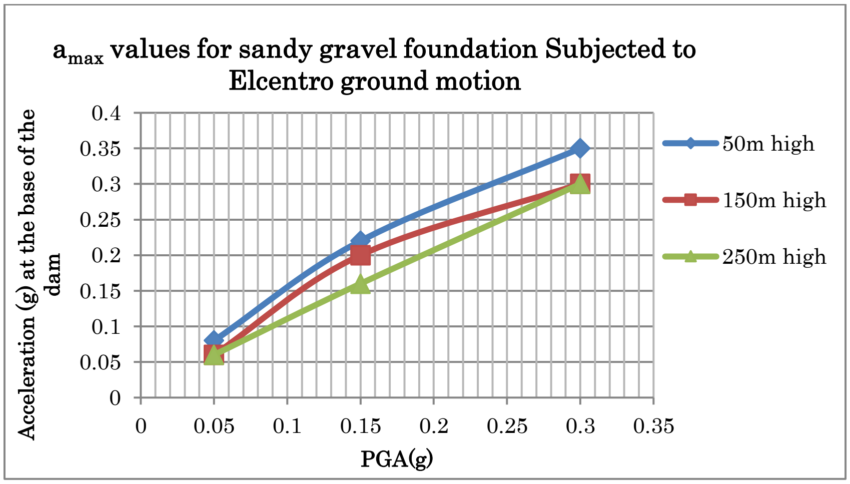

(c)

Figure 4-20: Comparison of a_{max} for sandy gravel foundation under different height dam subjected to motion (a) Kobe ground motion (b) Hachinohe ground motion (c) Elcentro ground motion

As it can be observed in Figure 4-18, Figure 4-19 and Figure 4-20, Rock foundation does not show amplification for the three dam heights under Kobe and Hachinohe ground motion but Elcentro ground motion shows amplification as the PGA increases. The amplification at the foundation level gets larger with increasing dam height in the case of Elcentro ground motion at high amplitude. Ground motion of high amplitude can induce strains consequently causing considerable damping with in the foundation. As the dam height decreases the over burden pressure on the rock decreases, lowering the confinement of the strains and allowing more damping to take place. Figure 4-21 shows the decrease of the strain at the top of the foundation with an increase in dam height. Hence, as the dam height increases the amplification increases.

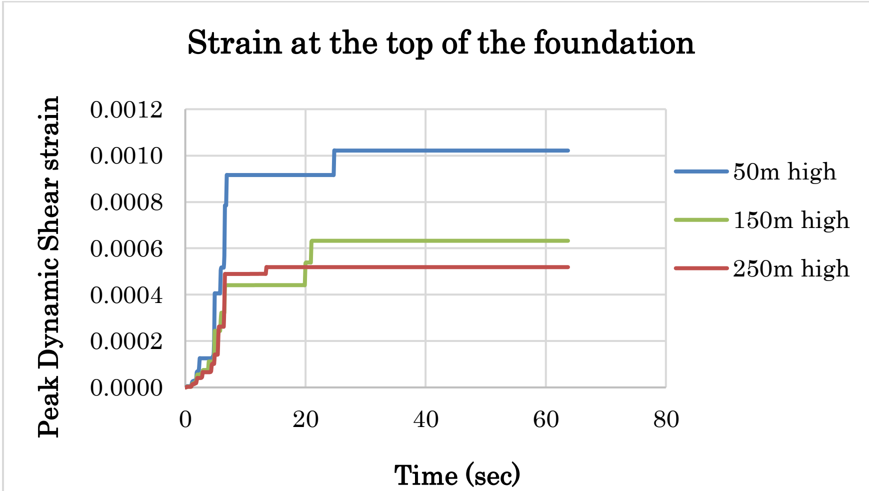

Figure 4-21: Peak Dynamic Shear strain at the top of the foundation.

4.3.1.2. Maximum acceleration in the dam

a) **Comparison a_{max} values for different ground motions under the same foundation**

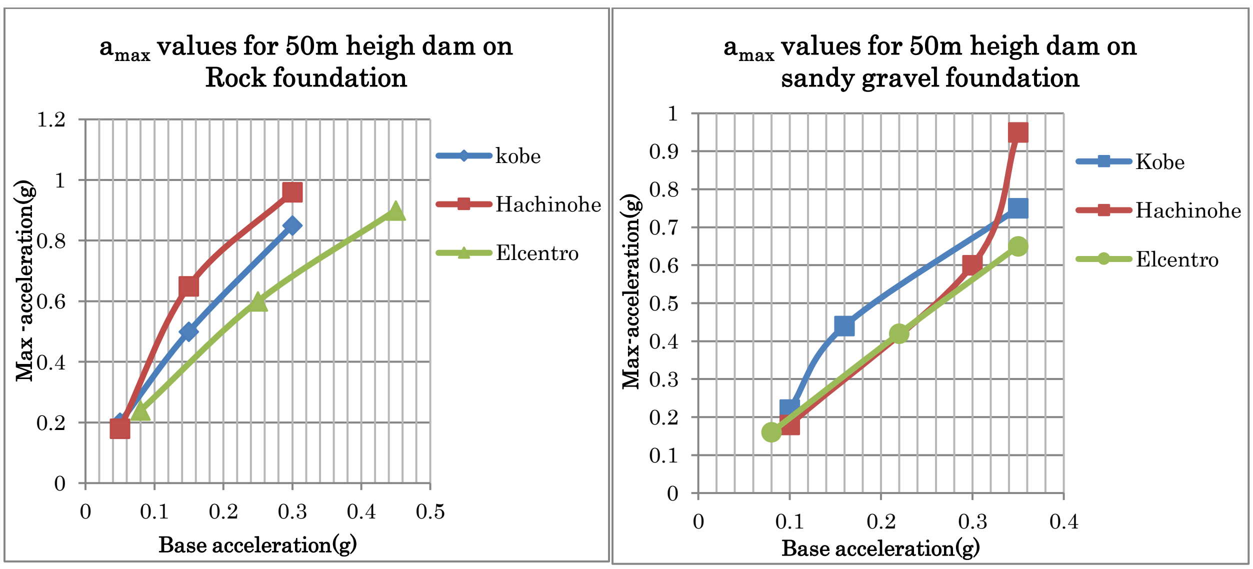

(a) (b)

Figure 4-22: a_{max} value for 50m high dam subjected to different ground motions on top of - (a) Rock foundation, (b) sandy gravel foundation.

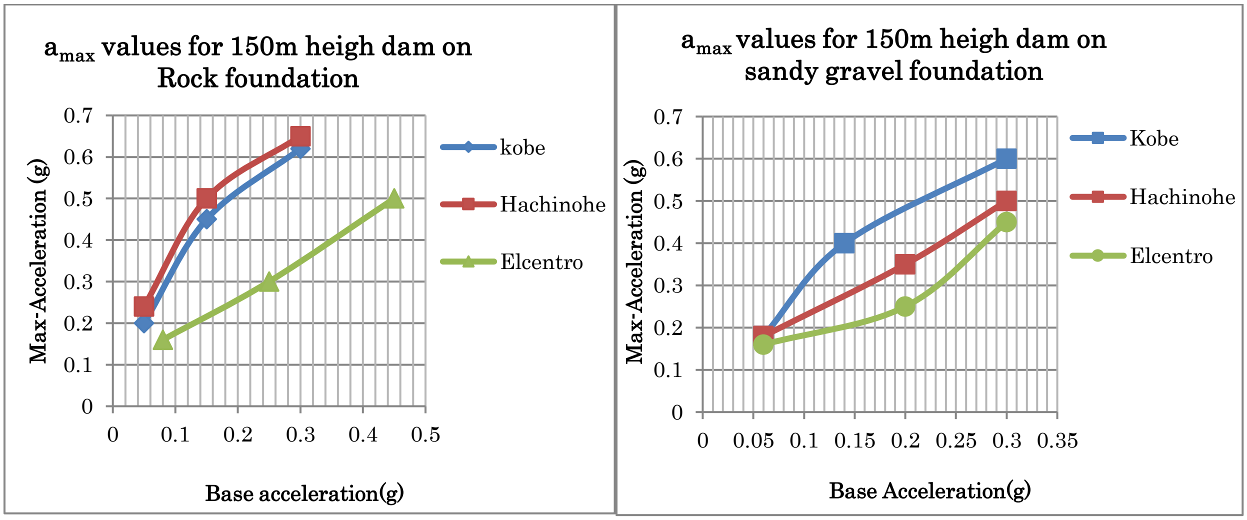

(a) (b)

Figure 4-23: a_{max} value for 150m high dam subjected to different ground motions on top of - (a) Rock foundation, (b) sandy gravel foundation.

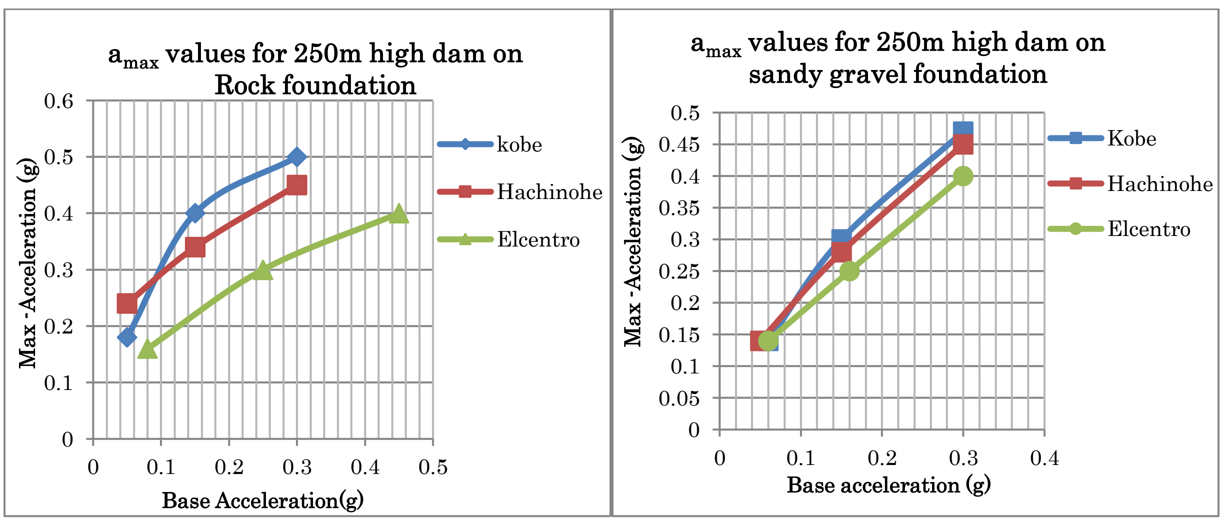

(a) (b)

Figure 4-24: a_{max} value for 250m high dam subjected to different ground motions on top of - (a) Rock foundation, (b) sandy gravel foundation.

From the Figure 4-23, Figure 4-23 and Figure 4-24 it can be observed that Kobe and Hachinohe ground motions with no consistent behaviors show relatively high amplification whereas all the results show low amplification of Elcentro ground motion when compared to the other ground motions regardless of the foundation type, dam height and PGA.

Elcentro and Hachinohe have closer significant duration which is 29.70 sec and 23.89 sec respectively. While Kobe has 8.34 seconds of significant duration showing that duration is not the main cause behind the lower amplification of Elcentro ground motion. If we consider frequency content, Kobe and Hachinohe have lower frequency than Elcentro ground motion. Hence, ground motions with relatively lower frequency is showing amplification on the dam profile regardless of foundation type, height and amplification.

b) Comparison a_{max} values for same ground motion under the different foundations

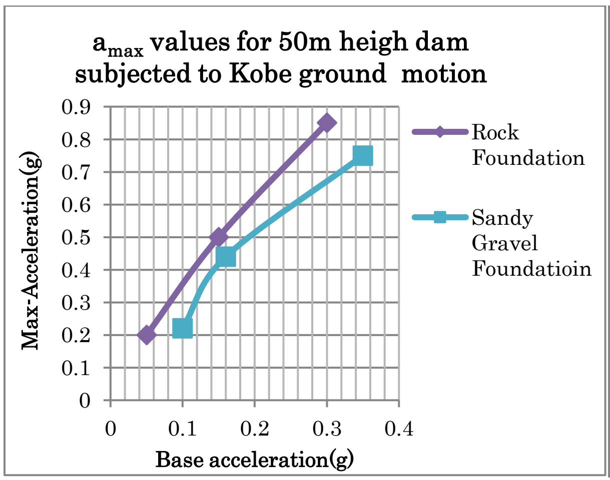

(a)

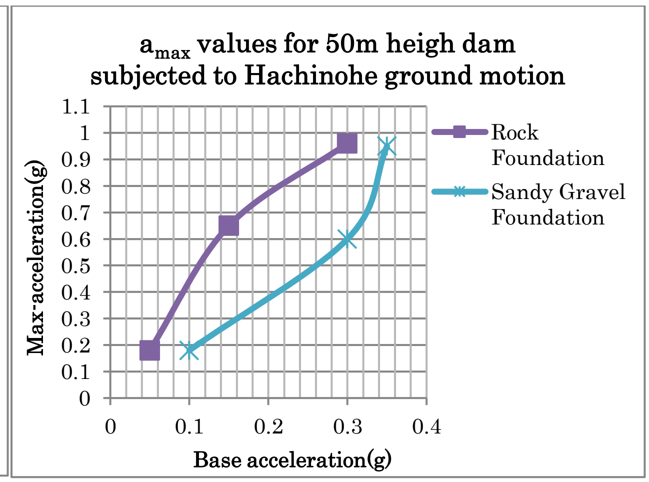

(b)

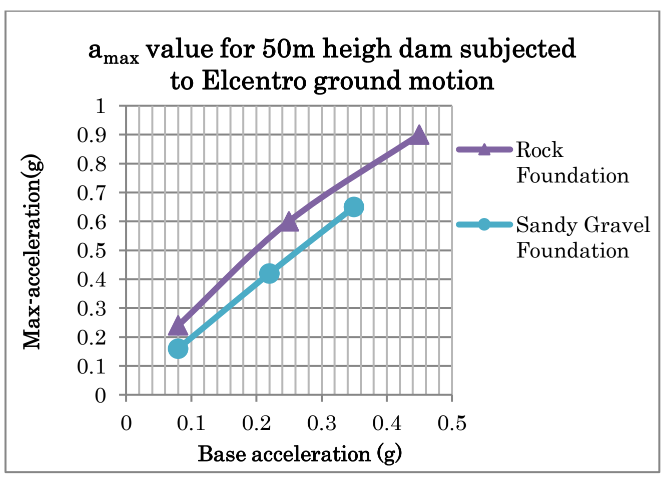

(c)

Figure 4-25: a_{max} value for 50m high dam on top of different foundation subjected to motion - (a)Kobe ground motion , (b) Hachinohe ground motion , (c) Elcentro ground motion

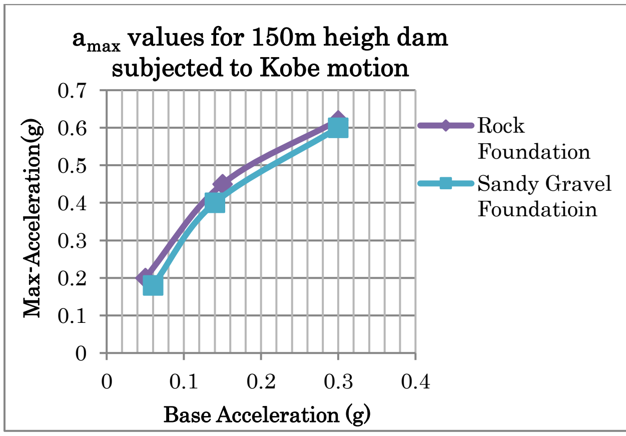

(a)

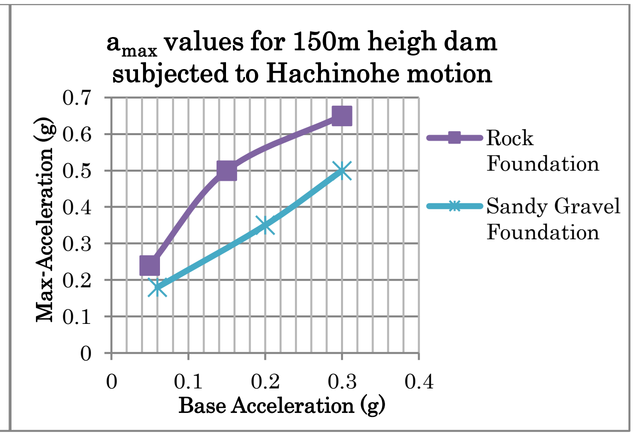

(b)

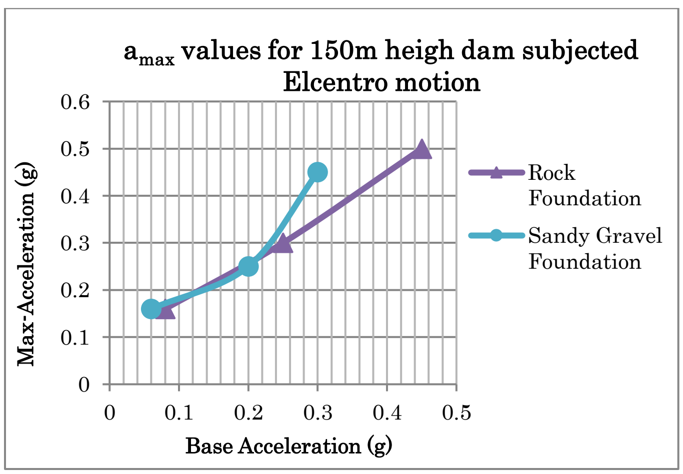

(c)

Figure 4-26: a_{max} value for150m high dam on top of different foundations subjected to the same ground motion - (a)Kobe ground motion , (b) Hachinohe ground motion, (c) Elcentro ground motion

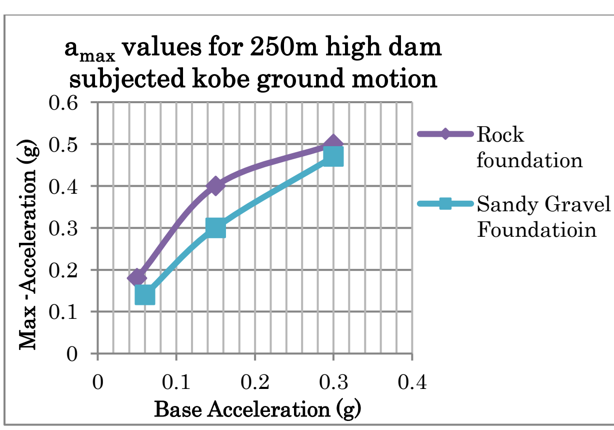

(a)

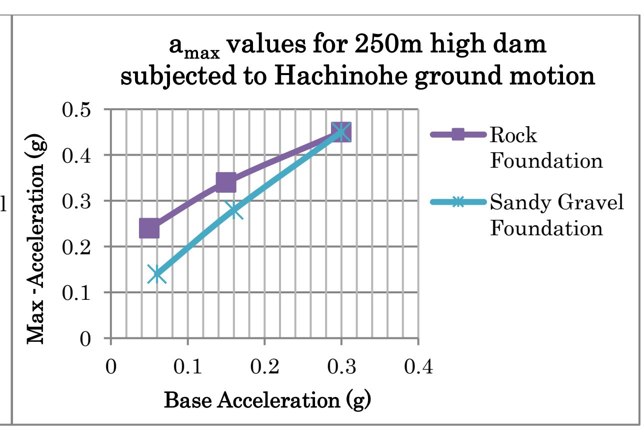

(b)

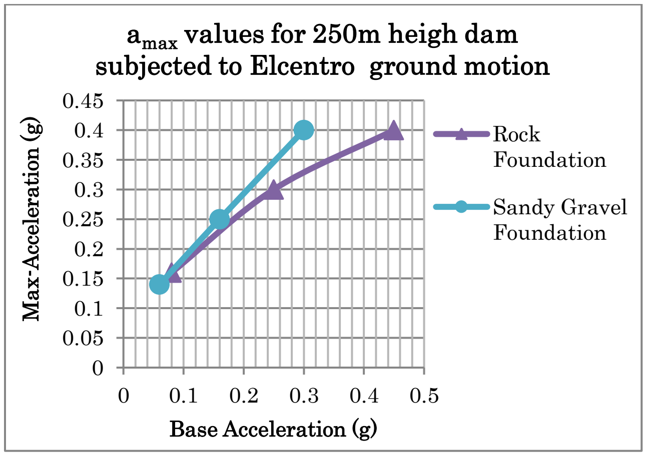

(c)

Figure 4-27: a_{max} value for250m high dam on top of different foundations subjected to the same ground motion - (a)Kobe ground motion , (b) Hachinohe ground motion, (c) Elcentro ground motion

Earlier in this chapter it was observed that base acceleration of dams on sandy gravel foundation are higher for low frequency ground motions. On the other hand, high frequency ground motions show relatively larger amplification on rock foundation.

When it comes to amplification of ground motion within the dam, as can be seen in Figure 4-24 to Figure 4-26, all dam profiles placed on rock foundation show relatively higher acceleration regardless of the base acceleration. As described by Kramer (1996), this might potentially be attributed to radiation/geometric damping, a tendency of an underlying medium to absorb the reflected ground motion waves, of the dam and lowering the overall effect of the ground motion. When the foundations is rock, by keeping the transmitted waves trapped within the dam, ground motion is relatively more amplified.

C. **Comparison a_{max} value for same ground motion and foundation but different height**

i. Rock foundation

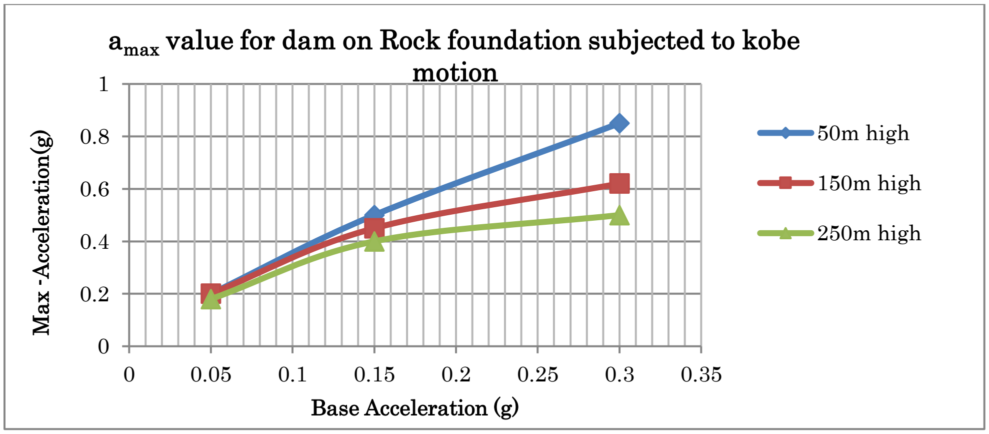

(a)

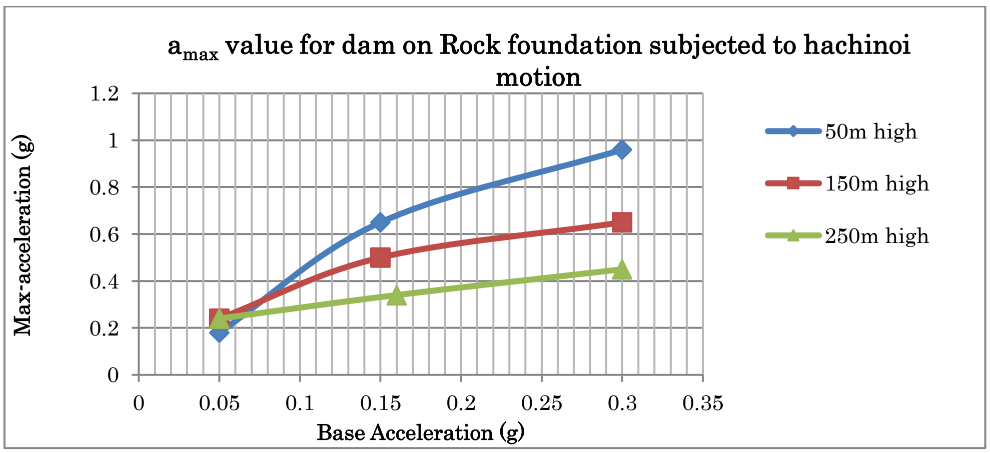

(b)

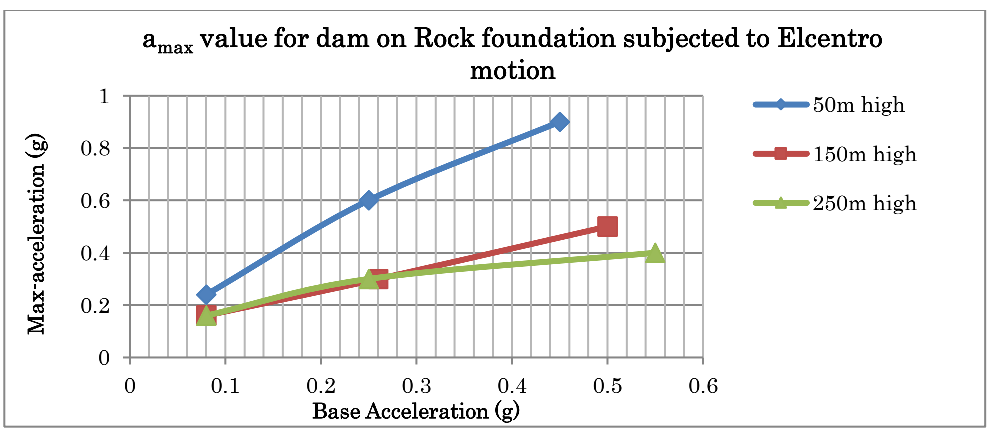

(c)

Figure 4-28: Comparison of a_{max} for dam on top of rock foundation subjected to ground motion (a) Kobe ground motion (b) Hachinohe ground motion (c) Elcentro ground motion.

ii. Sandy gravel foundation

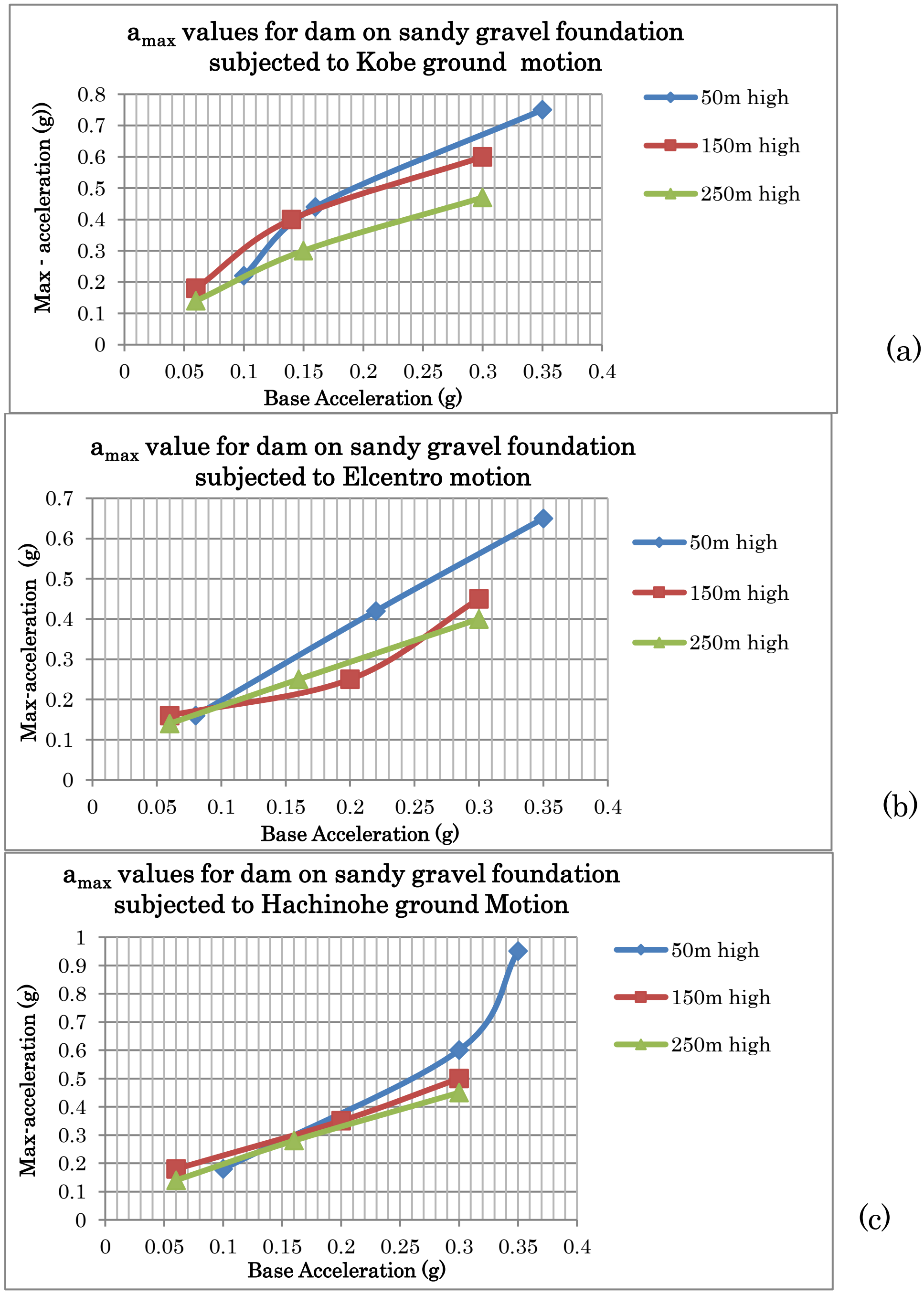

Figure 4-29: Comparison of a_{max} values for dam on top of Sandy gravel foundation subjected to motion (a) Kobe ground motion (b) Hachinohe ground motion (c) Elcentro ground motion

In Figure 4-28 and Figure 4-29 it can be observed that regardless of ground motion, PGA and type of foundation the amplification of ground motion increases with decrease in height. Radiation Damping is a concept that is related to the volume of a material, which increases with increasing height of the dam considered. Spreading of the energy with in the volume material will decrease the effect of the ground motion. Hence, 50m high dam will have higher amplification than 150m which also show higher amplification than 250m high dam.

4.3.1.3. Determining the pseudo-static coefficient (K_h)

Summary of a_{max} values

The plot Figures 4-28 summarize maximum accelerations generated when using three ground motions for each dam height on two different foundation types. Each figure consists of six results for each PGA value.

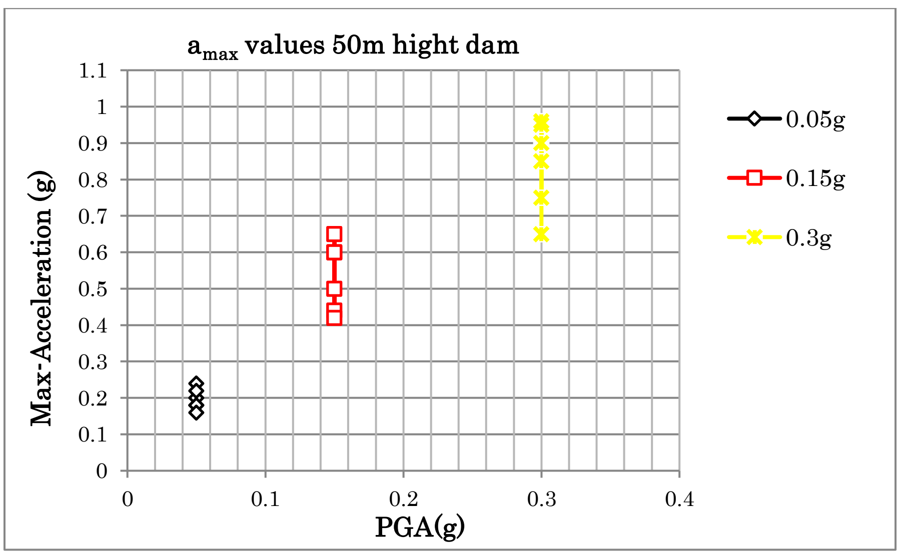

(a)

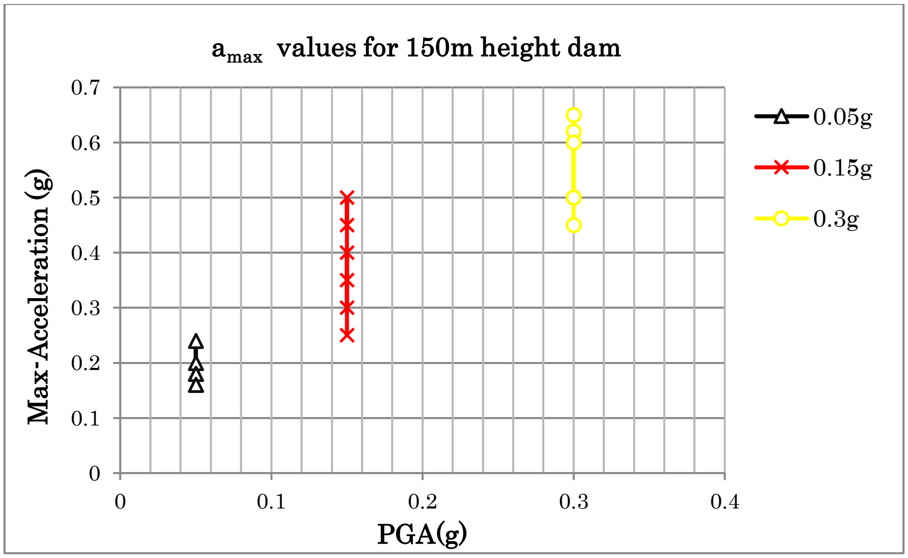

(b)

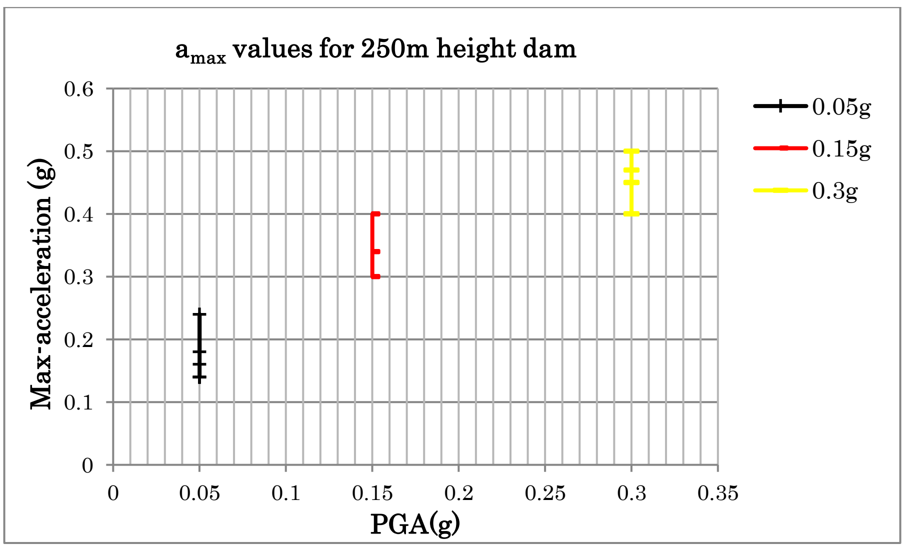

(c)

Figure 4-30: Summary of a_{max} values for the purpose of estimating the pseudo-static coefficient (K_h) for the height (a) 50m (b) 150m (c) 250m

There is some overlapping of the results since there might be results having the same value as can be seen in the Figures 4-28. But it can be observed that the results of each PGA have somehow closer values no matter the type of motion or the foundation type. Table 4-2 shows range of maximum acceleration values from the Figure 4-30.

Table 4-2: Maximum acceleration range

	Maximum acceleration range [a_{max}] range		
Dam Height	**0.05g**	**0.15g**	**0.3g**
50m high	0.14g - 0.26g	0.4g - 0.65g	0.65g - 0.96g
150m high	0.16g – 0.24g	0.25g – 0.5g	0.45g – 0.65g
250m high	0.14g – 0.23g	0.3g – 0.4g	0.4g -0.5g

-For PGA of 0.05g all three heights have closer values.

-For PGA of 0.15g and 0.3g the 50m high dam shows higher a_{max} value than the150m and 250 high dam.

After observing that the shorter dam amplifies more for higher PGA, a 15m height dam on top of rock foundation that has passed the requirements of both SEEP/W and SLOPE/W analyses was analyzed for comparison.

Table 4-3: Maximum acceleration range

	Maximum acceleration range [a_{max}] range		
Dam Height	**0.05g**	**0.15g**	**0.3g**
15m high	0.1g-0.38g	0.3g-0.95g	0.6g-1.4g
50m high	0.14g - 0.26g	0.4g - 0.65g	0.65g - 0.96g

The results with 50m high dam show that the values are close but still there is some greater amplification on 15m high dam when compared to 150m and 250m dam height as shown in Table 4-3.

The effect of an earth quake are represented by a constant horizontal acceleration (Pseudo-static acceleration) that produce inertial forces (pseudo-static force) on the sliding mass (Kramer, 1996). The magnitude of the pseudo-static force are:-

$$F = \frac{W}{g}\,a = \frac{a}{g}\,W \tag{4-1}$$

The ratio of $\frac{a}{g}$ is a represented by a dimensionless coefficient k (pseudo-static coefficient).The horizontal acceleration is considered in this study and the horizontal maximum acceleration is used.

$$k_h = \frac{a_{\max}}{g} \tag{4-2}$$

$$F_h = k_h W \tag{4-3}$$

Maximum acceleration ($a_{\max}$) is expressed in terms of g as presented in Table 4-2 and Table 4-3, there for by simple division and crossing out g, k_h can be found.

4.3.2. Summary of maximum acceleration location

To have a better view where the maximum acceleration is located within the full height of the dam, QUAKE/W output in contour representation is as shown in Figure 4-30. The red portion around the top of the dam corresponding to the area of maximum acceleration. The heights labeled "Max" and "Min" are heights that show the area range that maximum acceleration covers from the top of the dam. The average level between the two locations has been taken to represent the location of the maximum acceleration for every analysis result. This average value for each dam height is given in a range as shown in Table 4-5 with their corresponding PGA Values. The dam shown in Figure 4-31 is a 50m high dam resting on 50m deep sandy gravel foundation subjected to Kobe ground motion at an amplitude of 0.3g. The side slope is 3H: 1V and 2.5H: 1V for upstream and downstream respectively with 0.3H: 1V core side slope.

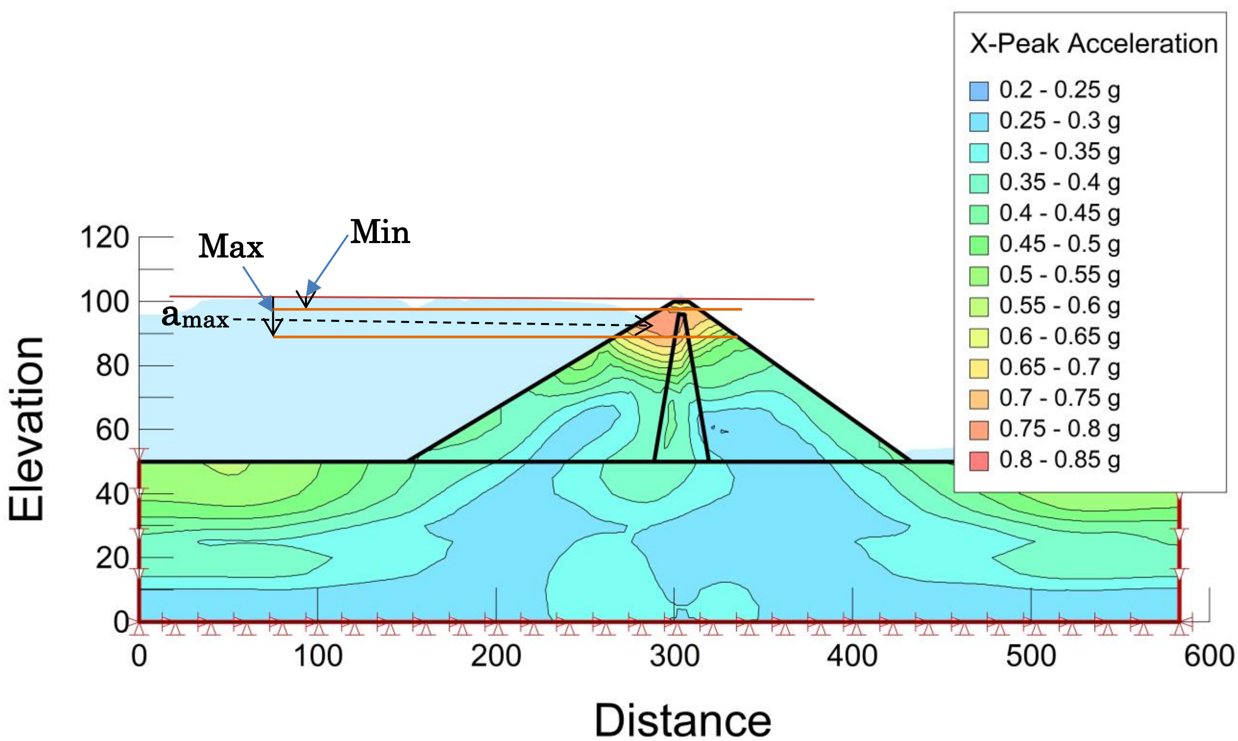

Figure 4-31: sample for showing location of Pseudo-Static coefficient

Table 4-4: Location of maximum acceleration

	Location of Maximum acceleration measured from the crest to the downwards					
Dam Height	0.05g	Avg.	0.15g	Avg.	0.3g	Avg.
50m high	4m - 9m	6.5 m	4m - 10m	7m	4m - 8m	6m
150m high	10m - 40m	25 m	12m - 40m	26m	9m - 36m	22.5m
250m high	6m - 70m	38 m	11m - 68m	39.5m	18m - 59m	38.5m

Approximate location of the maximum acceleration (a_{max}) is found below the top of the dam at a range of 6m- 7m, 22.5m-26m and 38.5m- 39.5m for 50m, 150m and 250m, respectively. It can also be given in form of a ratio of the dam height as shown in Table 4-6. Showing a small deviation from Yu (2012) finding, for 50m high dam the location is from 1/7 to 1/8 of the dam height measured from the crest to the bottom. And for 150m and 250m high dams the location lies in the range of 1/6 to 1/7 of the dam height measured from the crest to the bottom of the dam.

Table 4-5: Location of maximum acceleration in ratio (Average location of maximum acceleration / Dam height)

	Location of Maximum acceleration measured from the crest downwards (Avg. / Dam Height)					
	0.05g		0.15g		0.3g	
Dam Height	Avg.	In fraction (Avg. / Height)	Avg.	In fraction (Avg. / Height)	Avg.	In fraction (Avg. / Height)
50m high	6.5 m	1/8	7m	1/7	6m	1/8
150m high	25 m	1/6	26m	1/6	22.5m	1/7
250m high	38 m	1/7	39.5m	1/6	38.5m	1/6

4.3.3. Summary of earthquake induced permanent deformation

A sample output for Permanent deformation is shown in Figure 4-32. The dam shown is 50m high resting on 50m deep sandy gravel foundation subjected to Kobe ground motion at an amplitude of 0.3g. The side slope is 3H: 1V and 2.5H: 1V for upstream and downstream, respectively, with 0.3H: 1V core side slope. The earthquake induced permanent deformation on the dam are presented in this section.

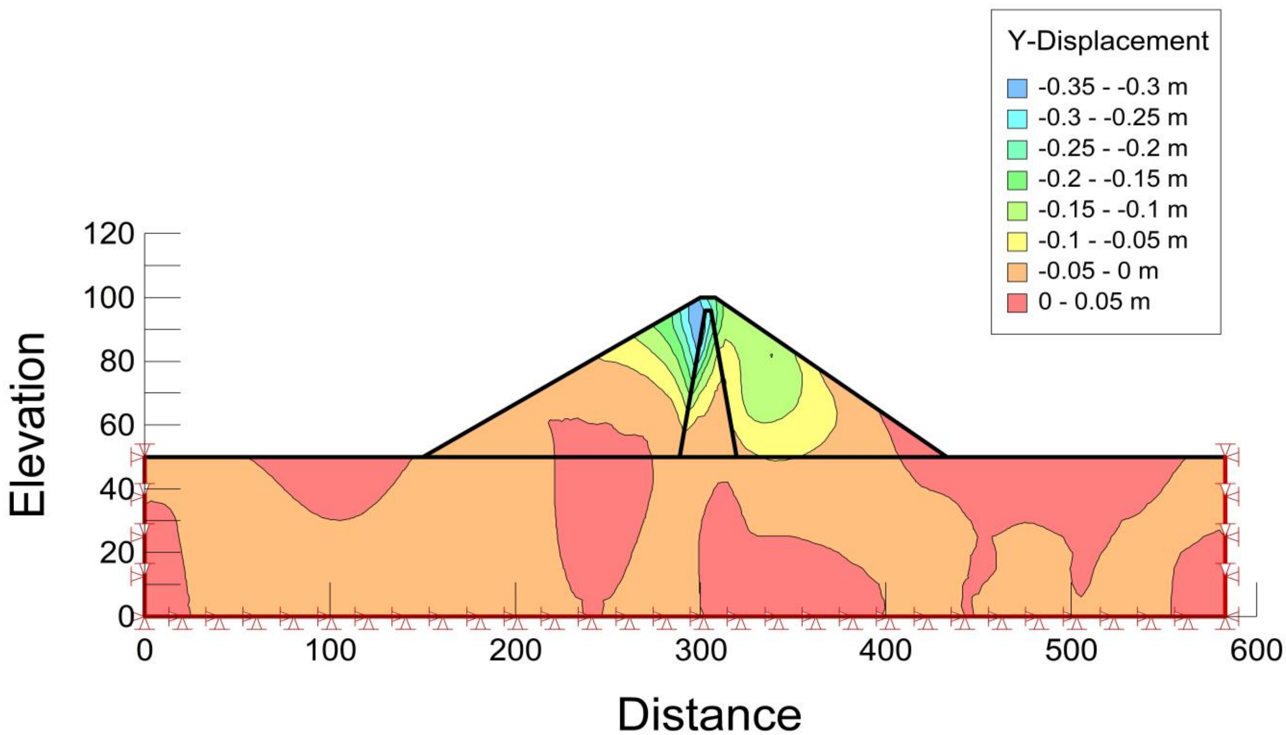

Figure 4-32: Sample software output for Permanent deformation

a) **Comparison of permanent deformation for different ground motions under the same foundation**

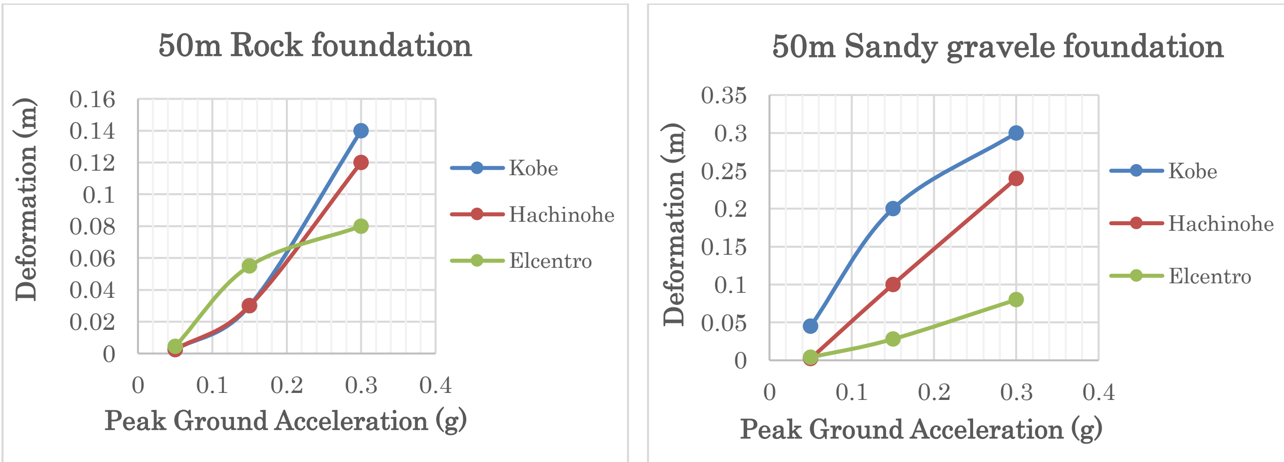

(a) (b)

Figure 4-33: Deformation measurement for 50m high dam subjected to different ground motion on top of- (a) Rock Foundation (b) Sandy Gravel foundation

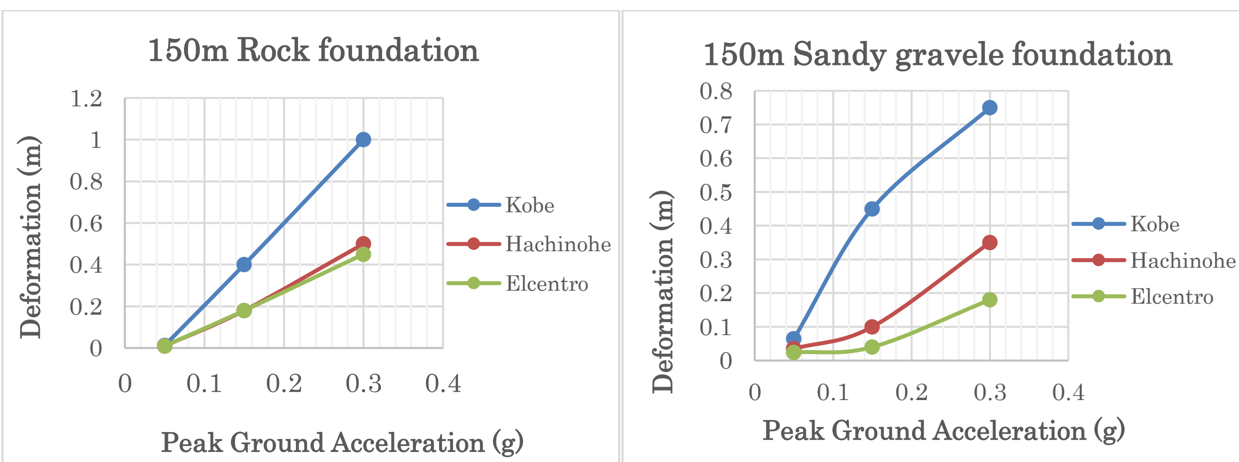

(a) (b)

Figure 4-34: Deformation measurement for 150m high dam subjected to different ground motion on top of- (a) Rock Foundation (b) Sandy Gravel foundation

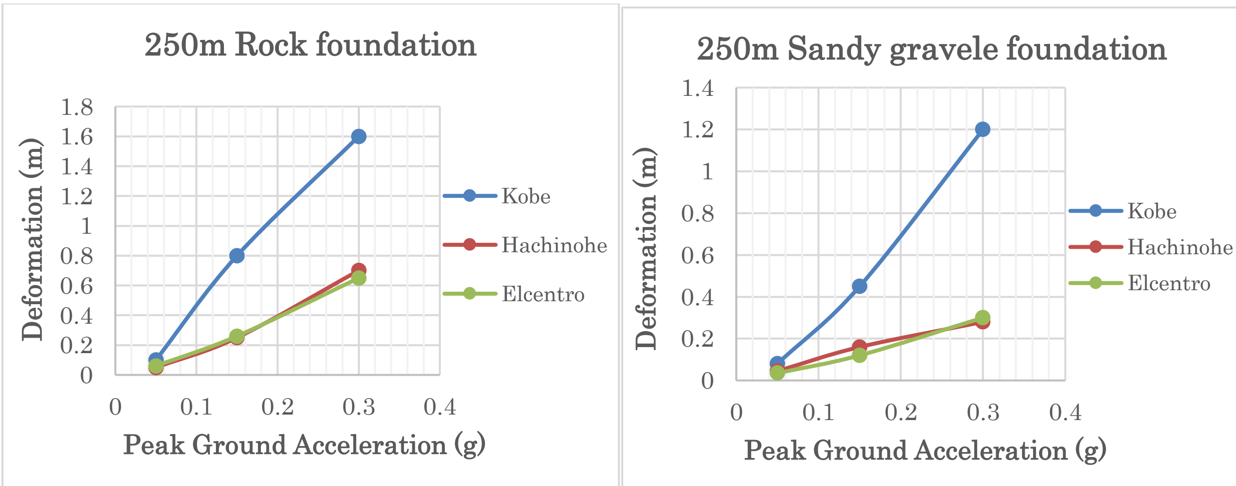

(a) (b)

Figure 4-35: Deformation measurement for 250m high dam subjected to different ground motion on top of- (a) Rock Foundation (b) Sandy Gravel foundation

While observing the maximum acceleration within the dam in the previous section, Kobe and Hachinohe ground motions showed more amplification. As shown in Figure 4-33 to 4-35, Kobe shows more deformation than Hachinohe ground motion. In contrary to what Kramer (1996) suggested ,this might be attributed to Kobe ground motion having more cycle of large amplitude impulse for a longer duration than Hachinohe ground motion as shown in Figure 3-21 and Figure 3-22. In addition to this, Kobe ground motion contains more small-frequency content as could be seen in Figures 3-23 and to Figure 3-24 compared with the other two ground motions.

b) Comparison of permanent deformation for same ground motion under the different foundations

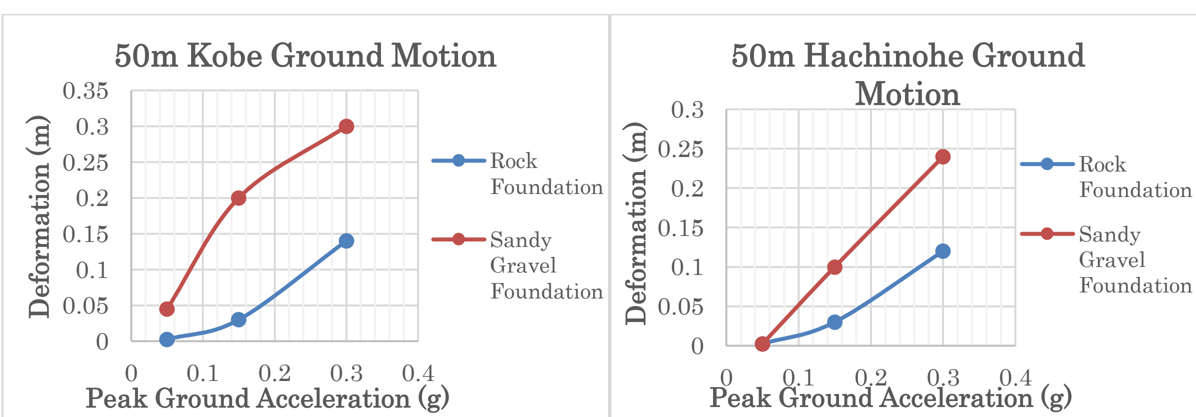

(a) (b)

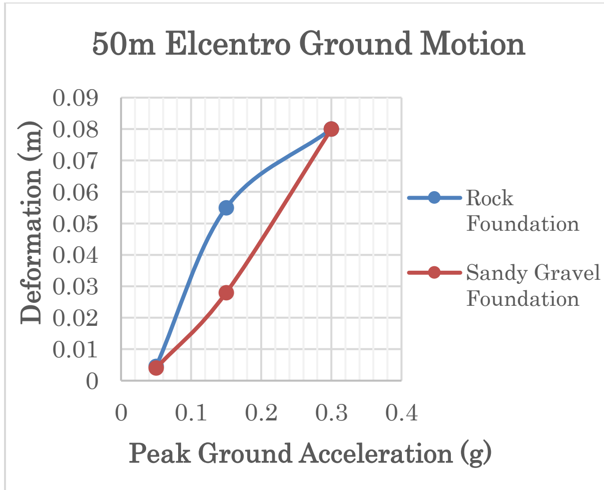

(c)

Figure 4-36: Deformation measurement for 50m high dam on top of different foundation subjected to- (a) Kobe ground motion, (b) Hachinohe ground motion, (c) Elcentro ground motion

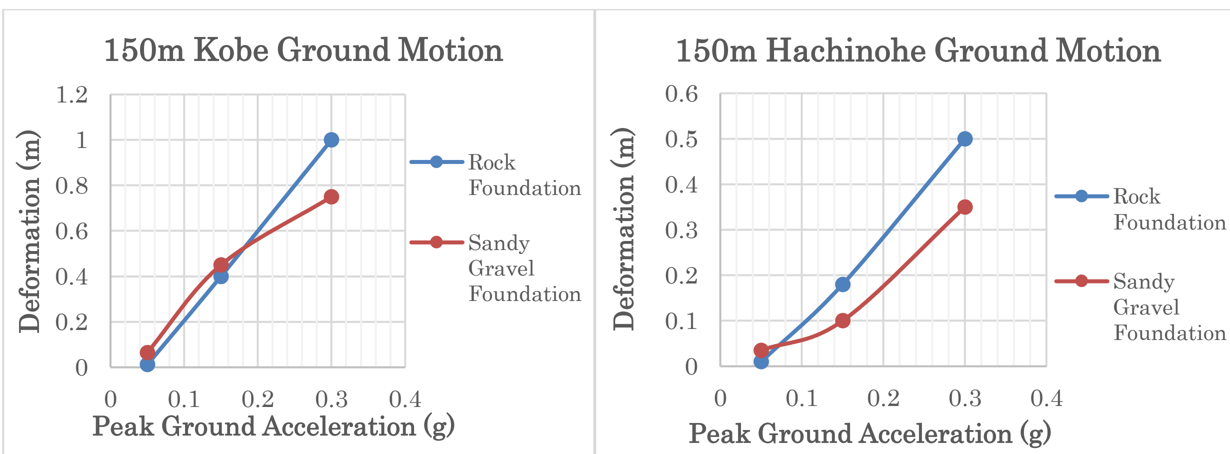

(a) (b)

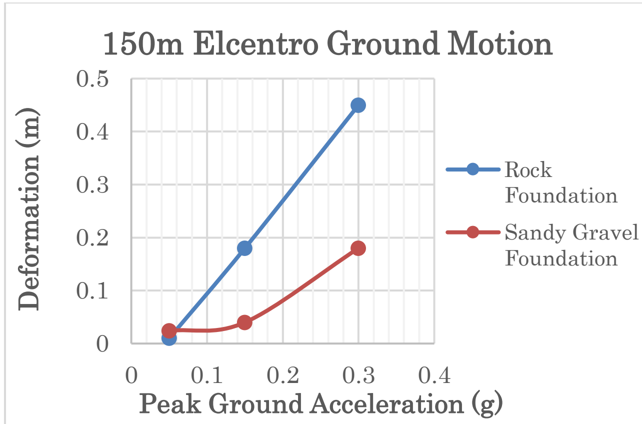

(c)

Figure 4-37: Deformation measurement for 150m high dam on top of different foundation subjected to- (a) Kobe ground motion, (b) Hachinohe ground motion, (c) Elcentro ground motion

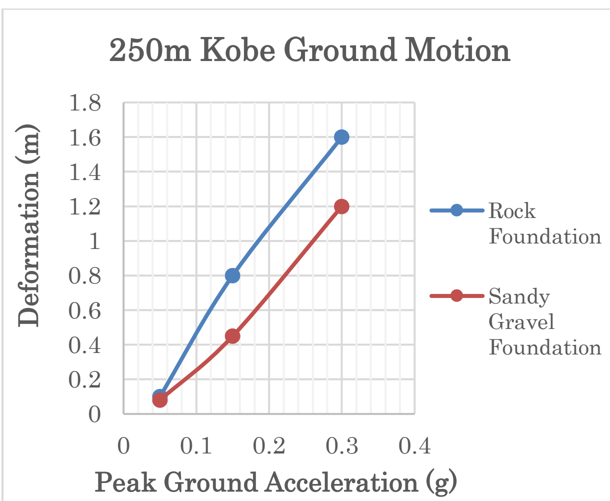

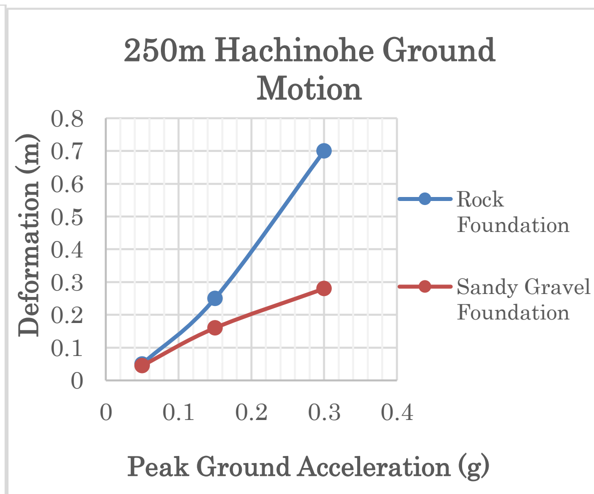

(a)

(b)

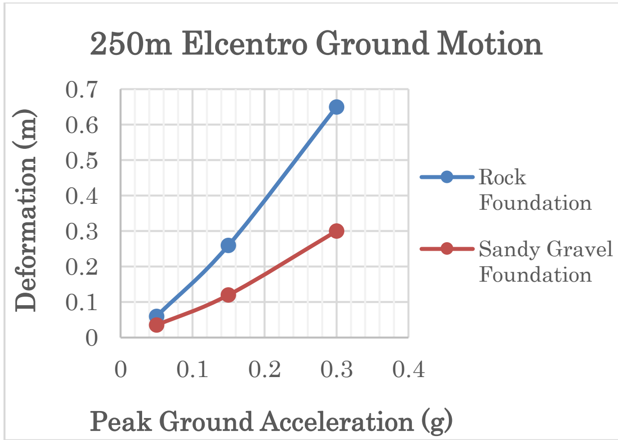

(c)

Figure 4-38: Deformation measurement for 250m high dam on top of different foundation subjected to- (a) Kobe ground motion, (b) Hachinohe ground motion, (c) Elcentro ground motion

Except from two 50m high dam cases (Figure 4-36 (a) and (b)), where dams on sandy gravel foundation show higher deformation, the remaining (Figure 4-36(c), Figure4-37 and Figure 4-38) show relatively higher deformation resting on rock foundation. It has been observed on the previous section that dam resting rock foundation seem to have higher Maximum acceleration values, hence the higher deformation.

c) **Comparison a_{max} value for same ground motion and foundation but different height**

i. Rock foundation

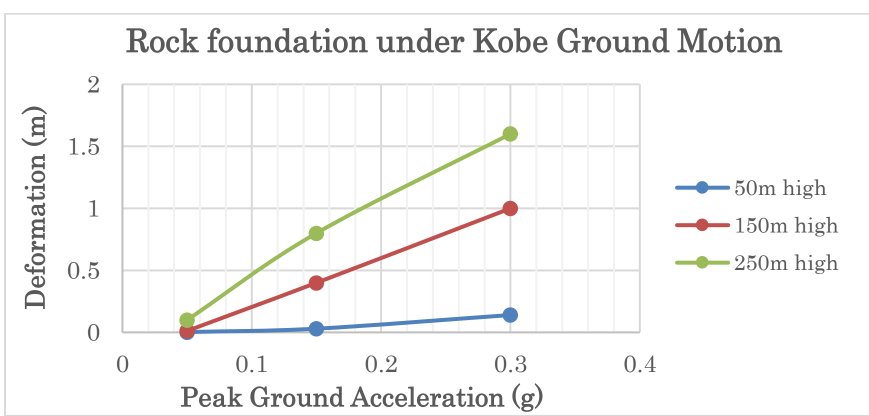

(a)

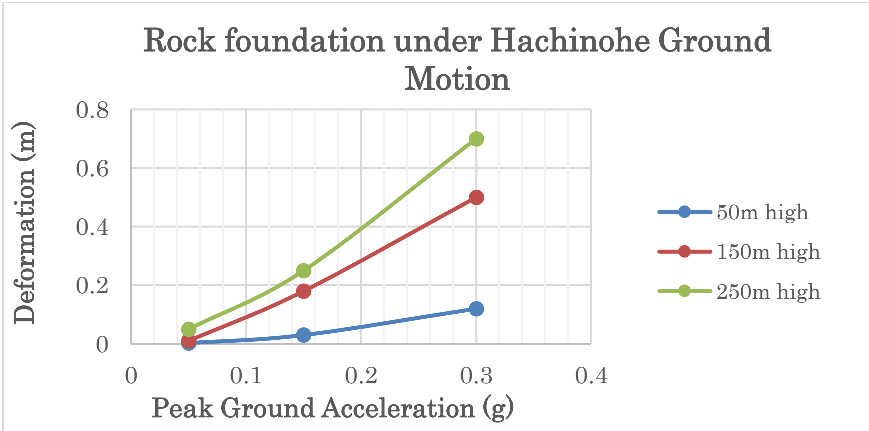

(b)

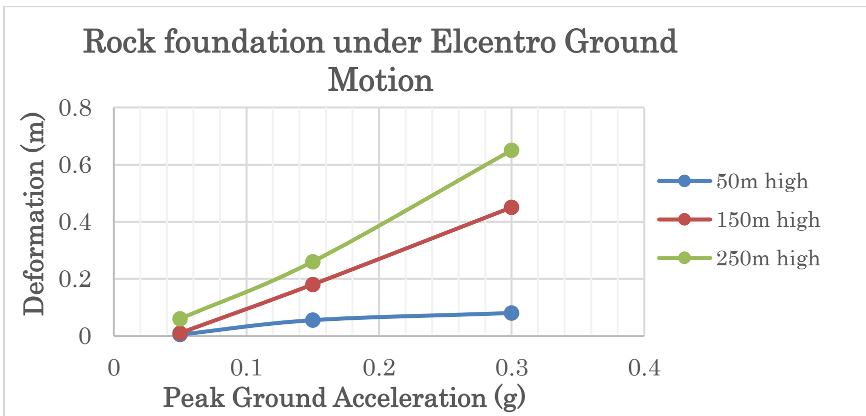

(c)

Figure 4-39: Deformation measurement for dam on top of rock foundation subjected to –(a) Kobe ground motion, (b) Hachinohe ground motion ,(c) Elcentro Ground motion

ii. Sandy Gravel foundation

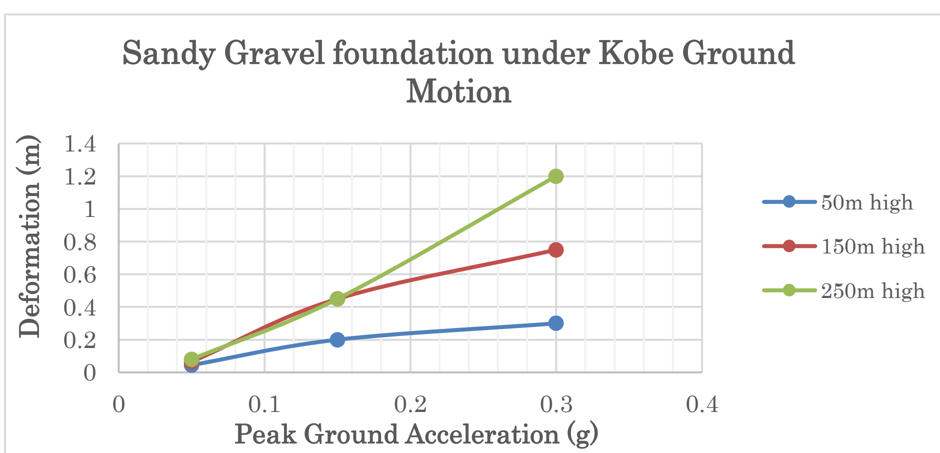

(a)

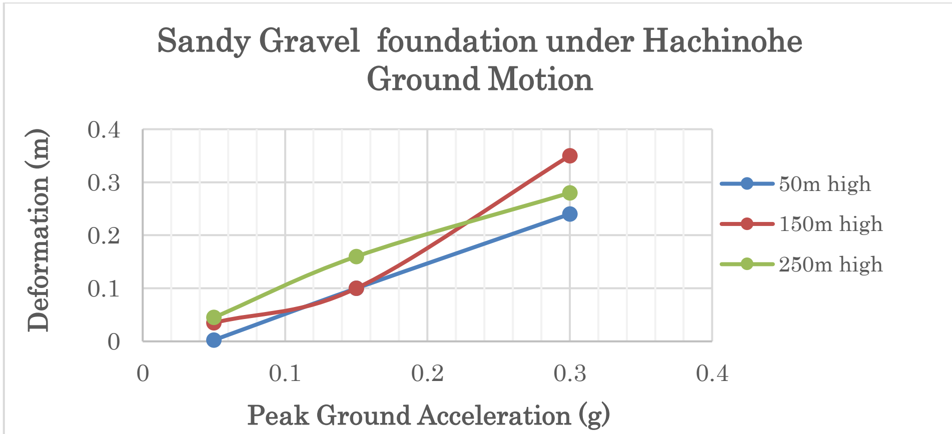

(b)

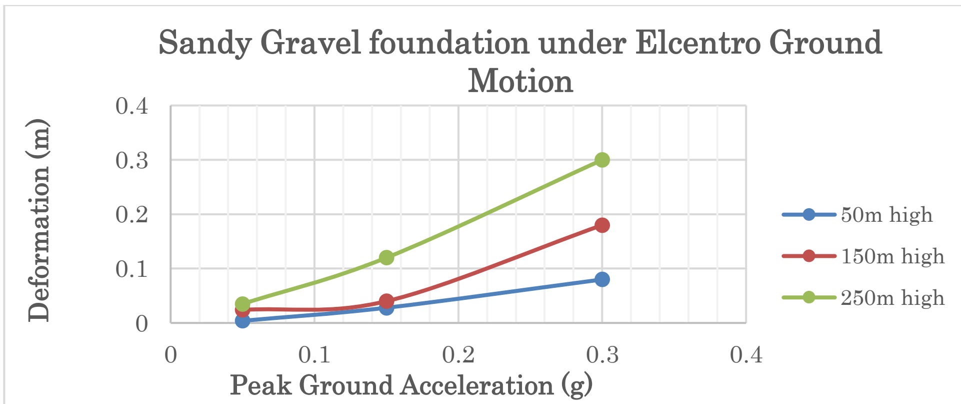

(c)

Figure 4-40: Deformation measurement for dam on top of Sandy Gravel foundation subjected to –(a) Kobe ground motion, (b) Hachinohe ground motion ,(c) Elcentro Ground motion

As the height of the dams increased, a higher permanent displacement was observed. The permanent deformation also increased with increasing intensity of ground motion as shown in Table 4-7, Figure 4-38, and Figure 4-39. For a certain peak ground acceleration, the ratio of the peak permanent deformation to the total height of the dam was found to be similar as shown in Table 4-8.

Table 4-6: Permanent deformation range in meter.

	Range of permanent deformation in meter		
Dam Height	**0.05g**	**0.15g**	**0.3g**
50m high	0.0024m-0.045m	0.028m-0.2m	0.08m-0.3m
150m high	0.01m-0.065m	0.04m-0.45m	0.18m-1m
250m high	0.035m-0.1m	0.12m-0.8m	0.28m-1.6m

Table 4-7: Permanent deformation range in percent.

	Range of permanent deformation in percent ((deformation in meter / height of the dam)*100)		
Dam Height	**0.05g**	**0.15g**	**0.3g**
50m high	0.0048%-0.09%	0.056%-0.4%	0.16%-0.6%
150m high	0.0067%-0.043%	0.0267%-0.3%	0.12%-0.66%
250m high	0.014%-0.04%	0.048%-0.32%	0.112%-0.64%

CHAPTER 5 - CONCLUSION AND RECOMMENDATION

5.1. Conclusion

The main goal of this study is to analyze, zoned earth dam behavior under the action of different ground motions with peak ground accelerations for two different types of foundations. Based on the study, the following conclusions may be drawn:-

- Ground motion amplification of a dam foundation is affected by the over lying dam weight. As the dam height resting on sandy gravel foundation increases, so does the weight of the dam, stressing the under laying foundation. This stress creates confinements making the foundation stiffer which shows lowering of amplification and similarity of $a_{max.}$
- Ground motions with lower frequency shows amplification on the dam profile regardless of foundation type, height and base acceleration.
- To observe the effect of foundation on amplification potential of a dam, three different profiles laying on both Rock and Sandy Gravel foundation have been analyzed with different ground motion and PGA. The dams placed on rock foundation show relatively higher amplification regardless of the base acceleration. This might potentially be attributed to radiation/geometric damping, a tendency of an underlying medium to absorb the reflected ground motion waves, of the dam and lowering the overall effect of the ground motion. When the foundations is rock, by keeping the transmitted waves trapped within the dam, ground motion is relatively more amplified.
- The concept of Radiation Damping is also related to the volume of a material, which increases with increasing height of the dam considered. Spreading of the energy with in the volume material will decrease the effect of amplification of the ground motion, which increases with decrease in height.
- Pseudo-static coefficient (k_h) can be seen to increase with decrease in dam height for larger PGA values. In the case of lower PGA's, however, k_h is

observed to have approximately the same value for the types of foundations and ground motions considered.

- Approximate location of the pseudo-static coefficient (k_h) is observed to move further from the crest with increasing dam height. The average distance measured from the crest, when expressed as a fraction of the dam height, is observed to be 1/7 to1/8 in shorter dams and 1/6 to 1/7 in higher dams for all PGA and ground motions considered.
- Permanent deformation caused by the earthquake were analyzed succeeding dynamic analysis. Dams placed on rock foundation show relatively higher deformation corresponding to the high amplification. And Ground motion having more cycle of large amplitude impulse for a longer duration happens to cause higher deformation irrespective of the total duration of the ground motion.

5.2. Recommendation

Further detailed investigation in dam amplification can be done by varying slope, material property, dam shape, zones and type of core so as to see the effect they bring on both the dam and foundation. Additional analyses can also be done to see the effect of changing parameters on liquefaction susceptibility of a dam.

References

Ambraseys, N. (1960). On the seismic behaviour of earth dams . *World conference on Earthquake Engineering*, (pp. 331-358).

Anastasiadis, A., Klimis, N., Makra, K., and Margaris, B. (2004). On seismic behavior of a 130m high rockfill dam: An integrated approach. . *In Proceedings of the 13th World Conference on Earthquake Engineering, Vancouver, BC, Canada*.

Anastasiadis,A.,Klimis,N., Makra,K., and Margaris,B. (2014). On seismic behavior of 130m high rockfill dam: an integrated approach. *13 WCEE,canada*.

Anis,M., and Jawaid,S.A. (2016). Seismic Slope Stability. *International Jornal Of Computational Engineering Research (IJCER)*.

Beadenkopf, E. (2013). *Federal Guidelines for Inundation Mapping of Flood Risks Associated With Dam Incidents and Failures.*

Bowels,J.E.,. (1997). *Foundation analysis and design.* Mc Graw- Hill companies.

Briaud, J. L. (2013). *Geotechnical Engneering: unsaturated and saturated soils.* New Jersey: John wiley &sons.

Budhu, M. (2010). *Soil Mechanics and foundation .* Arizona: john wiley &son.

Chern,J.C. and Tsai, M.S. (2001). Seismic safety analysis of Earth dam. *International Conference on recent earthquake Enineering and soil dynamics*.

Chopra,A.K. (2017). Dynamics Of Structures-Theory And Applications to. *Earthquake Engineering*.

Duncan,J.M., Wright,S.G., and Brandon,T.L. (2014). *Soil Strength and Slope Stabillity.* John Wiley & Sons,Inc.

Engomoen, B., Witter,D.T., Knight, K. and Luebke,T.A. (2014). *Design standards No 13: Embankment Dams.* U.S. Department of the interior Bureau of Reclamation.

Fell, R., Macgregor,P., and Stapedon,D. (2015). *Geotechnical Engineering of Dams.* Taylor & francis group.

Garg, S. K. (1980). *Irrigation Engineering and Hydraulic Structures.* Delhi: Khanna Publishers .

GEO-SLOPE International Ltd. (2007). *Dynamic Modeling with QUAKE/W.* canada: GEO-SLOPE International Ltd.

GEO-SLOPE International Ltd. (2007). *Seepage Modeling with SEEP/W.* canada: GEO-SLOPE International Ltd.

GEO-SLOPE International Ltd. (2007). *Stability Modeling with SLOPE/W.* canada: GEO-SLOPE International Ltd.

GEO-SLOPE International Ltd. (2007). *Stress-Deformation Modeling with SIGMA/W.* canada: GEO-SLOPE International Ltd.

Gikas V., and Sakellariou,M. (2008). Settlement analysis of the Mornos earth dam: Evidence from numerical mdeling and geodetic monitoring . *Engineering structures*.

Gopal, P., and Kumar ,D.T.K . (2014). Slope stability and seepage analysis of earthen dam of a summer storage tank. *International Jornal of Innovative Research in Advanced Engneering (IJIRAE)*.

Haile, M. (1996). *Critical assessment of site effect parameters for strong ground motion prediction(Ph.D.dissertation),.* Tokyo: Tokyo Institute of Technology.

Hardin, B. (1978). The nature of stress-strain behavior for soils. *Earthquake Engineering and soil Dynamics-Proceedings of the ASCE Geotechnical Engineering Division Speciality Conference*.

Hardin, B.O. and Drnevich,V.P. (1972). Shear modulus and damping in soils. *Journal of Soil Mechanics and Foundation Div*.

Hynes -Griffin, M.E and Franklin, A.G. (1984). *Rationalizing the seismic coefficient method.* Vicksburg , Mississipi : Army Engineer Waterways Experiment Station .

ICOLD. (2010). Selecting Seismic Parameteres For Large Dams-B148. *International Commision Of Large dams*.

Idriss,I.M. and Duncan,J.M. (1988). *Earthquake response analysis of embankment dams.* Boston: Springer.

Kandolkar,S.S. , Aldonkar,S.S., and Savoikar,P.P. (2010). Rational pseudo- static stability analysis of embankment. *Indian Geotechnical Confrence -2010, GEOtrendz*, pp.16-18.

Khanna, R.,Datta,M., and Ramana,G.V. (2017). Influence of core thickness on stability of down stream slope of earth and rockfll dams under end-of-constructtion and stesdy-state-seepage:comparison. *Internationa jornal of geotechnical Engineering*, 8.

Kramer, S. L. (1996). *Geotechnical Earthquake Engineering*. Upper saddle river: Prentice- hall.

Makdisi, F.I. & Seed, H.B . (1978). Simplified procedure for estimating dam and embankment earthquake - induced deformations. *Journal of Geotechnical and Geoenviromental Engineering* .

Makdisi, F.I., and Seed, H.B. (1977). *A simplified procedure for estimating earthquake induced deformation in dams and embankments.* Berkeley,California.

Marcuson, W. (1981). *Moderator's report for session on earth dams and stability of slopes under dynamic loads.* St. Louis Missouri: in proc. Int. conf. on recent adv. In Geotech. Earthquake Engrg. And Soil Dyn.

Mayne,P.W. and Rix, G.J . (1993). G max -qc relationship for clays. *Geootechnical Testing Journal*, 54-60.

Moayed, R. Z., and Ramzanpour, M. F. . (2008). Seismic behavior of zoned core embankment dam. *EJGE, Bundle C*.

Moayed,R.Z.,and Ramanpour,M.F. (2008). seismic behavior of zoned core embankment dam. *EJGE,Vol.13,Bund.A*.

Newmark, N. (1965). Effect Of Earthquake on Dams And Embankment. 22.

Novak,P.,Moffat, A.I.B.,Nalluri,C., and Narayanan,R. (2017). *Hydraulic Structures.* London & NewYork: Taylor & Francis.

Özener, P., & Beşli, B. K. (2014). Investigation of effect on seismic response characteristics of earthfill and rockfill dams.

Pariseau, W. G. (2006). *Design analysis in rock mechanics.* Taylor & Francis.

Parish, Y., Sadek, M, and Shahrour, I. (2009). Numerical analysis of the seismic behaviour of earth dam. *Natural Hazards & Earth system Sciences*.

Raja,M.A., and Mashwari,B.K. (2016). Behavior of earth dams under seismic load considering Nonlinearity of the soil. *open jornal of civil engineering*.

Rampello,S., Cascone,E., and Grosso,N. (2009). Evaluation of seismic response of a homogeneus earth dam. *Soil Dynamics and Earthquake Engineering*.

Rao, S. S. (2004). *The Finite Element Method In Engineering .* Miami: Elsevier Science & Technology Books.

Seed, H.B. (1979). Considerations in the earthquake-resistant design of earth and rockfill dams. *Geotechnique,29*.

Seed,H.B. and Idriss, I. M. (1970). *Soil Moduli and Damping Factors For Dynamic Response Analyses.* Berkeley,California: shannon and Wilson, Inc.

Seed,H.B., and Martin, G. R. (1966). The seismic coifficient in earth dam design. *Journal of soil Mechanics and Foundations*.

Seed,H.B., Wong,R.T., Idriss, I.M., and Tokimatsu, k. (1986). Moduli and Dampng Factors For Dynamic Analysis Of Cohesionless Soils. *J.Geotech Engrg.*, 17.

Seged,H., and Haile,M. (2010). Earthquake induced Liquefaction analysis of Tendaho Earth-fill Dam. *ERA Vol.27*, 10.

Selcuk,M., and Terzi,N.U. (2015). Seismi Response of Ambar Dam to Recorded Earthquake. *international journal of advanced research*.

Sun,J.I.,Golesorkhi,R., and Seed,H.B. (1988). *Dynamic Moduli and Damping Ratios For Cohesive Soils.* Berkeley: National Science Foundation.

Terzaghi, K. (1950). Mechanism of landslides. *Application of geology to engineering practice ,Geological society of america*.

United States Department Of Interior, B. O. (1987). *Design of Small Dams .* Washington, DC 20402-93238.

United States Department Of Interior, B. O. (2012). *Section27-Seismic Risk for Embankment.*

Yu, L., Kong,X., and Xu, B. (2012). Seismic Response Characteritics of Earth and Rock fill. *15WCEE,USBOA*.

Appendices

Appendix-1- Dam Dimension

Detailed dam dimension 50m, 150m and 250m high dam are presented in Figure A.1.1. to A.1.3.

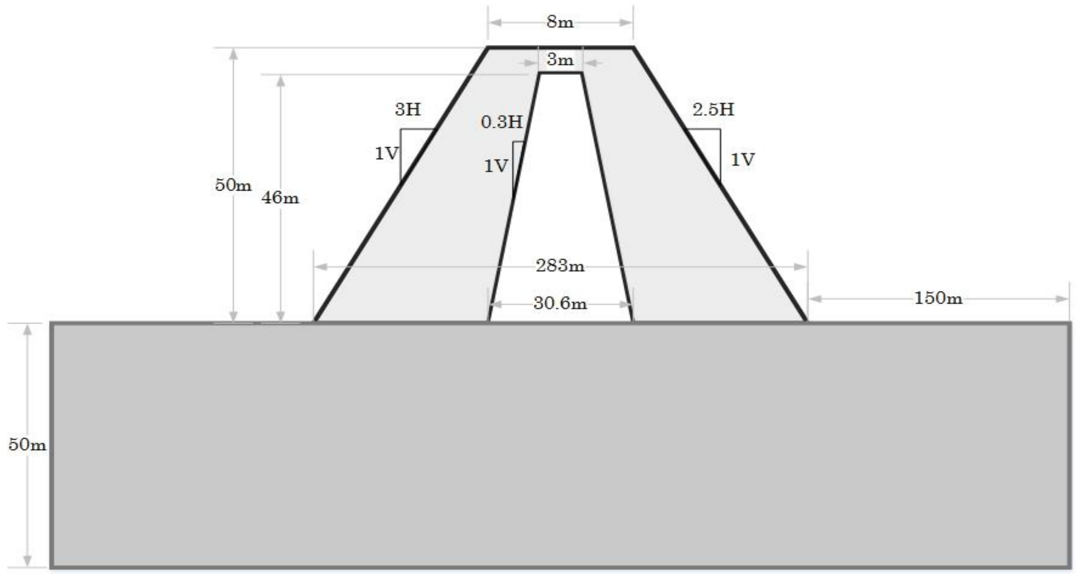

Figure A.1.1: 50m high dam

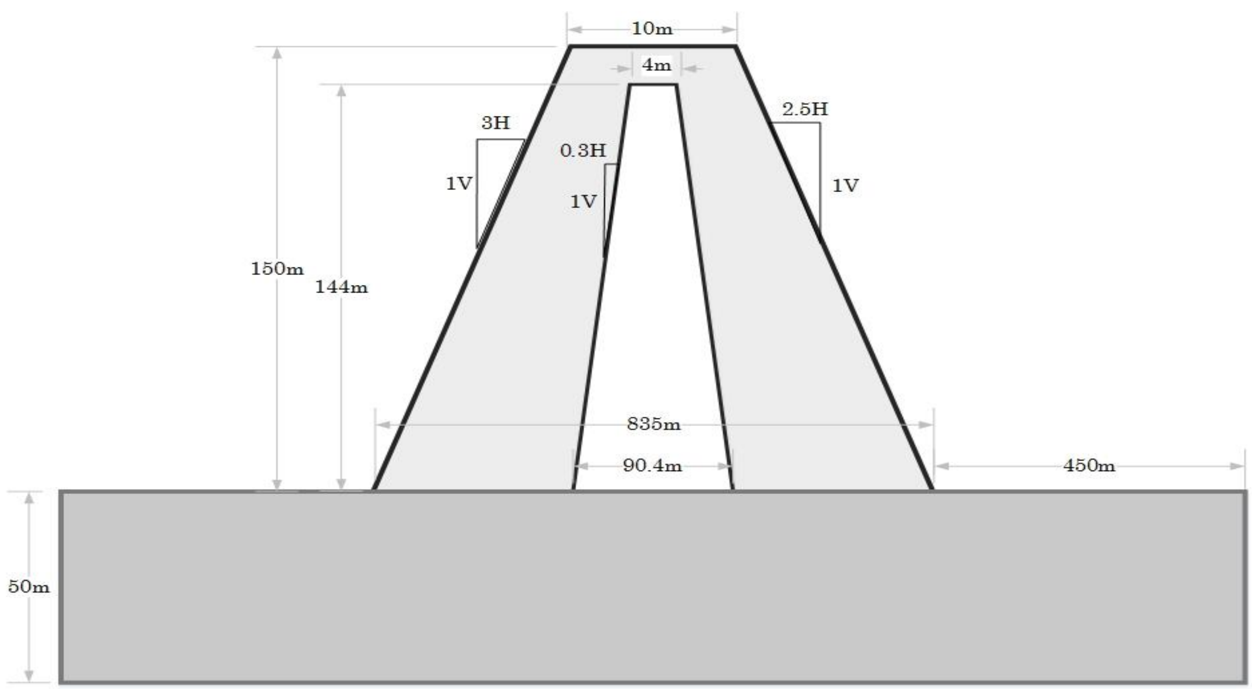

Figure A.1.2: 150m high dam

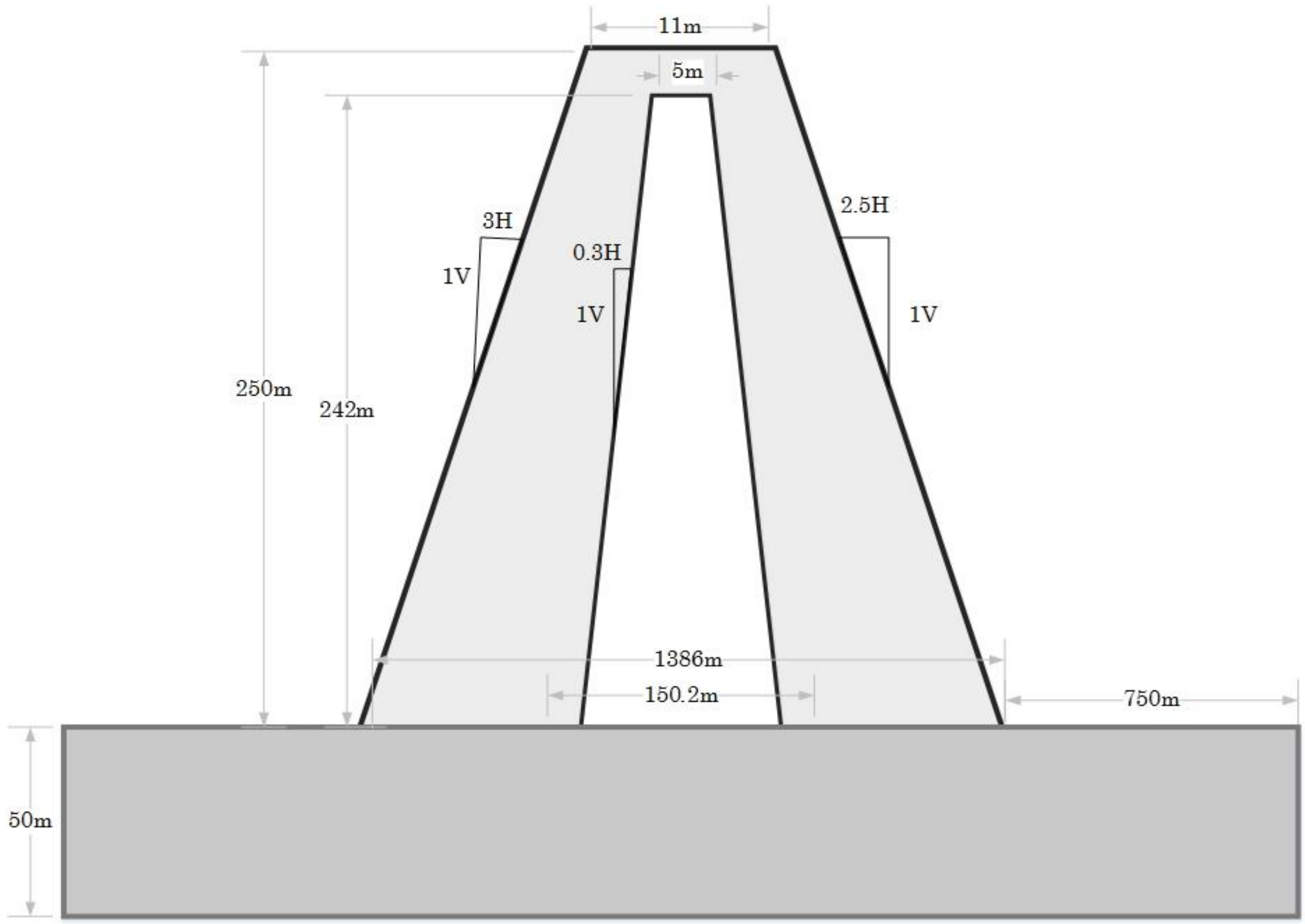

Figure A.1.3: 250m high dam

Appendix-2- GeoStudio modeling

Starting from modeling the cross section of the dam to assigning material property and a sample result is presented orderly in this section from Figure A.2.1 to A.2.9.

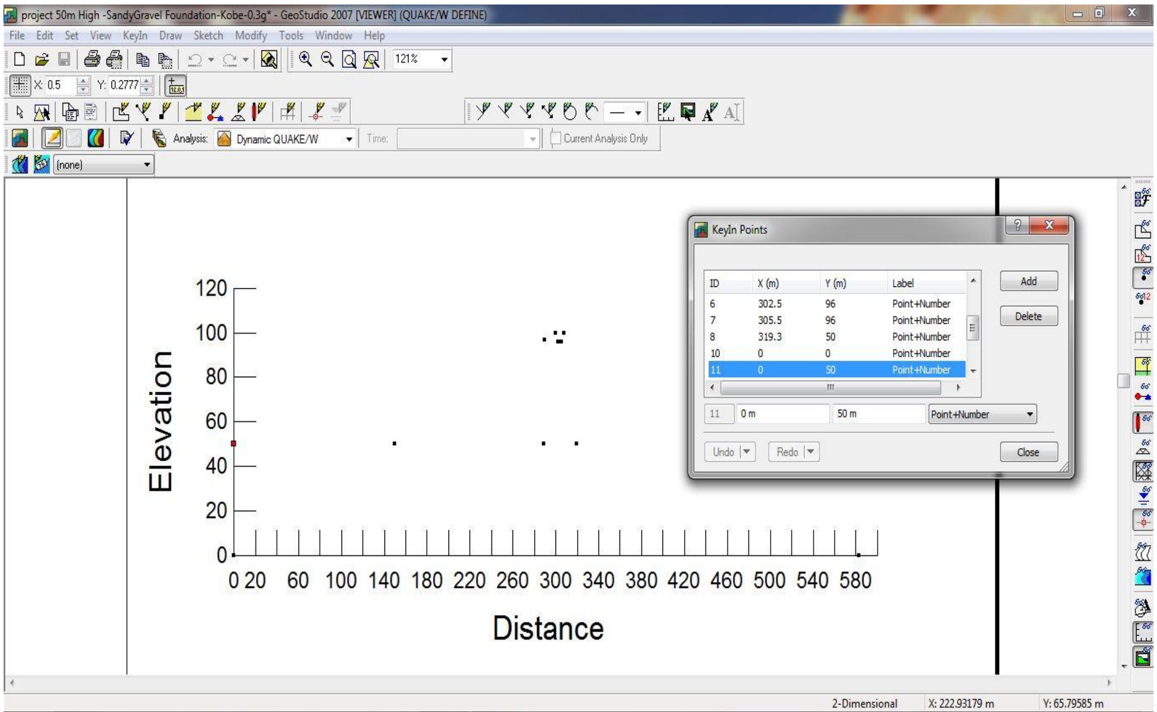

Figure A.2.1: Draw point

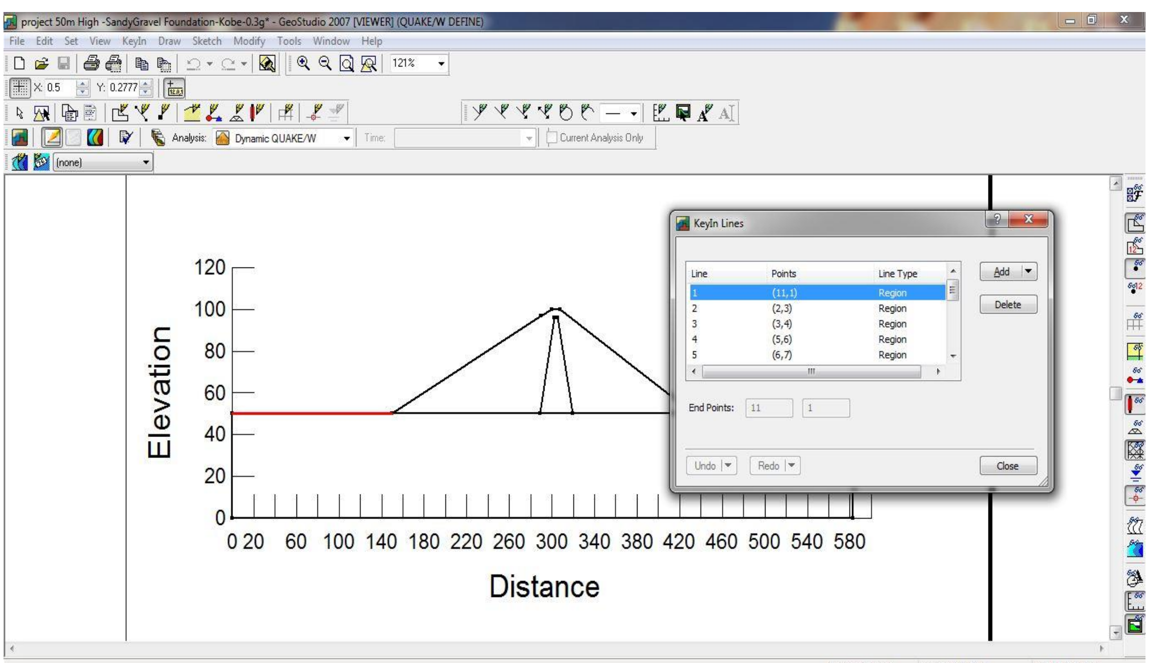

Figure A.2.2: Draw line

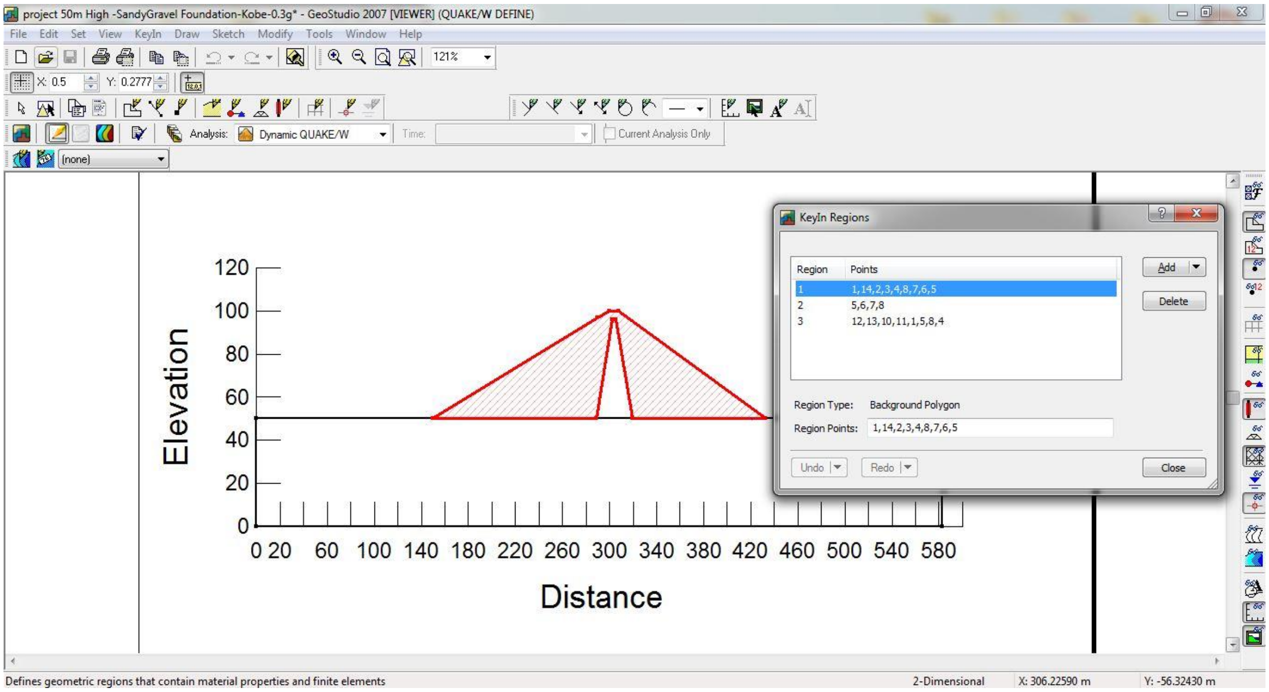
Figure A.2.3: Draw region

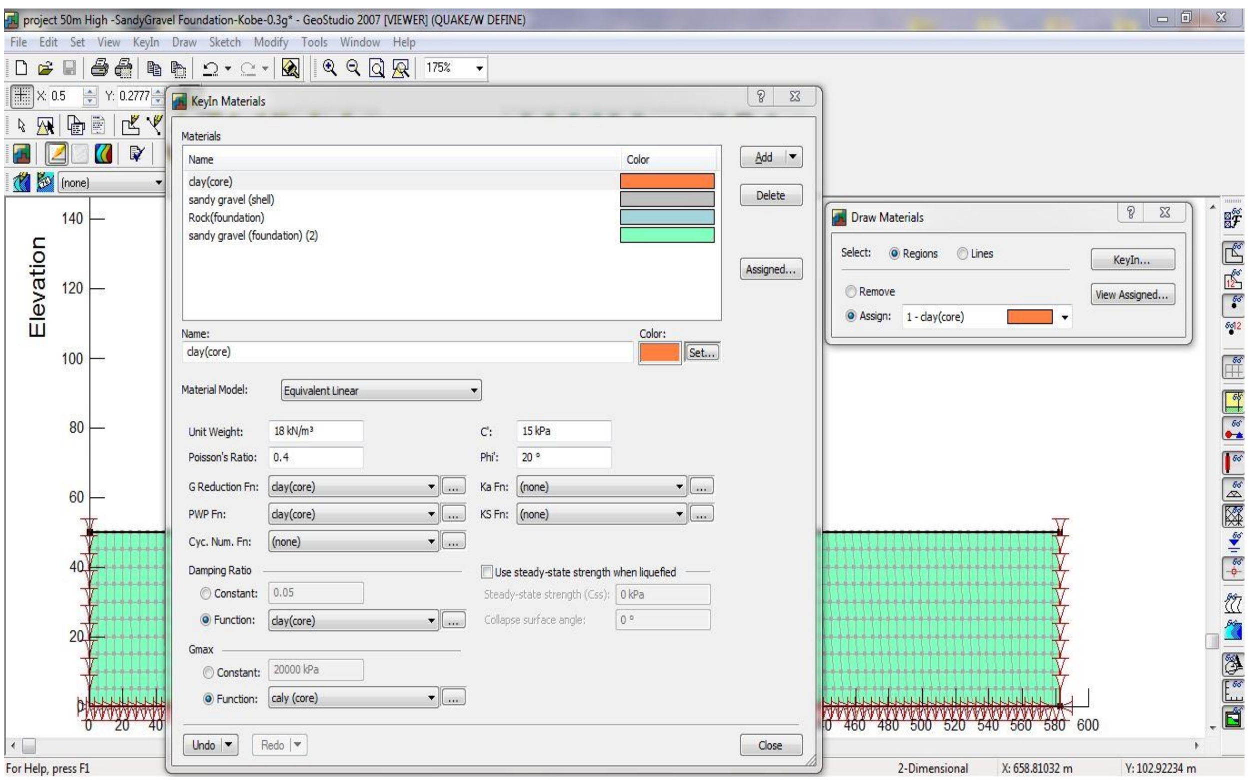
Figure A.2.4: Define material property

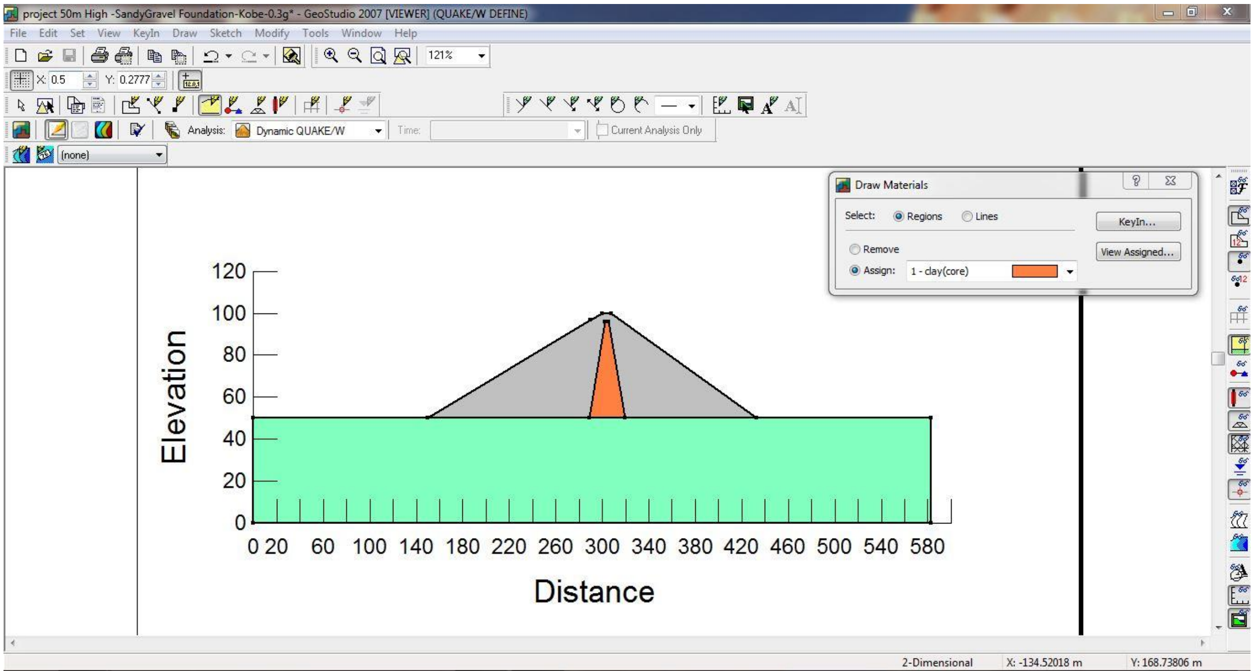

Figure A.2.5: Assign material property

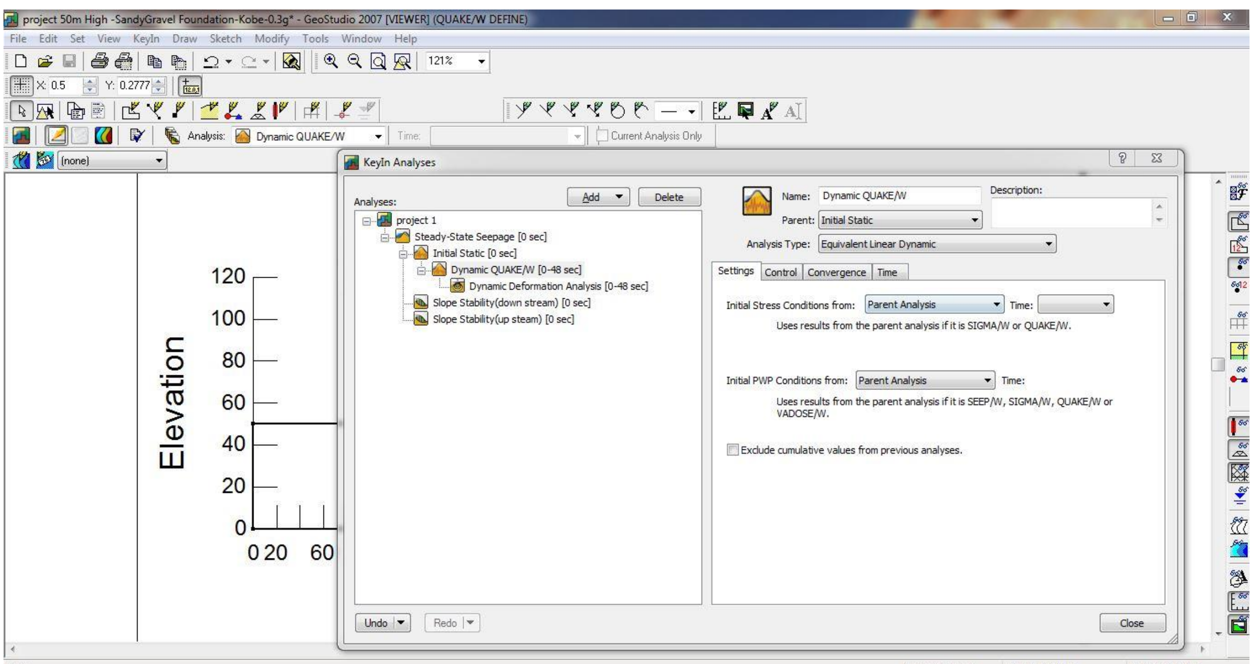

Figure A.2.6: Define analysis (Dynamic analysis taken as a sample)

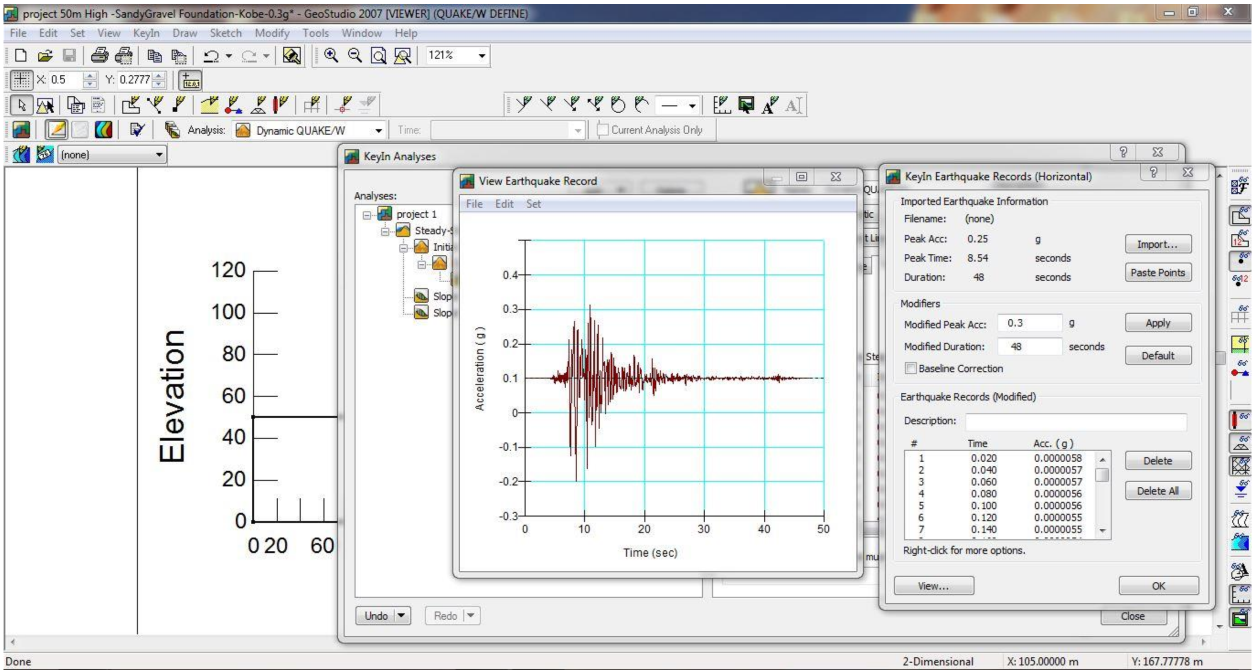

Figure A.2.7: Insert ground motion (Kobe ground motion at an amplitude of 0.3g taken as a sample)

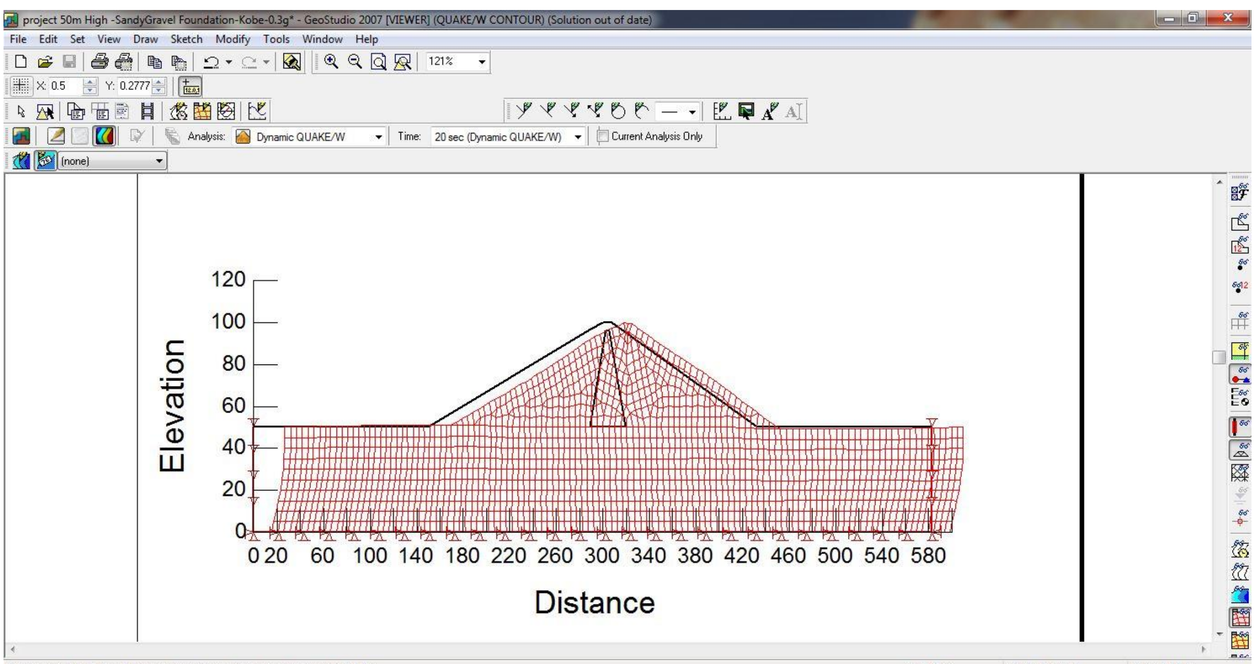

Figure A.2.8: Dynamic QUAKE/W deformed mesh result (at 20sec as sample)

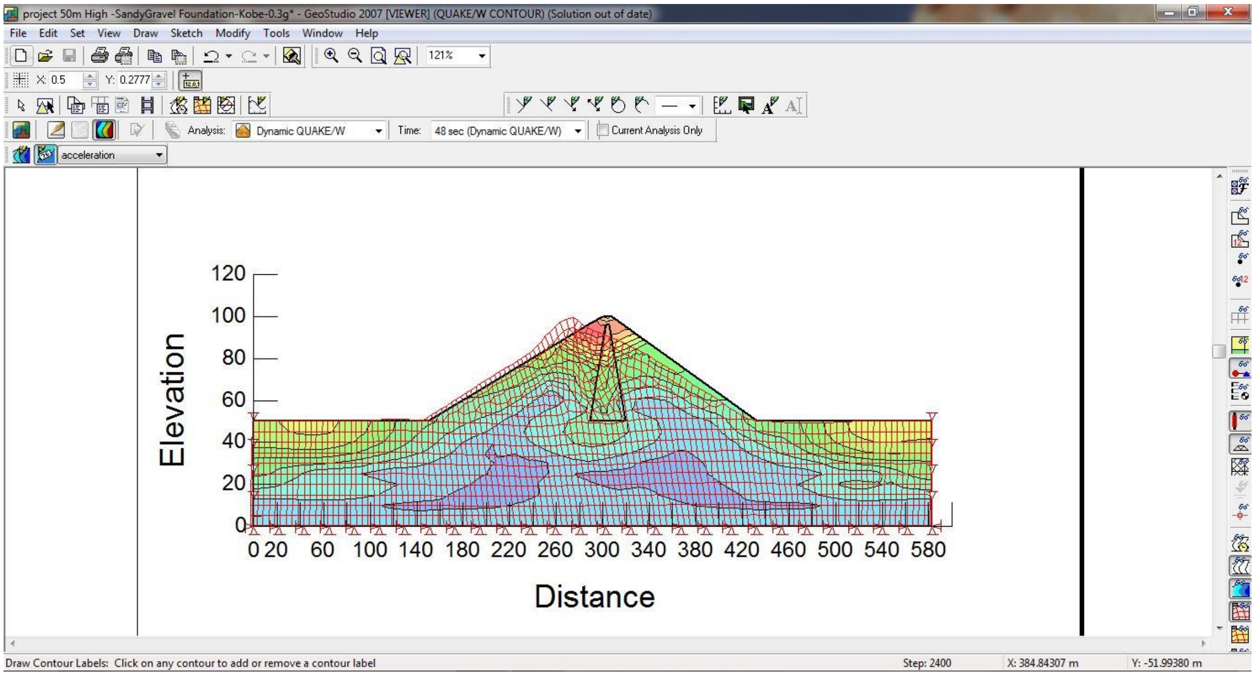

Figure A.2.9: Dynamic QUAKE/W deformed mesh result with contour presentation (at 48 sec as sample)

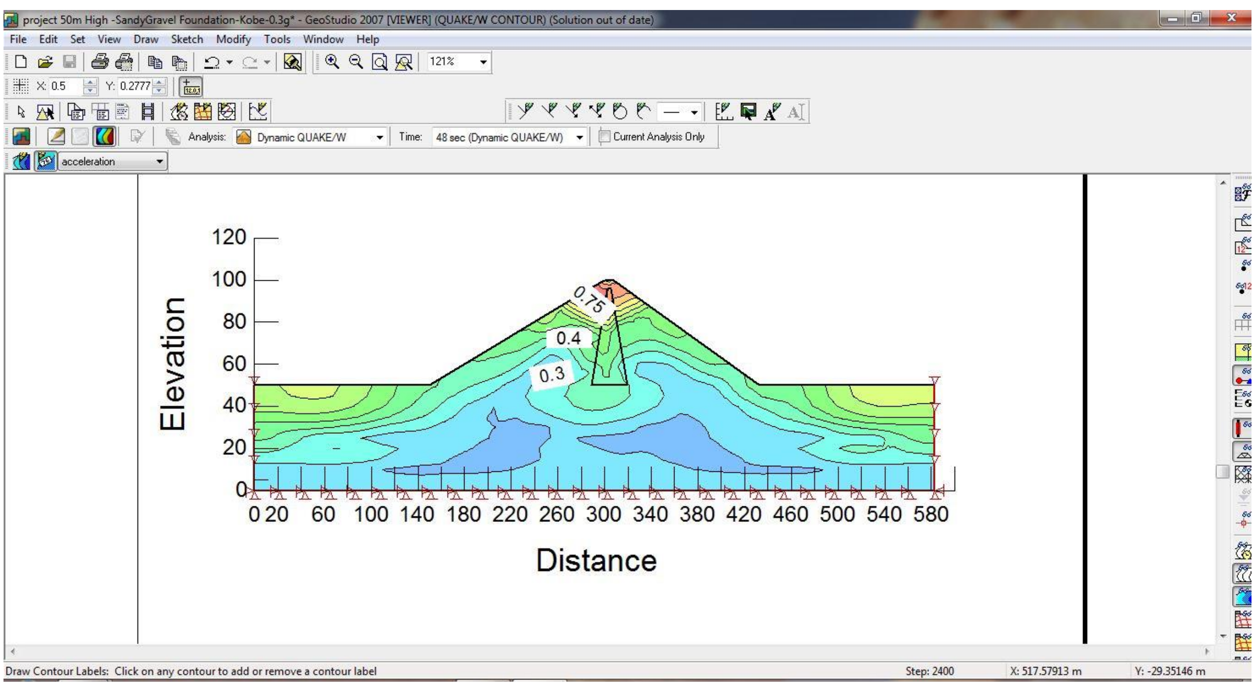

Figure A.2.10: Dynamic QUAKE/W result in contour representation (at 48 sec as sample)

Appendix-3- Sample results

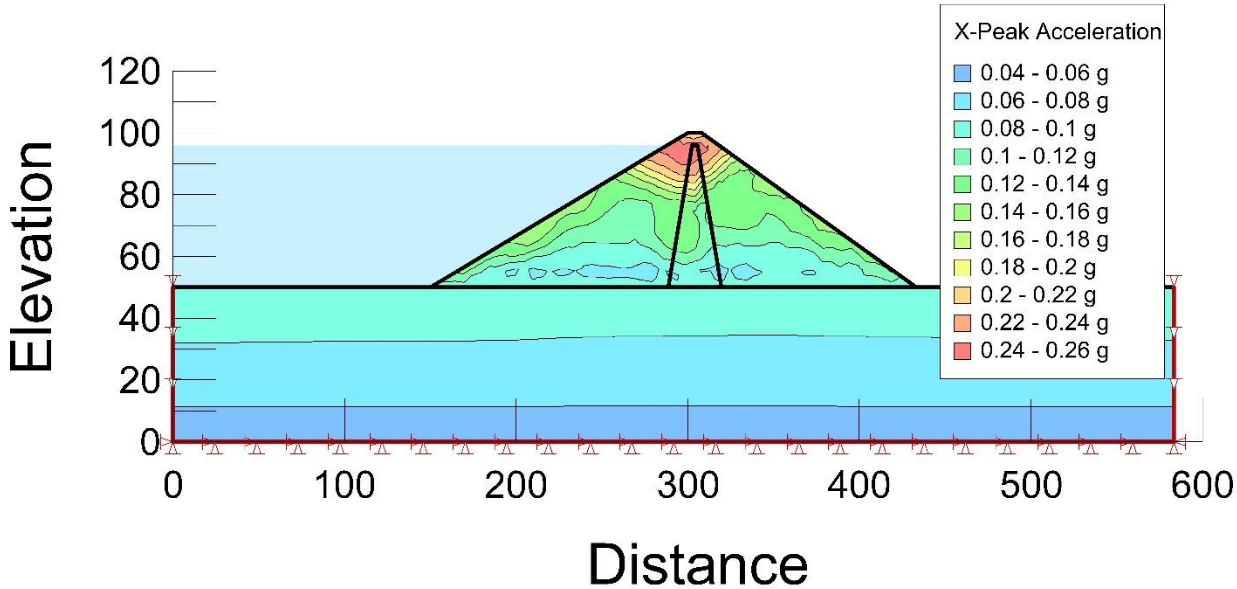

Figure A.3.1:Dynamic QUAKE/W result in contour representation (50m high dam on Rock foundation subjected to Elcentro ground motion at an amplitude of 0.05g)

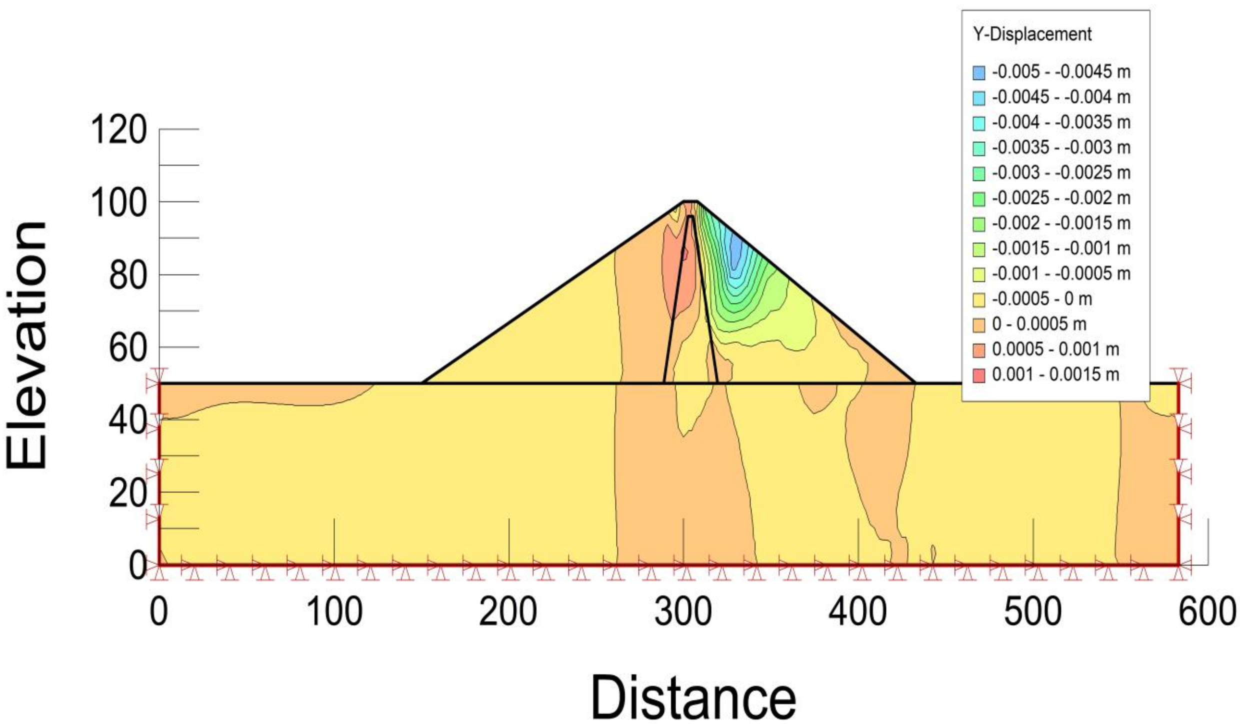

Figure A.3.2: Permanent deformation SIGMA/W result in contour representation (50m high dam on Rock foundation subjected to Elcentro ground motion at an amplitude of 0.05g)

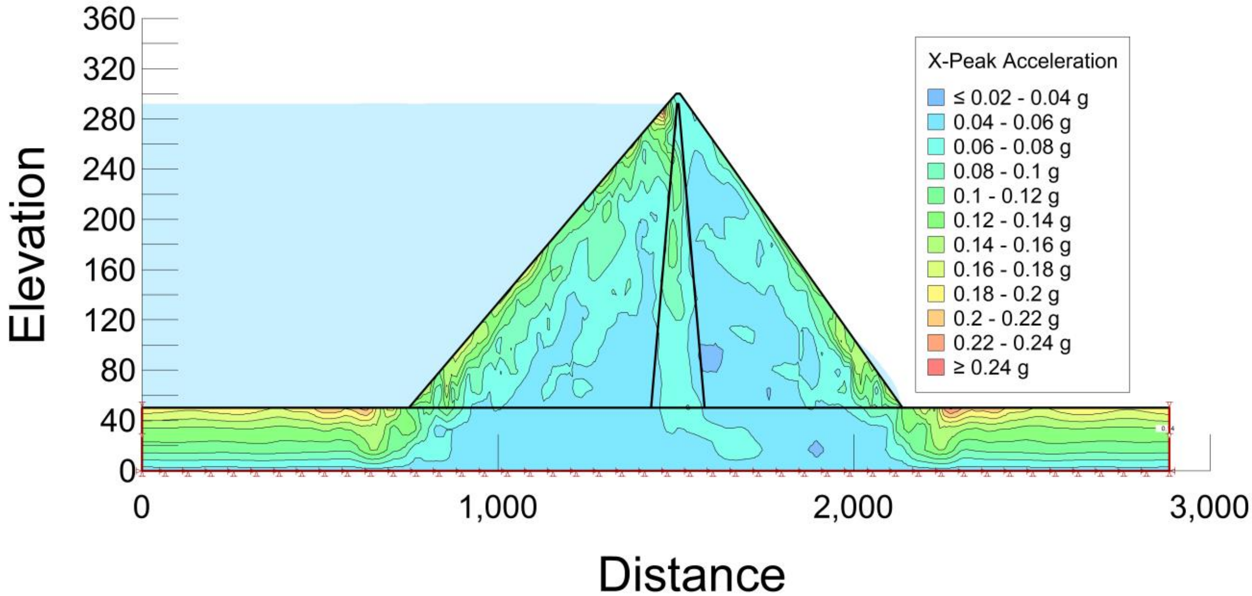

Figure A.3.3: Dynamic QUAKE/W result in contour representation (250m high dam on Sandy gravel foundation subjected to Hachinohe ground motion at an amplitude of 0.05g)

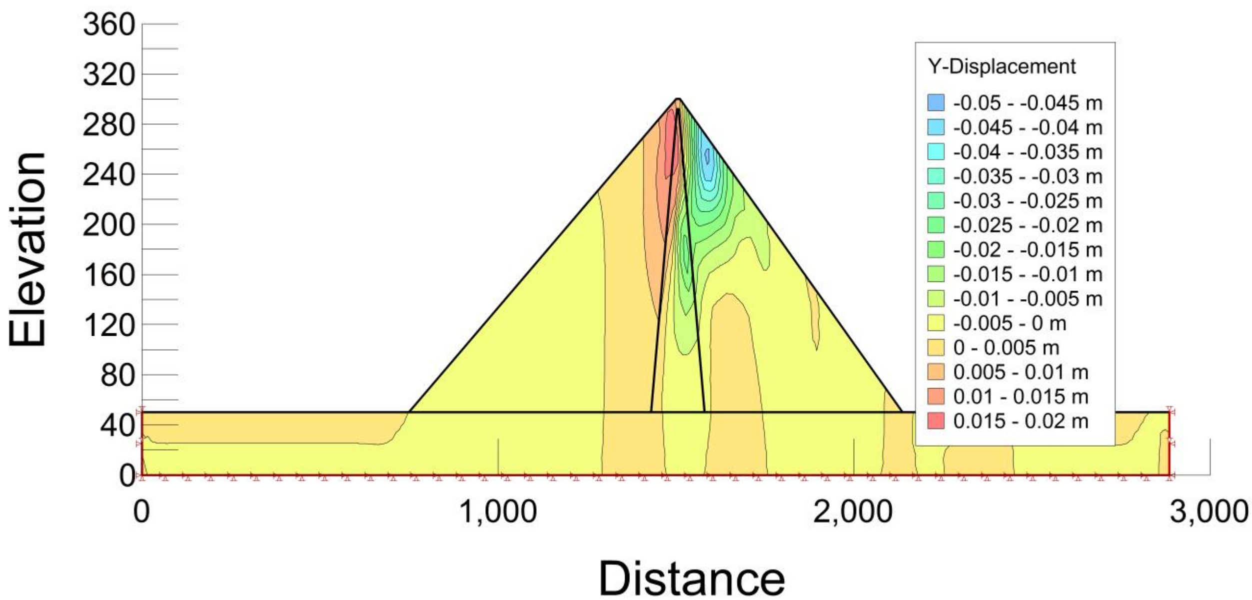

Figure A.3.4: Permanent deformation SIGMA/W result in contour representation (250m high dam on Sandy gravel foundation subjected to Hachinohe ground motion at an amplitude of 0.05g)

Appendix-4- Trial analiyses with 100m foundation

50m, 150m and 250m high dam resting on sandy gravel foundation subjected to Hachinohe ground motion with a PGA of 0.3g was taken as a trial model for checking the effect of changing the foundation depth. A foundation depth of 100m was considered and the comparison is placed in table Table A-4.

Table A-4: Comparison result for effect of foundation height difference

	50m high dam		**150m high dam**		**250m high dam**	
	50m Foundation	**100m Foundation**	**50m Foundation**	**100m Foundation**	**50m Foundation**	**100m Foundation**
Maximum acceleration on the top of the foundation	0.35g	0.25g	0.3g	0.3g	0.3g	0.3g
Maximum acceleration on the top of the dam	0.9g	0.5g	0.5g	0.5g	0.45g	0.45g

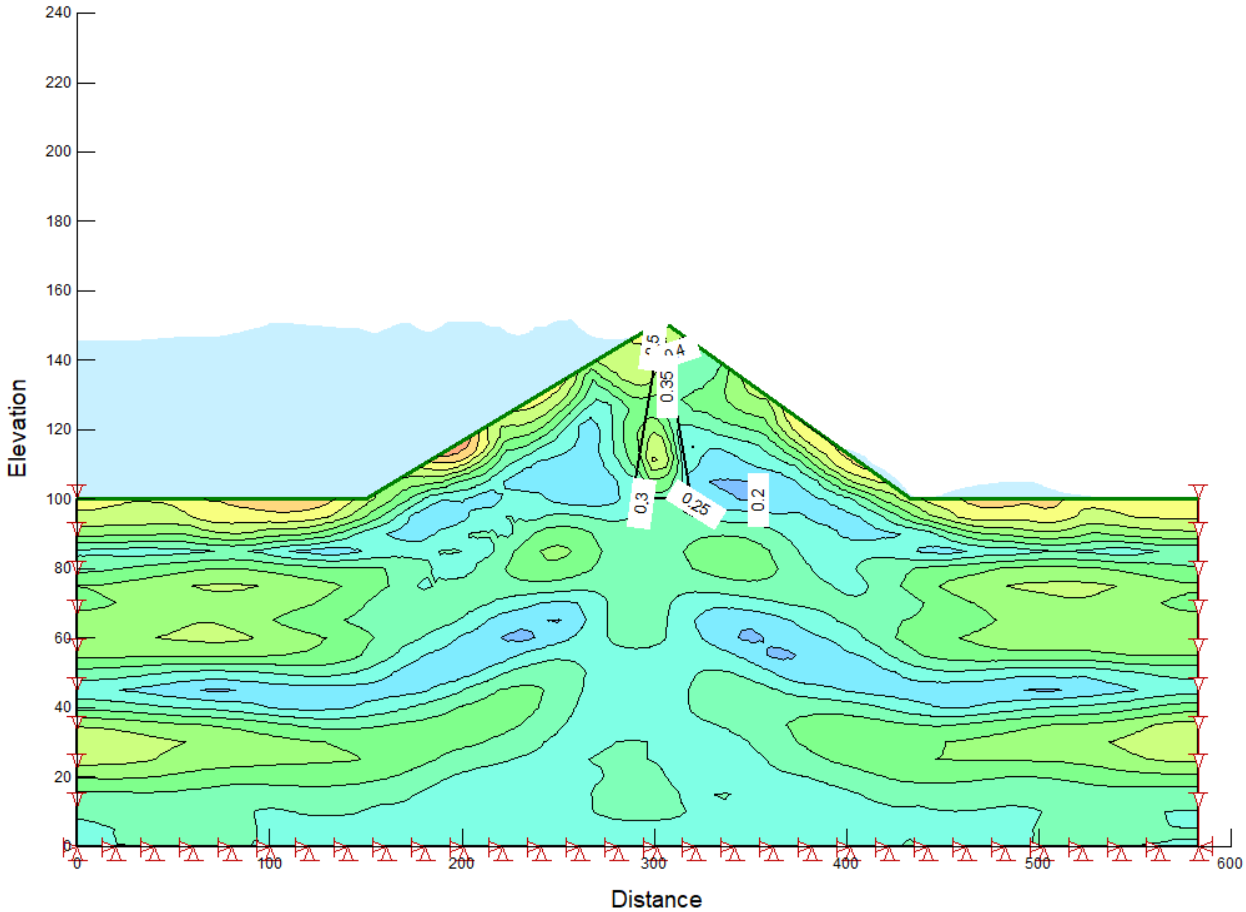

Figure A4.1: – 50m high dam as sample result for 100m Foundation